OTF DGPS FOR ESTUARINE DREDGING AND SOUNDING SURVEYS

R. B. PHELAN

April 1998

PREFACE

In order to make our extensive series of technical reports more readily available, we have scanned the old master copies and produced electronic versions in Portable Document Format. The quality of the images varies depending on the quality of the originals. The images have not been converted to searchable text.

OTF DGPS FOR ESTUARINE DREDGING AND SOUNDING SURVEYS

Richard B. Phelan

Department of Geodesy and Geomatics Engineering
University of New Brunswick
P.O. Box 4400
Fredericton, N.B.
Canada
E3B 5A3

April 1998

PREFACE

This technical report is a reproduction of a report submitted in partial fulfillment of the requirements for the degree of Master of Engineering in the Department of Geodesy and Geomatics Engineering, June 1997. The research was supervised by Dr. David Wells, and it was supported by Public Works and Government Services Canada, by Fisheries and Oceans Canada, and by the Natural Sciences and Engineering Research Council of Canada.

As with any copyrighted material, permission to reprint or quote extensively from this report must be received from the author. The citation to this work should appear as follows:

ABSTRACT

This report assesses the feasibility of using the On-The-Fly Differential Global Positioning System (OTF DGPS) satellite positioning technique for the accurate and reliable measurement of spatial variations in water's surface elevation in an estuarine region. The improvement of the accuracy and reliability of squat-dependent dredging and sounding surveys is assessed. Conventional dredging and sounding surveys require the installation and maintenance of temporary water level sensors, along with water level interpolation at the vessel location.

OTF DGPS feasibility is assessed through a practical field exercise on the Miramichi River, New Brunswick, using a representative OTF DGPS system -- the Ashtech Z12/PRISM system. Z12/PRISM results, obtained with the collaboration of the Department of Public Works, are compared with reviews on the performance of other OTF DGPS systems.

Under limited conditions: (1) PRISM/Z12 water surface elevation accuracy was acceptable, being +/- 0.034 metres at 95% confidence, and (2) PRISM/Z12 reliability was acceptable. Availability was: (1) acceptable at 90-99% for three out of four survey days, and (2) unacceptable at 25% for one survey day.

A squat-independent approach for OTF DGPS dredging and sounding surveys should be investigated. The use of multiple base and remote OTF DGPS stations needs to be

investigated. The accuracy and reliability of OTF DGPS needs to be assessed further, especially during the upcoming sunspot maximum.

TABLE OF CONTENTS

LIST OF FIGURES

LIST OF TABLES

ACKNOWLEDGMENTS

CHAPTER 1

INTRODUCTION

This report assesses the feasibility of using the OTF DGPS technology for the accurate and reliable measurement of spatial variations in water's surface elevation for squat-dependent dredging and sounding surveys in an estuarine region.

In this Chapter, section 1.1 outlines the need for in situ water levels. Section 1.2 covers the basics of water's surface elevation measurement using On-the-Fly Differential GPS (OTF DGPS). Section 1.3 discusses the feasibility assessment methodology. Section 1.4 gives a brief description of other applications requiring OTF DGPS water's surface elevations. Section 1.5 provides the summary of contributions. Finally, Section 1.6 gives an outline of the rest of the report.

1.1 The Need for Measuring Spatial Variations

In dredging and sounding surveys, it is necessary to measure the height of the water's surface above a known level (datum level). In a sounding survey, the distance from this datum level to the bottom of the estuary is then measured at many points in the survey area with an echosounder so that a detailed depth chart can be made. A

dredging survey may be needed to increase this distance from the datum water level to the sea bottom.

The traditional method of measuring the height of the water's surface above datum is to have **water level sensors** at one or more fixed locations on the shore. These sensors record the water's levels at fixed increments of time. Having obtained the water's level at the shore location(s), the water's level at a given time **at the vessel location** is then inferred from these records. Often the level is interpolated as a function of the distance from the two nearest water level sensor stations.

Factors such as variations in estuary shape can cause the water's surface elevation to vary as a function of location relative to the water level sensor stations. These spatial variations in water's surface elevation are better determined by **direct measurement**, rather than modeled by interpolation.

1.2 Using OTF DGPS for Water Level Measurement

The OTF DGPS water's level measurement technique is a satellite - based positioning technique that is capable of positioning **continuously moving platforms** with relative accuracies of around +/- 0.1 metres. On shore a base (reference) station is established with an OTF DGPS antenna (at a known elevation), an optional radio transmitter, and an OTF DGPS receiver. On the estuary, the **remote station**

2

(usually a ship), has similar equipment. A precise three-dimensional (3-D) vector is measured from the OTF DGPS antenna at the reference station to the remote OTF DGPS antenna. The remote and base stations do **not** have to be **stationary** to be able to measure this vector, but in practice the base station is usually stationary, while the remote moves. The term "On-The-Fly" refers to the fact that the integer carrier ambiguities are resolved while the remote receiver is moving [Leick, 1995]. The essential distinction between On-the-Fly DGPS and ordinary code Differential GPS (DGPS) is the fact that the carrier phase ambiguities are resolved [Wells, 1996].

In Figure 1.1 the desired quantity is the water's level - chart datum separation ΔD. We therefore measure the **height difference** $\Delta HDGPS$ between the OTF DGPS base station antenna and the OTF DGPS vessel antenna. We know the height f of the vessel's antenna above the water's surface, the elevation ELBM of the benchmark (BM) above datum, and the height HI of the DGPS base station antenna above the benchmark. We then calculate the elevation ΔD of the water's surface above or below datum **at the vessel location** from the following equation:

$$\Delta D = ELBM + HI - f - \Delta HDGPS \qquad (1.1)$$

This OTF DGPS water's level measurement technique will be referred to as a **squat-dependent** technique. This is be-

3
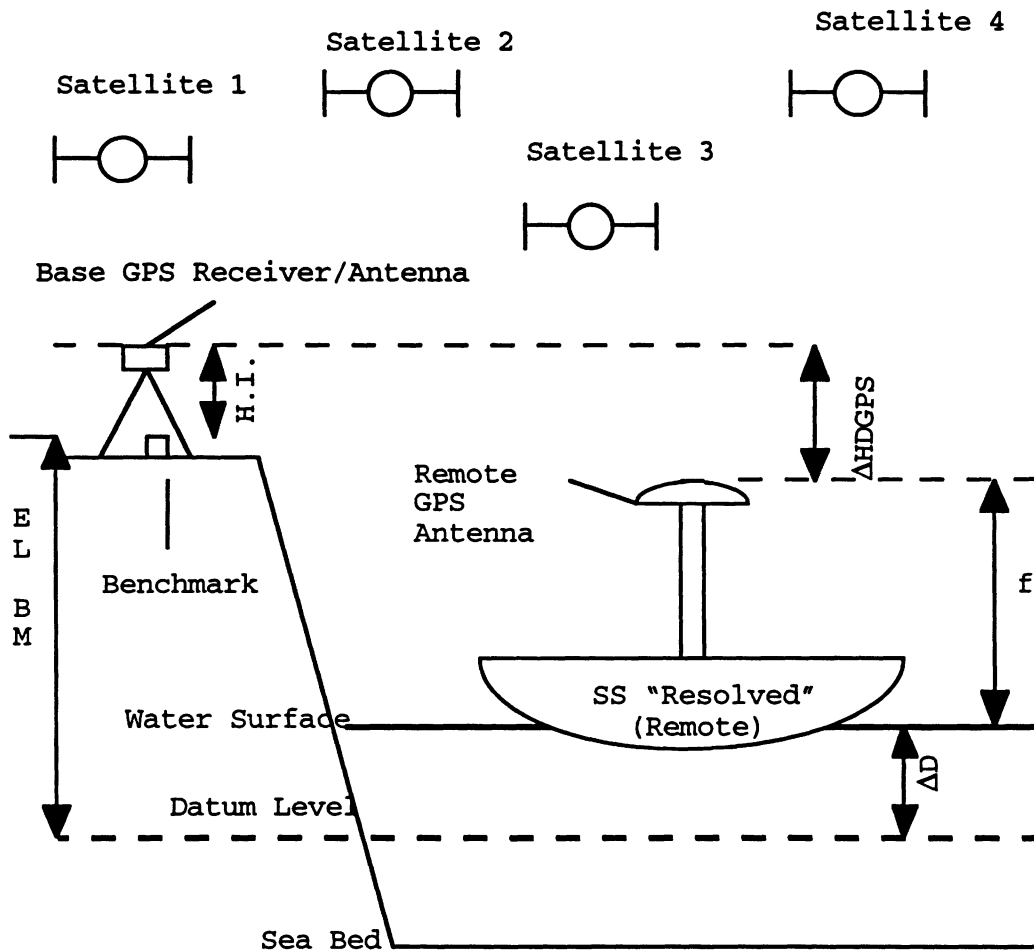
Figure 1.1

OTF DGPS water's surface elevation measurement technique
(after Wells [1995a]).

cause the accuracy of the water's surface elevations de-
pends on knowledge of the vessel squat -- the combined
effect of the vessel rising or sinking in the water, along
with changes in trim (i.e. the bow usually rises with
increasing speed, etc.) [Bowditch, 1984]. In contrast, a
squat-independent technique as suggested by Deloach
[1994] would use the elevation of the OTF DGPS remote

antenna and a known separation between the remote antenna and the echosounder to measure the elevation of the bottom.

Current OTF DGPS systems have ΔHDGPS **accuracies** of 0.02 to 0.10 metres out to 20 kilometres from a base station (Frodge et al [1993]; Lachapelle et al [1993]; Langley and Komjathy [1994]). Frodge et al [1994] indicate a reliability of roughly 99% or higher in finding the correct integer ambiguities. In the context of this report: (1) OTF DGPS **reliability** is defined as the ability to **correctly** flag integer ambiguities as **resolved or unresolved,** and (2) **availability** is the percentage of time that **resolved** ambiguities are available.

There are two modes of OTF DGPS. The calculation of the water's surface elevation can be done in **real - time mode** (water's surface elevation is computed immediately) by sending the observed OTF DGPS data from the reference station to the remote via a data link (essentially a radio broadcast). The real-time mode must be used when results are required immediately (for example to control dredging depth during dredging operations). One of the benefits of this mode is that very little data has to be stored. The water's surface elevation calculations can also be done in **post-processing** mode. Here, all the data from the reference station and the remote station is stored inside the OTF DGPS receivers or, more commonly, in PC laptops due to the large volume of data required. The data is then taken back to the office to be processed. Compared to real-

time, post-processing offers the advantage of being able to try several different strategies for processing the raw OTF DGPS data, but suffers somewhat from a requirement for large amounts of hard disk storage space.

1.3 Feasibility Assessment Methodology

The feasibility of using the OTF DGPS technique for dredging and sounding was assessed using a practical field exercise performed with the collaboration of the Department of Public Works (DPW) on the Miramichi River, New Brunswick. The field exercise used the Ashtech Z12 OTF DGPS receivers and the Ashtech PRISM post-processing OTF DGPS package, and involved comparing post-processed OTF DGPS water's levels with a network of digital water level sensors. The Department of Public Works requires a water level measurement/interpolation accuracy of **+/- 0.10 metres**. This report will determine if the OTF DGPS water's surface elevation accuracy meets this requirement. It was assumed that the performance of the Z12/PRISM package is indicative of the performance obtainable from any other OTF DGPS system. This assumption will be tested through comparisons between the PRISM field results and literature reviews of current OTF DGPS systems.

1.4 Other Applications for OTF DGPS Water Levels

There are several other applications for OTF DGPS

6

water's levels. They will be briefly mentioned here for the sake of completeness.

One additional application is UKC (Under Keel Clearance) real-time water level monitoring for marine navigation. This application is for estuaries with wide spacing between tidal stations, such as the Saint Lawrence River. Hare and Tessier [1995] have shown that water surface elevations at the midpoints of tidal stations can be as inaccurate as +/- 1.374 metres at the 1σ level. Ship groundings could result, especially when any previous sounding errors are considered as well.

Another application involves using OTF DGPS water's surface elevations for improving hydraulic models. Presently the models are used for water's surface elevation prediction in flood forecasting and real-time navigation. The models use estuary shape, river stage level, salinity, temperature, tide phase, current observations, and water level sensor elevations to determine the water's surface elevation. Burrells [1995] has stated that it may be possible to use OTF DGPS water's surface elevation profiles to check the validity of some of the model assumptions. This could be a real-time or post-processing application of OTF DGPS, depending on how quickly results are required.

1.5 Summary of Contributions

This report determines, on the basis of a practical

7

field exercise, if the OTF DGPS water's surface elevation measurement technique is sufficiently accurate and reliable to be used for squat-dependent dredging and sounding surveys in an estuarine region. Survey method recommendations are provided for real-time and post-processing OTF DGPS dredging and sounding surveys.

1.6 MEng Report Outline

Chapter Two outlines the need for accurate in situ water's surface elevation measurements.

Chapter Three discusses previous work which has been carried out in developing the OTF DGPS technology.

Chapter Four gives a brief overview of the forces influencing water's surface elevations in an estuarine region. A brief discussion of the basic types of hydraulic models is presented. The possibility of using OTF DGPS water's surface elevation observations for improving these models is investigated.

Chapter Five covers the Miramichi River OTF DGPS survey field data collection in detail.

Chapter Six presents the processing and interpretation of the OTF DGPS surveys on the Miramichi.

Chapter Seven contains the conclusions and recommendations.

CHAPTER 2

THE NEED FOR IN SITU WATER LEVELS

Present water level measurement techniques provide
measurements at discrete spatial locations. This can be
troublesome when accurate water levels are required at
locations other than where the water's level measurements
are made. It is then necessary to interpolate the water's
level at the desired locations. This interpolation can be
too inaccurate for certain applications.

Section 2.1 covers the need for accurate in situ
water's level information in dredging and sounding surveys.
Section 2.2 covers other applications for in situ water
levels.

2.1 The Need for Accurate in Situ Water's Level
Measurement in Dredging and Sounding Surveys

2.1.1 Datums and Water Levels

In the field of hydrography, accurate measurements of
the water's surface elevation above a known reference
height or **datum level** at specific times are needed. These
are the **water's levels.** These water levels are usually
measured by **water level sensors** at fixed increments of
time. Several digital (computerized) versions of these
sensors are now on the market. They can either be attached
to a dock, or placed on the sea bottom (seabed pressure

water level sensor). The dock-based water level sensors are "zeroed" against one of the following:

(1) A **tide staff**, which is a graduated wooden board that is placed into the water on a rigid support. These boards are read manually to obtain water levels at given times.

(2) A **tide tape**, which is an ordinary cloth survey tape with a weight attached.

The datum level represents the lowest water level observed during a given time period. Often the water's level will be lowest during a particular set of tides, known as **spring tides**, which repeat themselves approximately every two weeks during the year. The tide staff or tide tape reading is referred to the datum level through **benchmarks** which are stable, well defined markers with known datum elevations on them. The elevation of the tide staff or tide tape is referred to the benchmarks by using a **spirit level**, which is an optical device that is used to find the height difference between the benchmark(s) and the tide staff or tide tape.

The benchmark chart datum heights are commonly related to a mathematical model for the earth's gravity field, known as the geoid, which corresponds very closely to mean sea level. However, positioning systems such as GPS will likely require that datum heights be related to a reference ellipsoid [Wells et al, 1996]. Such a reference ellipsoid

is a best fit to the geoid.

2.1.2 Drawbacks in Traditional Sounding Methods

At the **same time** as the water level measurements, hydrographers measure the distances from the water's surface to the sea bottom at **specific locations**. These measurements are known as **soundings**. Knowing the water's levels and soundings, they produce **charts** that show how deep the water will be at these specific locations when the water's level falls to the **datum level**. These are the **charted depths** or **charted bathymetry**. The **accuracy** and coverage of these charted depths is **paramount**, as many different types of vessels depend on them for safely navigating harbors and bays. If the charted depths are thought to be dangerously shallow, a **dredging survey** will be performed to deepen the harbor. Traditionally, these depths have been assigned very pessimistic values (i.e. likely to be more shallow than actual) for safety reasons, due to the lack of in situ water's level information at the vessel location, and uncertainties in depth measurement, depth data point positioning, datum determination, etc.

Traditionally, hydrographers have used water's level measurements above datum taken at **fixed points** (for instance, at docks). When they do sound at **distant locations** (some distance away from the docks), they have to **interpolate** the water's level at that location, because

the water's surface elevation will display some form of trend as a function of relative position from the docks. In effect, they have a **spatial problem** that has to be solved: at a given instant of time, what is the water's surface elevation **in situ** -- i.e. at a given position which is well away from the water level sensors?

To do the interpolation, hydrographers use the simultaneous water's level observations above datum at two docks, and interpolate the water's surface elevation at selected locations between them. Essentially, they are trying to model the behavior of the water's surface elevation between the two docks. The **spatial variations** in the water's surface elevation are being modeled. As with all interpolation techniques, there are several strategies, each with varying degrees of complexity.

An excellent example of the spatial interpolation problem for hydrography is given in Hare and Tessier [1995]. Figure 2.1 shows the location of the tidal stations that Hare and Tessier [1995] evaluated on the Saint Lawrence River, Quebec. Table 2.1 shows the 1σ (68% confidence) error in water's surface elevation for the midpoints of these tidal stations. Hare and Tessier [1995] state that these accuracies are not good enough, especially for the stations that are nearest the Gulf of Saint Lawrence. Vessel groundings are a distinct possibility, with 1σ accuracies as large as +/- 1.374 metres, especially when any previous sounding errors are combined with the wa-

12
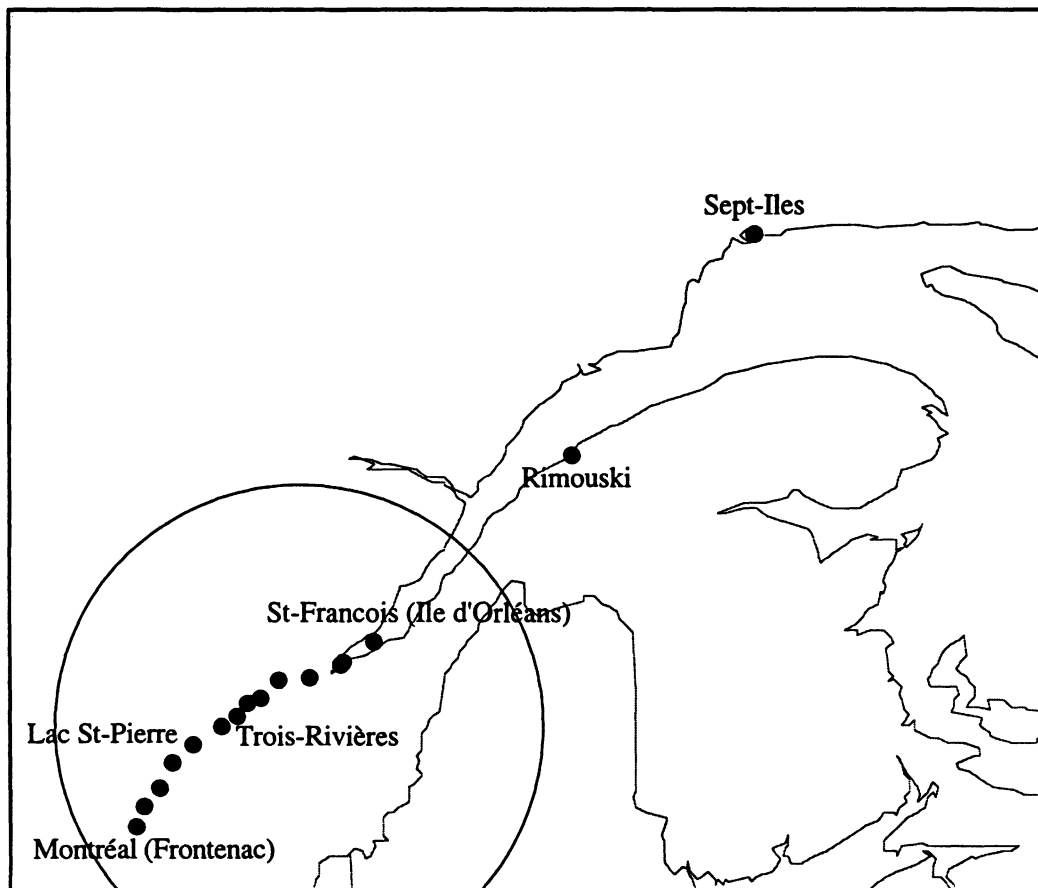
Figure 2.1

Tidal stations on the Saint Lawrence River
(from Hare and Tessier [1995, p. 1]).

ter surface modeling error [Hare and Tessier, 1995].

2.2 Other Requirements for In Situ Water Levels

The requirements of the Under Keel Clearance (UKC)
marine navigation application are more demanding than those
for hydrographic sounding and dredging surveys. Under Keel
Clearance represents a major change in thinking from the

13

traditional "worst-case" charted depths. At the vessel
location, the requirement is for an accurate in situ
water's level elevation above the **same** datum level as was

Table 2.1

Spatial prediction errors for the midpoints of tidal
stations on the Saint Lawrence River
(after Hare and Tessier [1995, p. 1]).

From Gauge	To Gauge	Distance Between Stations (Kilometres)	1 σ Error at Midpoint (Metres)
Sept-Iles	Rimouski	246	0.208
Rimouski	St-Francois	238	1.374
St-Francois	Quebec	35.4	0.190
Quebec	Lauzon	3.3	0.058
Lauzon	Neuville	35.2	0.190
Neuville	Portneuf	23.3	0.155
Portneuf	Deschaillons	22	0.067
Deschaillons	Batiscan	12.7	0.051
Batiscan	Becancour	15	0.055
Becancour	Trois-Rivieres	13.9	0.018
Trois-Rivieres	Lac St-Pierre	32	0.027
Lac St-Pierre	Sorel	23.6	0.023
Sorel	Contrecoeur	27.2	0.025
Contrecoeur	Varennes	20.7	0.021
Varennes	Montreale	18.9	0.020

used for the charted depths, along with an accurate
estimate of the distance from the ship's keel to the
bottom. In addition, **accurate predictions** of the water's
level along the vessel's projected course are **mandatory**
[Lacroix and Kightley, 1996].

One additional application involves using OTF DGPS to "ground truth" present hydraulic models. These models can then be used to improve flood forecasting and the UKC navigation application. **Hydraulics** is the study of fluid flow and the forces influencing that flow. Hydraulic **models** for water's surface elevation along an estuary can incorporate many factors, including the shape of the river/harbor, wind speed, salinity, and currents. Burrells [1995] has stated that a continuous spatial water's surface profile could possibly be used to determine if some of the assumed parameters in these models are correct. No conventional water's surface elevation measurement techniques can provide such a profile.

The UKC marine navigation option could benefit from a hydraulic model which has been verified with OTF DGPS observations. Such a model could provide better knowledge of the water's levels along the ship's intended course, and help to diminish the possibility of groundings.

Willis [1995] and Burrells [1995] have also indicated that accurate water's surface spot elevations at ice jam locations are very useful in flood forecasting. The current strategy is to use a spirit level to measure the water's surface elevation, and to tie this elevation to geodetic control, which can be a considerable distance from the ice jam location. It would be more efficient to have a method of obtaining accurate water's level elevations without the need for a time-consuming spirit level tie to control.

CHAPTER 3

RECENT ADVANCES IN OTF DGPS

Section 3.1 begins by covering the basic principles behind GPS positioning for navigation as given in Leick [1995]. Section 3.2 outlines some preliminary work in OTF DGPS. Section 3.3 covers the John E. Chance and Associates (JECA) OTF DGPS algorithm as used in the U.S. Army Corps of Engineers' real-time OTF DGPS system. Section 3.4 outlines results from the recent testing of three OTF DGPS systems. Section 3.5 covers the basics of the PNAV-PRISM OTF DGPS package, which was used in the OTF DGPS water's surface elevation ground truthing surveys (see Chapter Six for results).

3.1 Basic GPS Positioning Principles for Navigation

3.1.1 Space Segment, Control Segment, and User Segment

The GPS space segment consists of the satellite hardware and software. The GPS satellite constellation currently contains 24 satellites in total. Figure 3.1 shows a general view of the satellite orbits. These satellites are in a 20,000 kilometre high orbit above the earth, with an orbital period of about 12 hr.

16
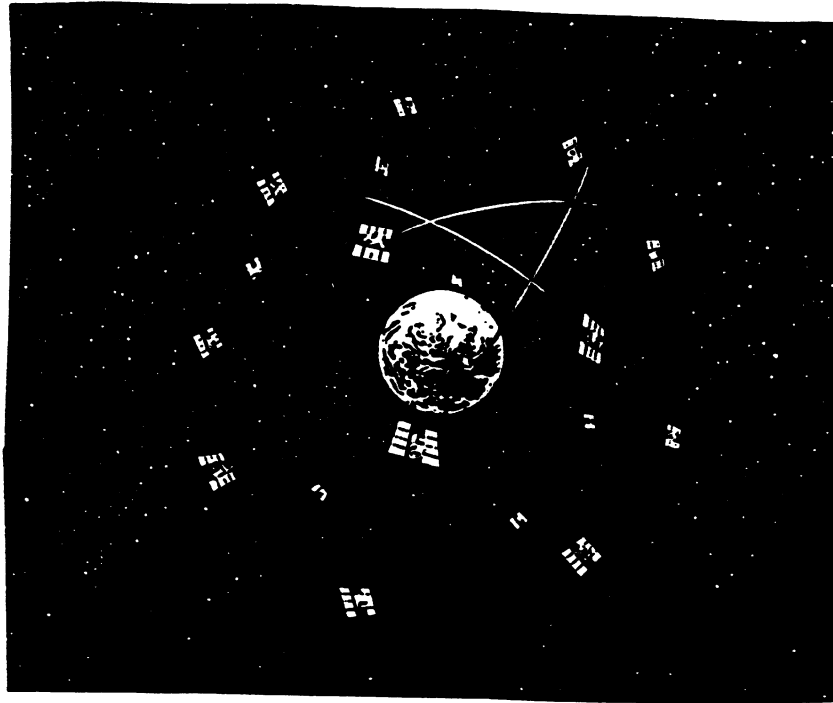
Figure 3.1

GPS satellite orbits
(from Leick [1995, p. 2]).

Every GPS satellite outputs two carrier waves
operating in the microwave band of the spectrum: L1, at a
frequency of 1575.42 MHz., and L2, at a frequency of
1227.60 MHz. The L1 carrier has a modulated wave
superimposed on it -- the C/A or coarse acquisition code.
This modulation can be represented as a series of zeroes
and ones in what is termed a pseudorandom noise sequence.
This sequence is unique to each satellite. The sequence
repeats itself over exact intervals of time, allowing for
the calculation of pseudoranges (see section 3.1.2). The

accuracy of pseudoranges obtained from the C/A code is deliberately degraded for military security reasons. This degradation is known as Selective Availability (SA).

The L1 and L2 carriers each have another modulation -- the P-code or precise code. The P-code is encrypted so that only the military can use it fully, with special receivers. However, civilian techniques have been developed to use certain features of the P-code.

In addition to the P-code and C/A code modulations, the L1 and L2 frequencies have a navigation message modulated on them. This message contains information about satellite ephemerides, clock behavior, GPS time (reference time for the satellites, based on atomic clocks), and system status messages.

The GPS control segment is made up of a master control segment near Colorado Springs, along with other stations located around the globe. These control stations have very accurate geocentric cartesian coordinates. Figure 3.2 shows a sample control station "DI" in a geocentric cartesian coordinate frame. The control segment performs three functions:

(1)   Monitors the satellite transmissions continuously.

(2)   Calibrates the satellite clocks.

(3)   Updates the navigation message periodically. This message contains information such as satellite health and predicted satellite positions in the

WGS '84 (World Geodetic System) '84 cartesian coordinate frame. WGS '84 is a geocentric crust-fixed coordinate system.
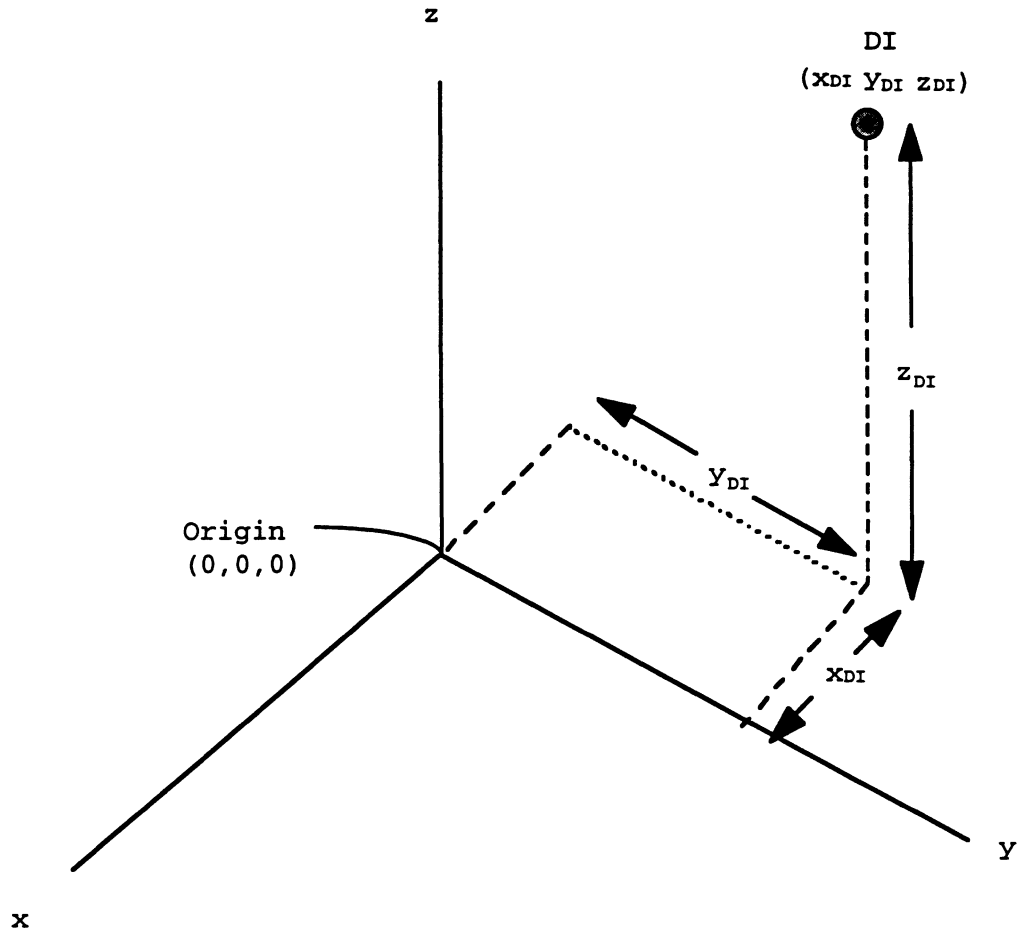
Figure 3.2

Control station "DI" in a geocentric cartesian coordinate system

The GPS user segment includes all the users of the GPS system, along with their hardware and software. Global Positioning System receivers are used to receive the microwave signals from the satellites.

19

3.1.2 Point Positioning

Point positioning in GPS navigation is a low-accuracy real-time or post-processing method of obtaining geocentric positions for the moving user (vessel) receiver. For a 3-D position fix, the requirement is that at least four satellites be visible at the vessel receiver. Figure 3.3 shows the minimum of four measurements needed for 3-D point positioning. The ρ_k^p, p=1,2,3,4 terms are the true geometric ranges from satellite p to receiver k at a given epoch of receiver time.

In practice, due to several error sources, it is **not possible** to measure the true geometric ranges ρ_k^p. What is actually measured is a biased range called a **pseudorange:** $P_k^p(t_k)$, p=1,2,3,...n. t_k is the nominal reception time of the satellite signal in the receiver time frame. To measure the pseudorange, the receiver and satellites both generate the same pseudorandom code. The receiver receives a signal from the satellite at a given instant of receiver time. The receiver code is then shifted in time to match the satellite code. This time offset between the satellite and receiver codes is nominally equal to the **travel time** of the signal from the satellite to the receiver. The measured time offset is converted into the pseudorange using the va-
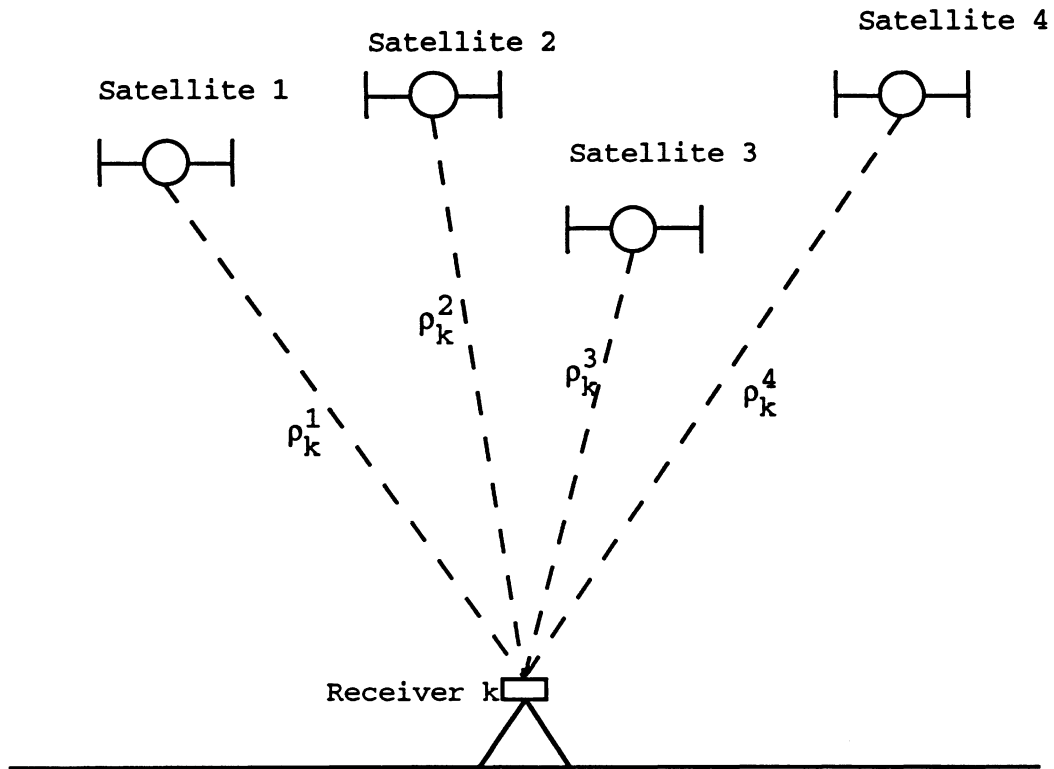
Figure 3.3

Minimum measurements for 3-D point position
(after Leick [1995, p. 248]).

ccuum speed of light c according to the following equation:

$$P_k^p(t_k) = (t_k - t^p)c, \tag{3.1}$$

where t^p is the nominal instant of signal emission in the satellite time frame, and t_k is the nominal instant of signal reception in the receiver time frame.

The receiver and satellite times are related to true time (GPS time, for example) by the following set of equations:

$$t_{r,k} = t_k + dt_k, \qquad\qquad (3.2)$$

$$t_r^P = t^P + dt^P, \qquad\qquad (3.3)$$

where the subscript "r" indicates true time; dt_k is the unknown offset in the receiver clock; dt^P is the unknown offset in satellite clock.

The pseudorange equation, with general epoch "t" is:

$$P_k^P(t) = \rho_k^P(t) - c\left[1 - \frac{\dot{\rho}_k^P(t)}{c}\right]dt_k + cdt^P + I_{k,P}^{P}(t) + $$

$$+ T_k^P(t) + d_{k,P}(t) + d_{k,P}^{P}(t) + d_P^P(t) + \varepsilon_P \qquad (3.4)$$

where $\rho_k^P(t) = \sqrt{(x^P - x_k)^2 + (y^P - y_k)^2 + (z^P - z_k)^2}$ is the estimated true geometric distance that the signal traveled. It contains **the unknown receiver coordinates** $\mathbf{x_k}$, $\mathbf{y_k}$, $\mathbf{z_k}$ (metres); $\dot{\rho}_k^P(t)$ is the rate of change of the estimated true geometric range; c is the vacuum speed of light; dt_k is the unknown offset from receiver time to true time; dt^P is the unknown offset from satellite time to true time; $I_{k,P}^{P}(t)$ is the unknown signal delay due to the ionosphere (metres); $T_k^P(t)$ is the unknown signal delay caused by the troposphere (metres); $d_{k,P}(t)$ is the unknown receiver hardware delay (metres); $d_{k,P}^{P}(t)$ is the unknown multipath at the receiver (metres); $d_P^P(t)$ is the unknown satellite

22

hardware delay (metres); ε_p is the unknown pseudorange measurement noise (metres).

For a 3-D point position, at **least four** simultaneous equations (one for each pseudorange) are formed using equation (3.4) [Leick, 1995]. All error terms except the receiver clock error dt_k are dropped, because all errors other than dt_k are dominated by the SA error [Langley, 1997]. It is not practical to try and estimate the smaller errors when the larger SA effect **cannot** be modeled. A least-squares solution is possible if there are more than four satellites visible -- i.e. p > 4.

3.1.3 Carrier Phase Observables

At time "t", when a receiver first locks on to the carrier phase signal from a satellite, the fractional difference in phase between a reference sine wave in the receiver and the received satellite signal is measured. This measured fraction can range from 0 cycles to 2π cycles. Figure 3.4 shows a fractional value of $\pi/4$ (90 degrees).

The **carrier phase observable** $\varphi_k^p(t)$ for receiver k and satellite p represents the **accumulated** measured carrier phase since the receiver initially locked on to satellite p. The general epoch "t" is used to avoid confusion in later developments of the carrier phase equa-
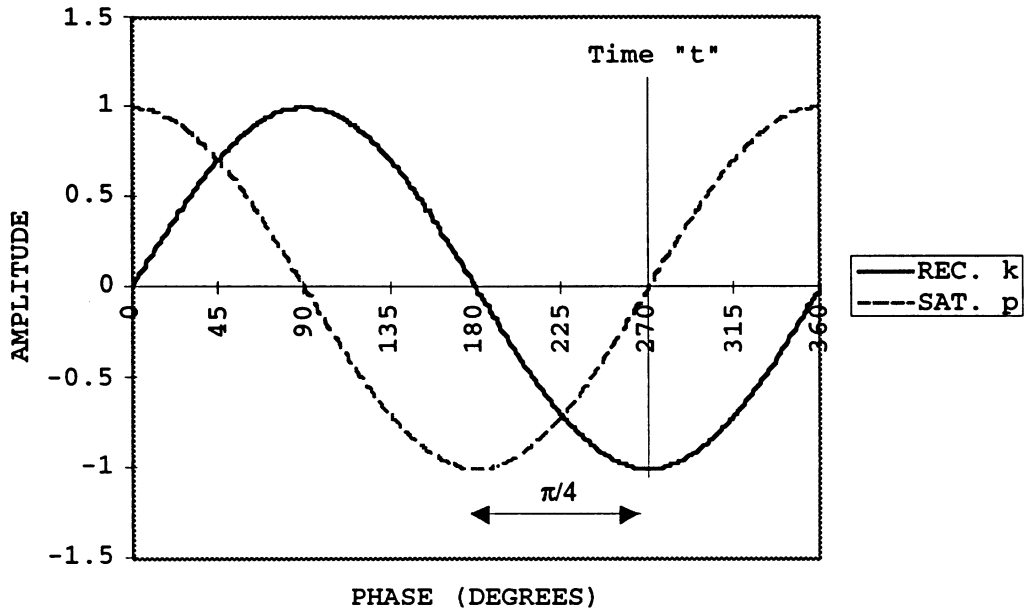
Figure 3.4

Fractional carrier phase difference at initial lock-on

tions. The carrier phase equation for a vacuum at epoch "t" is, with all terms in cycles [Leick, 1995]:

$$\varphi_k^p(t) = \varphi_k(t) - \varphi^p(t) + N_k^p(1) - \frac{f}{c}I_{k,\varphi}^p(t) + \frac{f}{c}T_k^p(t) +$$
$$+d_{k,\varphi}(t) + d_{k,\varphi}^p(t) + d_{\varphi}^p(t) + \varepsilon_{\varphi} \qquad , \qquad (3.5)$$

where $\varphi_k^p(t)$ is the carrier phase observable; $\varphi_k(t)$ is the observed reference phase for the receiver k; $\varphi^p(t)$ is the received satellite phase; $N_k^p(1)$ is the initial arbitrary counter setting of the receiver tracking register at the instant of phase lock on satellite p; $-\frac{f}{c}I_{k,\varphi}^p(t)$ is the signal advance due to the ionosphere; $\frac{f}{c}T_k^p(t)$ is the signal

24

delay due to the troposphere; $d_{k,\varphi}(t)$ is the receiver hardware delay; $d_{k,\varphi}^p(t)$ is the multipath; $d_\varphi^p(t)$ is the satellite hardware delay; ε_φ is the noise on the carrier phase measurement.

Note that the "φ" subscript is used to indicate quantities whose values are unique to phase observations.

Every time the measured phase difference $\varphi_k(t)-\varphi^p(t)$ increases or decreases by one cycle, the carrier phase observable $\varphi_k^p(t)$ increases or decreases by one count (cycle) correspondingly. Leick [1995] uses an excellent example to illustrate $\varphi_k^p(t)$. Imagine that the receiver and satellite are stationary on two survey monuments. Also assume that the measured phase difference at the receiver is zero at the instant of initial lock-on. Now, if the receiver moves one wavelength closer to the satellite in one second, the carrier phase observable $\varphi_k^p(t)$ will **increase** by **one cycle**. It is immaterial whether the satellite moves toward the receiver or vice versa. Table 3.1 shows a simulated example of L1 carrier phase observables for **10** epochs, **one** receiver, and **two** satellites. Note that L1 has a wavelength of about 0.1903 metres.

With simplification, Leick [1995] arrives at the scaled form of the undifferenced carrier phase equation, with all units in **metres**:

Table 3.1

Sample carrier phase observables

Receiver Epoch t (Seconds)	Distance to Satellite 1 (Metres)	$\varphi_1^1(t)$ (Counts)	Distance to Satellite 2 (Metres)	$\varphi_1^2(t)$ (Counts)
1	21000019.03	0.00	20000000.00	0.00
2	21000000.00	100.00	20000019.03	-100.00
3	20999980.97	200.00	20000038.06	-200.00
4	20999961.94	300.00	20000057.09	-300.00
5	20999942.91	400.00	20000076.12	-400.00
6	20999923.88	500.00	20000095.15	-500.00
7	20999904.85	600.00	20000114.18	-600.00
8	20999885.82	700.00	20000133.21	-700.00
9	20999866.79	800.00	20000152.23	-800.00
10	20999847.77	900.00	20000171.26	-900.00

$$\Phi_k^p(t) = \rho_k^p(t) - cdt_k + cdt^p + \frac{c}{f}N_k^p(1) -$$

$$I_{k,P}^{\ p}(t) + T_k^p(t) + d_{k,\Phi}(t) + d_{k,\Phi}^{\ p}(t) + \qquad\qquad (3.6)$$

$$+ d_\Phi^p(t) + \varepsilon_\Phi$$

where $\rho_k^p(t)$ is the geometric range at time t; $-cdt_k$ is the error due to receiver clock bias; $+cdt^p$ is the error due to satellite clock bias; $-I_{k,P}^{\ p}(t)$ is the signal advance due to the ionosphere; all other terms are simply scaled values of the terms in equation (3.5).

Note that the "Φ" symbol indicates that we are dealing with the **scaled** carrier phase equations. Also, assuming the same carrier frequency, $\text{ABS}\left(-I_{k,P}^{\ p}(t)\right)$ from equation

(3.6) $= I_{k,P}^{p}(t)$ from equation (3.4) since the ionosphere advances the code and delays the carrier. Absolute value is given by ABS.

3.1.4 Differencing Methods in Relative Positioning

The goal of relative positioning in GPS navigation is to accurately find the **difference in coordinates** from a fixed base station k (usually a stationary point on land) to the moving remote receiver m. A **baseline** is a straight line from the base station to the remote in a cartesian coordinate frame. For a 3-D position, the desired components of this baseline are the Δx Δy Δz baseline components in the Cartesian coordinate frame. Four satellites are a required minimum. Figure 3.5 shows a typical baseline.

In relative positioning, it is possible to use pseudorange measurements, carrier phase measurements, or a combination of the two (as is done in OTF DGPS). Relative positioning is more accurate than point positioning for two reasons: (1) cancellation/minimization of some of the point positioning errors in equation (3.4), and (2) the carrier phase signal can be used, resulting in solutions that are less noisy than pseudorange solutions.

3.1.4.1 Single and double differenced pseudoranges

Mathematical techniques called single and double differencing are used on the measured pseudoranges. Let us start with **single differences,** also known as **between**
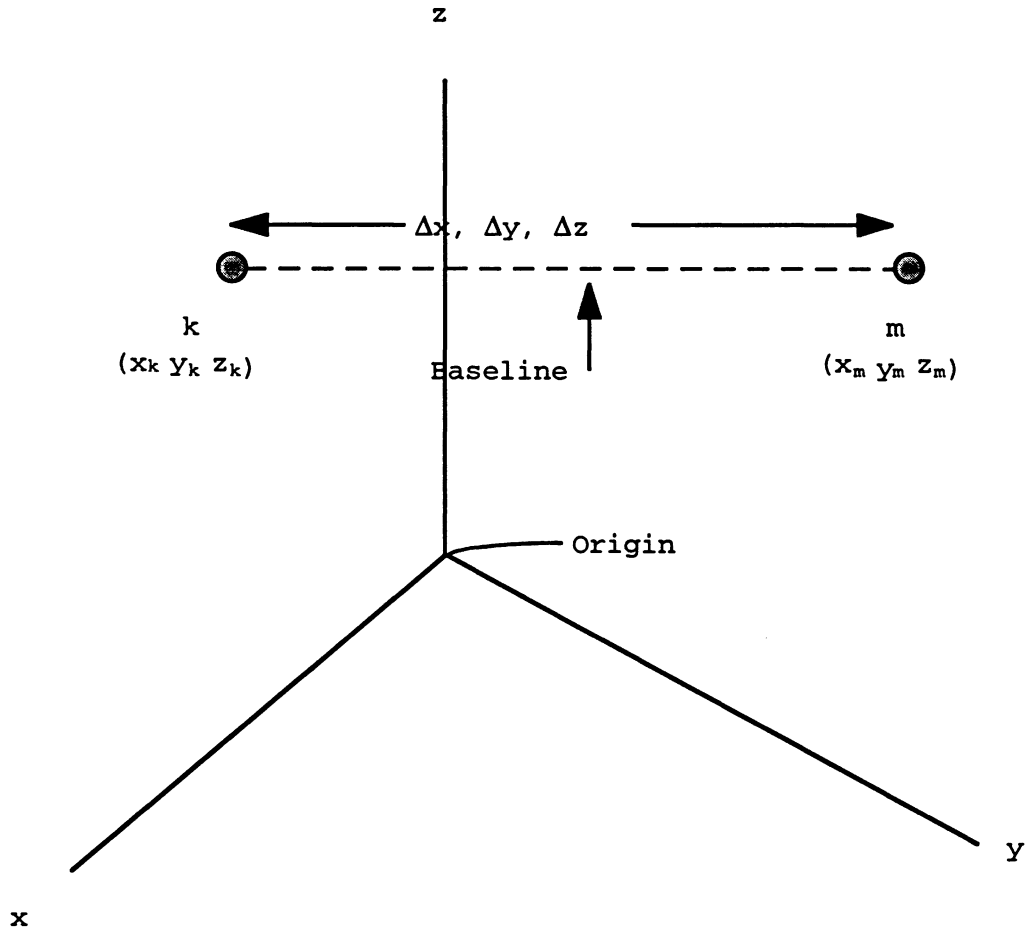
Figure 3.5

Typical baseline in relative positioning

receiver single differences. A single difference uses two receivers and one satellite. Figure 3.6 illustrates the

measurements needed for one single difference. The single difference is the scalar difference of the two pseudoranges. With **five** satellites and **two** receivers, there are **five** single differences. The single difference eliminates the satellite clock error, which is part of SA, and greatly reduces the ionospheric and tropospheric errors if the baseline is short. The equation (in metres) for a single differenced pseudorange $P_{km}^{p}(t)$ with **base receiver k, remote receiver m**, and **satellite p** is:

$$P_{km}^{p}(t) = \rho_{km}^{p}(t) + cdt_{km} + I_{km,P}^{p}(t) + T_{km,P}^{p}(t) + d_{km,P}(t) +$$
$$+d_{km,P}^{p}(t) + \varepsilon_{km,P}^{p}(t)$$

(3.7)

Satellite p
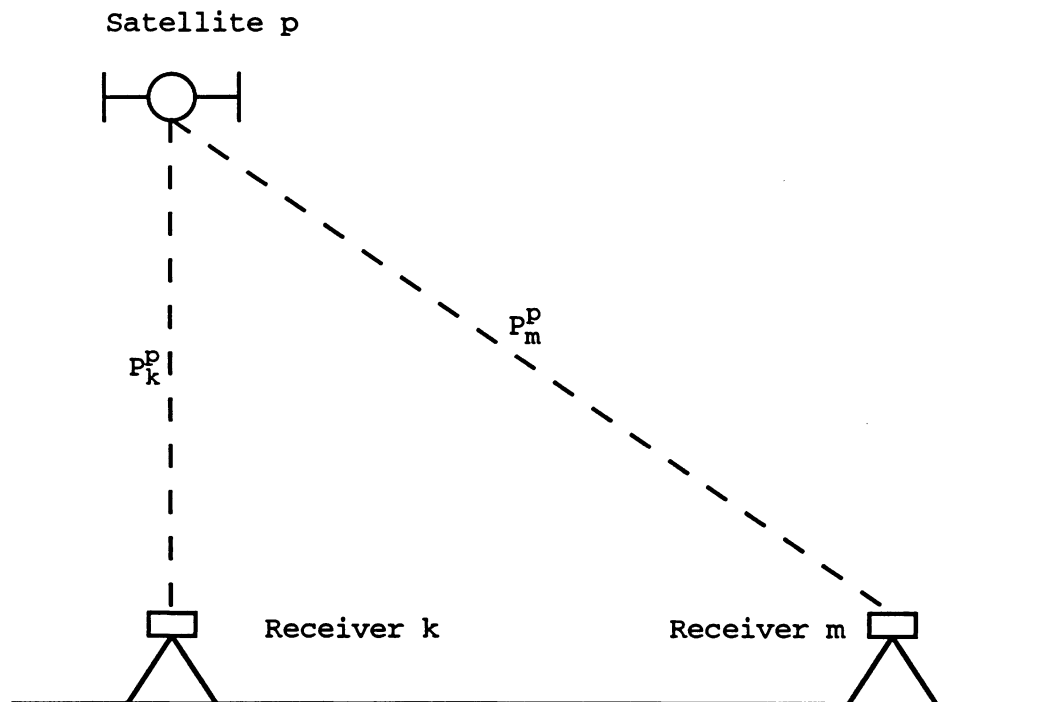
Figure 3.6

Required observations for one single differenced
pseudorange observable
(after Leick [1995, p. 260]).

where $\rho_{km}^p(t)$ is the single difference of the two geometric ranges; cdt_{km} is the unknown single differenced receiver clock error; $I_{km,P}^p(t)$ is the unknown single differenced ionospheric delay; $T_{km,P}^p(t)$ is the unknown single differenced tropospheric delay; $d_{km,P}(t)$ is the unknown single differenced receiver hardware delay; $d_{km,P}^p(t)$ is the unknown single differenced multipath; $\varepsilon_{km,P}^p(t) = \sqrt{\varepsilon_{kP}^2(t) + \varepsilon_{mP}^2(t)}$ is the single differenced pseudorange measurement noise, with $\varepsilon_{kP}^2(t)$ being the squared pseudorange measurement noise for receiver k, and $\varepsilon_{mP}^2(t)$ being the squared pseudorange measurement noise for receiver m.

The single difference has the following effects on pseudorange point positioning errors:

(1)   Eliminates satellite clock offset dt^p, along with the satellite hardware delay $d_P^p(t)$ (if it is constant in time).

(2)   Sharply reduces ionospheric and tropospheric errors on **short** baselines.

Significant errors remain in remote station coordinates obtained from the single difference observable. Therefore, it is better to use double differences.

A **double difference** is the scalar difference of two single differences. Figure 3.7 shows the observations nec-

30
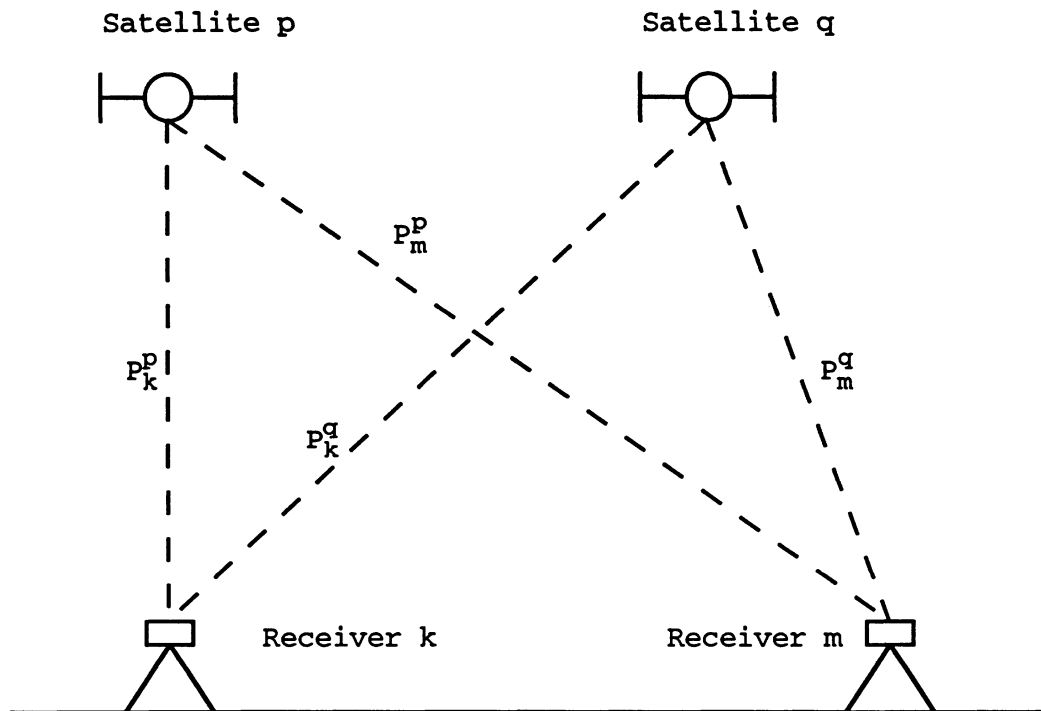
Figure 3.7

Required observations for one double differenced
pseudorange observable
(after Leick [1995, p. 262]).

essary for one double differenced pseudorange. Thus, for **five satellites** and **two receivers**, there is the possibility of **four** double differences. Table 3.2 shows some simulated single and double differenced pseudorange measurements for five satellites and two receivers. The double difference is free of the satellite clock errors and receiver clock errors. The effects of the ionosphere and troposphere are greatly reduced if the baseline is short. The equation for the double differenced pseudorange $P_{km}^{pq}(t)$ with **base receiver k, remote receiver m,** and

satellites p and q is:

$$P_{km}^{pq}(t) = \rho_{km}^{pq}(t) + \varepsilon_{km,P}^{pq}(t),$$ (3.8)

where $\rho_{km}^{pq}(t)$ represents the double differenced geometric ranges (metres); $\rho_{km}^{pq}(t) = (\rho_k^p(t) - \rho_m^p(t)) - (\rho_k^q(t) - \rho_m^q(t))$; $\varepsilon_{km,P}^{pq}(t) \cong 2\varepsilon_P(t)$ is the double differenced pseudorange measurement noise. Least squares can be applied to equation (3.8) to get the **remote receiver coordinates** x_m, y_m, z_m.

In equation (3.8) all the error terms that were originally present in equation (3.4), except for the double differenced pseudorange measurement noise $\varepsilon_{km,P}^{pq}(t)$, have been dropped, implying the following assumptions:

Table 3.2

Simulated single and double differenced pseudoranges

Satellite	Pseudo-ranges	Pseudo-ranges	Single	Double
	Receiver 1	Receiver 2	Differences	Differences
	(Kilom-etres)	(Kilom-etres)	(Kilom-etres)	(Kilom-etres)
1	$P_1^1 = 20000$	$P_2^1 = 20010$	$P_{12}^1 = 10$	-----------
2	$P_1^2 = 21000$	$P_2^2 = 20990$	$P_{12}^2 = -10$	$P_{12}^{12} = -20$
3	$P_1^3 = 19500$	$P_2^3 = 19501$	$P_{12}^3 = 1$	$P_{12}^{13} = -9$
4	$P_1^4 = 22000$	$P_2^4 = 22002$	$P_{12}^4 = 2$	$P_{12}^{14} = -8$
5	$P_1^5 = 21900$	$P_2^5 = 21905$	$P_{12}^5 = 5$	$P_{12}^{15} = -5$

(1) All satellite and receiver clock errors have been

canceled out in the differencing process.

(2)   The ionospheric error term has been canceled or greatly reduced in the differencing process.

(3)   The tropospheric error has either been canceled or greatly reduced in the differencing process or modeled out of the observed pseudoranges.

(4)   The multipath error is not present.

(5)   The receiver and satellite hardware delays are constant, and therefore cancel out in the differencing process.

3.1.4.2 Single differenced carrier phase observable

The between-receiver single differenced carrier phase observable (or single difference observable) is given by $\varphi_{km}^{p}(t)$. Two receivers must observe the same satellite at the same nominal time. **Five** satellites and **two** receivers give **five** single differences. The equation (in **cycles**) [Leick, 1995]:

$$\varphi_{km}^{p}(t) \equiv \varphi_{k}^{p}(t) - \varphi_{m}^{p}(t)$$

$$= \frac{f}{c}[\rho_{k}^{p}(t) - \rho_{m}^{p}(t)] + \frac{a^{p}}{c}[\rho_{k}^{p}(t) - \rho_{m}^{p}(t)]$$

$$+ \frac{f}{c}[\dot{\rho}_{k}^{p}(t)dt_{k} - \dot{\rho}_{m}^{p}(t)dt_{m}] + N_{km}^{p}(1)$$

$$- f(dt_{k} - dt_{m}) + I_{km,\varphi}^{p}(t) + \frac{f}{c}T_{km}^{p}(t)$$

$$+ d_{km,\varphi}(t) + d_{km,\varphi}^{p}(t) + \varepsilon_{km,\varphi}^{p}$$

(3.9)

33

where $\dot{\rho}_k^p$ and $\dot{\rho}_m^p$ are rates of change of geometric range with time; a^p is satellite frequency offset; $N_{km}^p(1) = N_k^p(1) - N_m^p(1)$ is the unknown difference in initial integer ambiguities; $I_{km,\varphi}^p(t) = I_{k,\varphi}^p(t) - I_{m,\varphi}^p(t)$ is the unknown difference in ionospheric advance; $T_{km}^p(t) = T_k^p(t) - T_m^p(t)$ is the unknown difference in tropospheric delay; $d_{km,\varphi}(t) = d_{k,\varphi}(t) - d_{m,\varphi}(t)$ is the unknown difference in receiver hardware delay; $d_{km,\varphi}^p(t) = d_{k,\varphi}^p(t) - d_{m,\varphi}^p(t)$ is the unknown difference in multipath; $\varepsilon_{km,\varphi}^p = \sqrt{\left(\varepsilon_{k,\varphi}^p\right)^2 + \left(\varepsilon_{m,\varphi}^p\right)^2}$ is the unknown difference in carrier phase noise, with $\left(\varepsilon_{k,\varphi}^p\right)^2$ being the squared carrier phase noise for receiver k and satellite p; similarly, $\left(\varepsilon_{m,\varphi}^p\right)^2$ = the squared carrier phase noise for receiver m and satellite p.

3.1.4.3 Double differenced carrier phases

The carrier phase double differenced observable $\varphi_{km}^{pq}(t)$ is similar to the pseudorange double differenced observable in that it requires two receivers k and m observing two satellites p and q at the same nominal time t. As with the double differenced pseudorange, **four** double differences can be formed from **five** satellites and **two** receivers. Table 3.3 shows some simulated single and double differenced carrier phase observables for two satellites and two

34

receivers. The double difference equation, with all units in **cycles** is [Leick, 1995]:

$$\varphi_{km}^{pq}(t) \equiv \varphi_{km}^{p}(t) - \varphi_{km}^{q}(t)$$

$$= \frac{a^{p}}{c}[\rho_{k}^{p}(t) - \rho_{m}^{p}(t)] - \frac{a^{q}}{c}[\rho_{k}^{q}(t) - \rho_{m}^{q}(t)] +$$

$$+ \frac{f}{c}[\rho_{k}^{p}(t) - \rho_{m}^{p}(t)] - \frac{f}{c}[\rho_{k}^{q}(t) - \rho_{m}^{q}(t)]$$

$$+ \frac{f}{c}[\dot{\rho}_{k}^{p}(t)dt_{k} - \dot{\rho}_{m}^{p}(t)dt_{m}] - \frac{f}{c}[\dot{\rho}_{k}^{q}(t)dt_{k} - \dot{\rho}_{m}^{q}(t)dt_{m}]$$

$$+ N_{km}^{pq}(1) + I_{km,\varphi}^{pq}(t) + \frac{f}{c}T_{km}^{pq}(t) + d_{km,\varphi}^{pq}(t) + \varepsilon_{km,\varphi}^{pq}(t)$$

(3.10)

where a^{p} and a^{q} are the frequency offsets for satellites p and q respectively; $N_{km}^{pq}(1) = N_{km}^{p}(1) - N_{km}^{q}(1)$ are the unknown double differenced initial integer ambiguities; $I_{km,\varphi}^{pq}(t) = I_{km,\varphi}^{p}(t) - I_{km,\varphi}^{q}(t)$ are the unknown double differenced ionospheric advances; $T_{km}^{pq}(t) = T_{km}^{p}(t) - T_{km}^{q}(t)$ are the unknown double differenced tropospheric delays; $d_{km,\varphi}^{pq}(t) = d_{km,\varphi}^{p}(t) - d_{km,\varphi}^{q}(t)$ is the unknown double differenced multipath; $\varepsilon_{km,\varphi}^{pq}(t) \cong 2\varepsilon_{\varphi}$ is the double differenced carrier phase noise.

3.2 Preliminary Software Investigation

Euler, Hein, and Landau [1992] performed some investigations for the U.S. Army Topographic Engineering Center (USATEC). They indicate that centimetre - level carrier phase positioning is possible in real-time. In particular, they present an algorithm and software for OTF

35

DGPS ambiguity resolution using single or dual frequency data.

Table 3.3

Single and double differenced carrier phase observables

Sat-ellite Number	Carrier Phase Observable Receiver 1 (Counts)	Carrier Phase Observable Receiver 2 (Counts)	Single Differenced Observable (Counts)	Double Differenced Observable (Counts)
1	$\varphi_1^1(t)=900.$	$\varphi_2^1(t)=-900$	$\varphi_{12}^1(t)-1800$	- - - - - - - - - - - - -
2	$\varphi_1^2(t)=150.$	$\varphi_2^2(t)=-50.$	$\varphi_{12}^2(t)-200.$	$\varphi_{12}^{12}(t)=+1600.$

Euler, Hein, and Landau [1992] discuss several key points. They concentrate on the use of the civilian C/A code. They state that it may be possible to reduce the C/A code noise level to +/- 0.10 metres, but multipath effects can commonly introduce errors of 2-3 metres. This is the justification they state for using the carrier phase differencing vs code differencing. As stated by Wells [1995b] C/A code noise has actually been brought down to around +/- 0.040 metres for the Ashtech Z12 system.

Euler, Hein, and Landau [1992] state several facts about their technique for OTF DGPS. It involves first finding a position based on the differential code solution.

The true vessel position lies within a specific error region located around the initial position. This is also known as a **search space.** The number of possible solutions inside the region depends on the number of satellites available, and on the size of the error region. For a dual-frequency system, there is the possibility of introducing the wide-lane observable, which is the difference between the L1 and L2 carriers. The number of possible solutions in the error region is drastically reduced with the use of the wide-laning technique. Following Abidin [1994], we see that this reduction occurs because the wide-lane observable has a longer wavelength than either L1 or L2 (about 0.86 metres). This means that for a fixed search space size, there are less integer ambiguity combinations that can be contained within it.

Euler, Hein, and Landau [1992] mention three methods for determining the correct integer ambiguity:

(1)   The method of Remondi [1991], which uses a combination of code and carrier, and smoothes the data before and after the epoch of interest, producing approximate values for the ambiguities. Remondi then applies a technique called the "ambiguity function method", based on an exponential function, which must be maximized to find the optimal solution. The method applies for single and dual frequencies [Euler, Hein, and Landau, 1992].

(2)   The method used by Hatch [1989]. This technique

        is based on a least-squares method together with

        a search strategy. Using four satellites,

        ambiguity combinations are chosen from a search

        window. Then, redundant satellites are checked

        for their integer nature. Using a predefined

        threshold, Hatch [1989] accepts or rejects

        combinations leading to the best solution. This

        approach has the disadvantage of not testing all

        the ambiguity combinations [Euler, Hein, and

        Landau, 1992].

(3)   The method used by Euler, Hein, and Landau

        [1992]. Here, all ambiguity combinations are

        checked, and a factorization method is used to

        reduce the computational load. Their method is

        well suited to real-time usage, as the algorithms

        can handle several thousands of combinations in

        less than half a second, using a 386 PC [Euler,

        Hein, and Landau, 1992].

Many more techniques for OTF DGPS have developed since
1992. See for example Abidin [1994].

        Euler, Hein, and Landau [1992] make several
recommendations for their algorithm and software. The
recommendations are:

(1)   Increase reliability of the software.

(2)   Refine test criteria for internal ambiguity

combination testing.

(3)   Implement a technique to instantaneously provide
       the correct ambiguity combination for an upcoming
       satellite.

(4)   Use the dual-frequency data with an ionospheric
       model for longer baselines (they had no trouble
       with ionospheric effects on a 4.7 kilometre
       baseline, but significant error appeared for a 26
       kilometre baseline).

(5)   Provide real time accuracy and reliability
       estimates.

(6)   Use the Kalman filter prediction to stabilize the
       ambiguity resolution.

3.3 OTF DGPS Algorithm for USATEC OTF System

In Frodge et al [1994], a general description of the
OTF DGPS algorithm employed in the U.S. Army Corps of
Engineers real-time prototype OTF DGPS system was given.
This system was developed by John E. Chance and Associates
under contract with the U.S. Army Corps of Engineers. The
goal was to achieve an operational, real - time prototype
system from a previous post-processing version of the
system.

There are three steps in the algorithm:

(1)   A metre-level (or better) accuracy first guess is

generated from a differential code solution.

(2)   A search region is formed.

(3)   Grid candidates within the search region are evaluated, and the best candidate selected.

3.3.1 Meter-Level Solution

Least squares estimation can be applied to the double-differenced pseudorange equation (3.8) to obtain geocentric coordinates for the remote receiver m. It is not clear whether Frodge et al [1994] have applied a dual-frequency ionospheric correction to the observed carrier phases. The accuracy of the double-differenced solution is somewhat limited due to the noisiness of the pseudorange measurements.

Leick [1995] and Frodge et al [1994] state that better results can be obtained by using a carrier phase smoothed range equation. The first step is to modify equation (3.8) to obtain the following in metres:

$$\lambda[\varphi_{km}^{pq}(t) + N_{km}^{pq}(t)] = \rho_{km}^{pq}(t) + \lambda[\varepsilon_{km,\varphi}^{pq}], \qquad (3.11)$$

where λ is the wavelength of the carrier signal; $\varphi_{km}^{pq}(t)$ is the double differenced carrier phase observable; $N_{km}^{pq}(t)$ is the unknown double differenced integer ambiguity; $\rho_{km}^{pq}(t)$ are the double differenced geometric ranges; $\lambda[\varepsilon_{km,\varphi}^{pq}] \cong \lambda[2\varepsilon_{\varphi}]$ is the double differenced carrier phase

noise.

A time difference of equation (3.8) is then taken, and $\rho_{km}^{pq}(t)$ from equation (3.11) is substituted into the time difference, yielding the carrier phase smoothed range equation with all units in metres:

$$[P_{km}^{pq}(1)]_i = P_{km}^{pq}(t_i) - \lambda[\varphi_{km}^{pq}(t_i) - \varphi_{km}^{pq}(1)] + \varepsilon_{\varphi P}(t_i) \quad , \qquad (3.12)$$

where $[P_{km}^{pq}(1)]_i$, $i=1,2,...r$ is the rth determination of the double differenced pseudorange at initial epoch 1, based on measurements from the later epoch t_i; $\varepsilon_{\varphi P}(t_i)$ is the noise on the smoothed double differenced pseudorange solution.

Given **five** satellites, **two** receivers, and **10** epochs, **r** would be equal to **10**, with a total of **40** double differenced pseudorange observables.

We then have to get an averaged estimate for the double differenced pseudorange at initial epoch 1 from:

$$[P_{km}^{pq}(1)]_{AVG} = \frac{1}{r} \sum_{i=1}^{r} [P_{km}^{pq}(1)]_i \qquad (3.13)$$

where $[P_{km}^{pq}(1)]_{AVG}$ is the average of the r initial double differenced pseudorange value estimates.

Equation (3.13) simulates having a large number of $P_{km}^{pq}(1)$

measurements at the initial epoch one. A large series of these measurements are averaged, and the $[P_{km}^{pq}(1)]_{AVG}$ used to replace $P_{km}^{pq}(t)$ in equation (3.8). Least squares is then used to obtain the **smoothed geocentric Cartesian coordinates** x_{sm}, y_{sm}, z_{sm} of the remote receiver m at initial epoch 1.

3.3.2 Search Region

Leick [1995] states that the search region is formed around the smoothed initial estimate x_{sm}, y_{sm}, z_{sm} for the remote receiver position obtained in the previous section 3.3.1. The smoothed initial estimate is used because the search region must contain the true position. The more accurate the initial position is, the smaller the search region is, resulting in quicker ambiguity resolution.

The simplest search region is a cube (see Figure 3.8), with sides equal to multiples of the standard deviation of the smoothed solution for x_{sm}, y_{sm}, z_{sm} from section 3.3.1. The region is centered on the initial smoothed receiver code position for receiver m. In reality, the cube is a very inefficient search region -- ellipsoids are much better [Abidin et al, 1992]. Although it is necessary to have at **least five** satellites for OTF DGPS, four will be used in some of the following examples for simplicity.

If there is sufficient geometric strength in the double differenced solution, and the ambiguity search routines are

True position
of station m

Initial approximate
position for station m

Search volume
for station m at epoch t

Trial solution

Receiver k
(position
known)
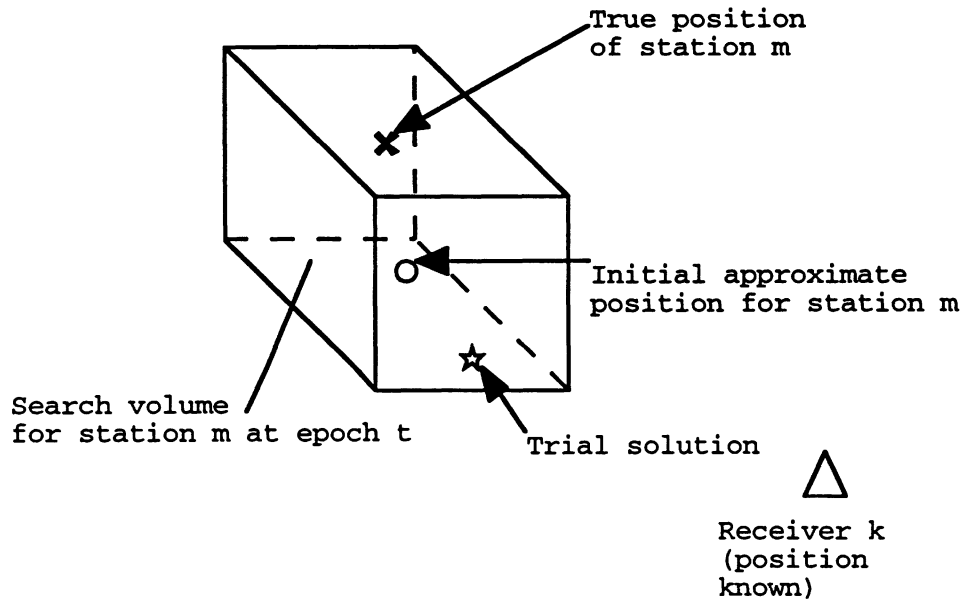
Figure 3.8

Sample OTF DGPS search region
(after Leick [1995, p. 385]).

fast enough (i.e. small search volume, high speed computer, etc.), it is possible to find the position of receiver m independently at each epoch. Frodge et al [1994] mention that real-valued estimates $(N_{km}^{pq}(1))_R$ of the double differenced integer ambiguities are computed at the initial smoothed code position from a modified version of equation (3.8). This modified version is:

$$(N_{km}^{pq}(1))_R = \frac{f}{c}[P_{km}^{pq}(1)]_{AVG} - \varphi_{km}^{pq}(1) + \varepsilon_{km,\varphi}^{pq}.$$ (3.14)

These initial real-valued estimates are rounded to initial closest integer values $(N_{km}^{pq}(1))$, and placed into some form

43

of the double-differenced carrier phase equations (3.10) to obtain initial double differences DD1, DD2, DD3,...DDn for station m. An n-dimensional Cartesian coordinate system is constructed, and centered on the initial double differences for station m (see Figure 3.9). The dimension n of the system is equal to the number of double differences (three for a four-satellite constellation with two receivers). A **search grid** is formed in this system by intersecting three double-difference planes. Each intersection defines a point in the n-dimensional system.

3.3.3 Testing Grid Candidates

The final step in the OTF DGPS initialization process is the search for the best grid candidate. Frodge et al [1994] state that some form of the carrier phase equations is used to determine the integer ambiguities for a given test candidate. A modeled range ρ is computed along with a residual. The correct grid candidate will have low residuals, whereas incorrect candidates will not.

In terms of statistical acceptance criteria, Frodge et al [1994] state that the statistical norm they have chosen is based on a mean of the absolute values of the computed real-valued double difference ambiguities from their rounded integer values. The appropriate equation is:

$$\frac{1}{n} \sum_{q=2}^{n+1} \left| (N_{km}^{pq}(t))_R - N_{km}^{pq}(t) \right| \quad , \qquad (3.15)$$

where m=2 and k=p=1 (for one base station and one remote).

ΔDD3

(DD1,DD2,DD3)

ΔDD1 ΔDD2
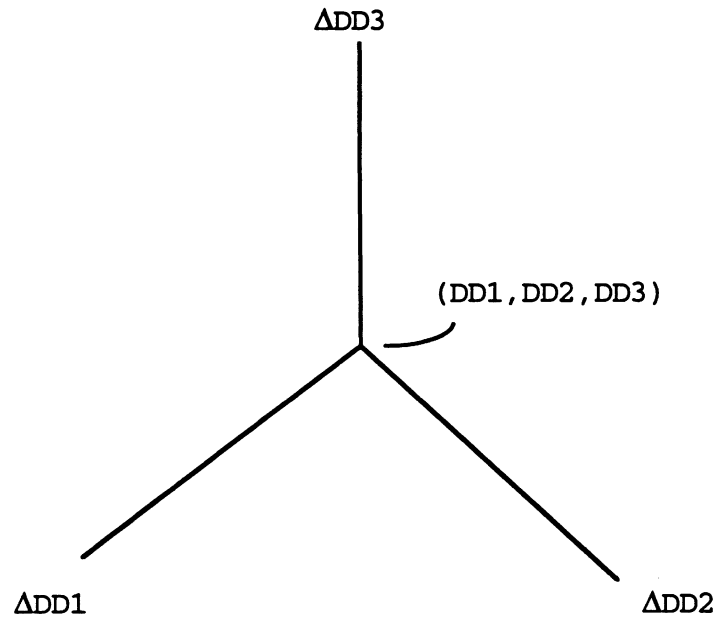
Figure 3.9

Cartesian coordinate system for three double differences.

The OTF DGPS ambiguity resolution is accepted if it gives at least three percent discrimination among the top candidates. This criterion yields roughly a 99 percent success rate of the real-time system ambiguity resolution. When a still higher level of certainty is required, 5 percent is used [Frodge et al 1994].

3.4 Recent Tests on Three OTF DGPS Systems

In this section, we summarize the results of testing that was performed for three OTF DGPS systems:

(1) The U.S. Army Corps of Engineers (USACE) real-time system, which uses the dual-frequency Trimble Geodesist SSE receiver [Frodge et al, 1993].

(2) The Ashtech L12 single frequency receiver, using the PRISM post-processing package.

(3) The Ashtech P-XII dual-frequency receivers [Lachapelle et al, 1993].

In Table 3.4 the difference column shows error estimates for the differences between the OTF DGPS elevation and the elevation obtained from the reference measurements. Sdev is the standard deviation of these differences. RMS is the root mean square error of these same differences.

3.5 Ashtech PNAV - PRISM OTF DGPS Package

The type of receivers which were used on the Miramichi River surveys are Ashtech Z12 receivers. As stated by Wells [1995b], they have the advantage of being dual frequency receivers, with about +/- 0.04 metres noise on the measured pseudoranges. If many satellites are available, very fast

46

ambiguity resolution is possible with these receivers (on the order of a few seconds).

The post-processing for the Miramichi River Z12 OTF DGPS data was done with the PRISM-PNAV software package. We shall discuss the basics of the PRISM-PNAV version 2.100P OTF DGPS algorithm as described by Langley and Komjathy [1994] in this section.

Table 3.4

Comparison of three OTF DGPS systems.

Receiver Type	Type of GPS Observation	Baseline Length (kilom-etres)	Type of Vertical Reference Observations	Difference (Metres)
Geodesist Trimble SSE receivers	Dual frequency	0.290 1.900	Spirit Level wat.lev.sens spirit level wat.lev.sens	0.019 (Sdev) 0.014 (Sdev) 0.015 (Sdev) 0.016 (Sdev)
Ashtech	Single frequency	<10	Predicted tides	0.014 (RMS) - 0.028 (RMS)
Ashtech P-XII	Dual frequency	<20	First order orthometric heights	0.060 (RMS)

PNAV is a sub-program which is located within the main PRISM software processing package. The PRISM-PNAV 2.100 P

OTF DGPS algorithm is designed for post-processing only. Later versions of the Z12 receiver have an OTF DGPS algorithm built into the receiver for real-time positioning [Ashtech, 1995]. The observed data can consist of single or dual frequency code and carrier phase observations. See Table 3.5 for the 1σ RMS accuracies available from PNAV, along with the expected length of time required to get these accuracies, once **continuous** carrier phase observations are available. PNAV uses a Kalman filter to compute predicted positions, compares these positions with positions derived from the data, and then computes the estimated positions with the covariance matrix of the predictions and the measurements.

Forward and backward processing means that for a given period of observed OTF DGPS data, PNAV calculates positions from the early end of the data series to the late end, and vice versa. This is helpful if lock on the satellites is lost at one point in the data. As an example, assume that a satellite blockage occurred at 12:00 PM GPS time. It could take five minutes to regain lock, as PNAV sorts out which satellites to use. Processing backward from the later end of the time series allows this interval of lost lock to be decreased, because good data exists on the later side of the blockage, without the complications introduced by loss of lock.

Several conditions must be present to ensure that the values in Table 3.5 are valid. They are, as given by

48

Ashtech [1994]:

Table 3.5

Achievable OTF DGPS accuracies with PNAV
(from Ashtech, 1994, p.7).

Data Type	Accuracy
C/A Code pseudorange, L1 carrier phase observations, float ambiguities	1-3 metres in the first 2-10 minutes, 0.1 - 1.0 metres thereafter. The best results (0.05 - 0.3 metres overall) can be achieved with forward and backward processing
Dual frequency P code + full wavelength carrier phase observations, fix ambiguities	0.5 to 2 metres in first 2-5 minutes, 0.01 to 0.1 metres when ambiguities are fixed

(1) PDOP (Position Dilution of Precision) < 4.

(2) At least five usable satellites in view.

(3) A minimum number of cycle slips due to obstructions.

(4) Separation (bsep) between the OTF DGPS base station and the remote OTF DGPS station < 10 kilometres.

(5) Low amount of multipath.

It should be noted that although no static

49

initialization or antenna swap needs to be performed during the collection of the PNAV data, there is a "settling down period". This is the time required for PNAV to converge to a solution, once **continuous** carrier phase observations are available. It is a function of several factors: (1) number of satellites observed, (2) PDOP, (3) baseline separation, (4) recording interval, and (5) type of data used. Ashtech [1994] states that for dual frequency observations, and fixed ambiguities, the settling time (tfix) is given by (note the dimensional in homogeneity!):

$$tfix(minutes) = [bsep(km) + rci(secs)]/2 \; , \qquad (3.16)$$

where rci is the recording interval in seconds.

Thus, for a 10 kilometre baseline separation, and a one second recording rate, tfix is equal to **5.5 minutes**. This would represent the expected worst case scenario in terms of baseline length for the Miramichi River OTF DGPS surveys.

Within PNAV, the GPS data is processed in three steps:

(1) Double differencing of the pseudoranges to obtain a differential solution for the receiver position. The integer ambiguities have **not** been resolved at this point. These approximate positions will be used as linearization points for a Taylor series expansion in the carrier

phase processing.

(2) Carrier phase observation processing to produce updated positions. The carrier phase data is checked at each update for cycle slips.

(3) The third and final step involves searching for an optimal carrier-phase ambiguity combination. An attempt is made to find an ambiguity - fixed solution.

In terms of quality assurance, the accuracy of the results is indicated by the 1σ root-mean - square (RMS) position error at each epoch. This position error is reliable if two conditions are met: (1) a Chi-square test on the weighted sum of the squared carrier phase residuals passes, and (2) the RMS of the carrier-phase residuals at any epoch is less than a predefined value.

Step three above will commence when the variances of the estimated integer ambiguities reaches a predefined threshold. When this threshold is reached, the integer ambiguity search is carried out around the estimated ambiguities.

CHAPTER 4

OVERVIEW OF HYDRAULIC MODELING OF WATER'S SURFACE ELEVATIONS

Section 4.1 begins with a simplified discussion on the factors influencing water's surface elevations in steady flow situations. Then, in section 4.2, some fairly recent techniques for modeling water's surface elevations in estuarine regions are briefly outlined, along with their strengths and weaknesses. The validity of combining such models with OTF DGPS water's surface elevation observations is briefly discussed.

4.1 Factors Influencing Water's Surface Elevations in Steady Flow Situations

The information in this section was obtained from Daugherty et al [1985]. Let us first assume:

(1) Open channel flow **without** the influence of tides or long time scale fluctuations in velocity and pressure (i.e. we are looking at **steady** flow).

(2) We are dealing with channels of rectangular cross section only. This is **uniform flow**.

The entire length of channel under consideration must be broken up into subsections which fit the criteria for rectangular cross section. See Figure 4.1 for the

quantities involved in **gradually varied flow**, which is similar to uniform flow, except that the channel cross section varies **gradually** within the subsection under consideration.
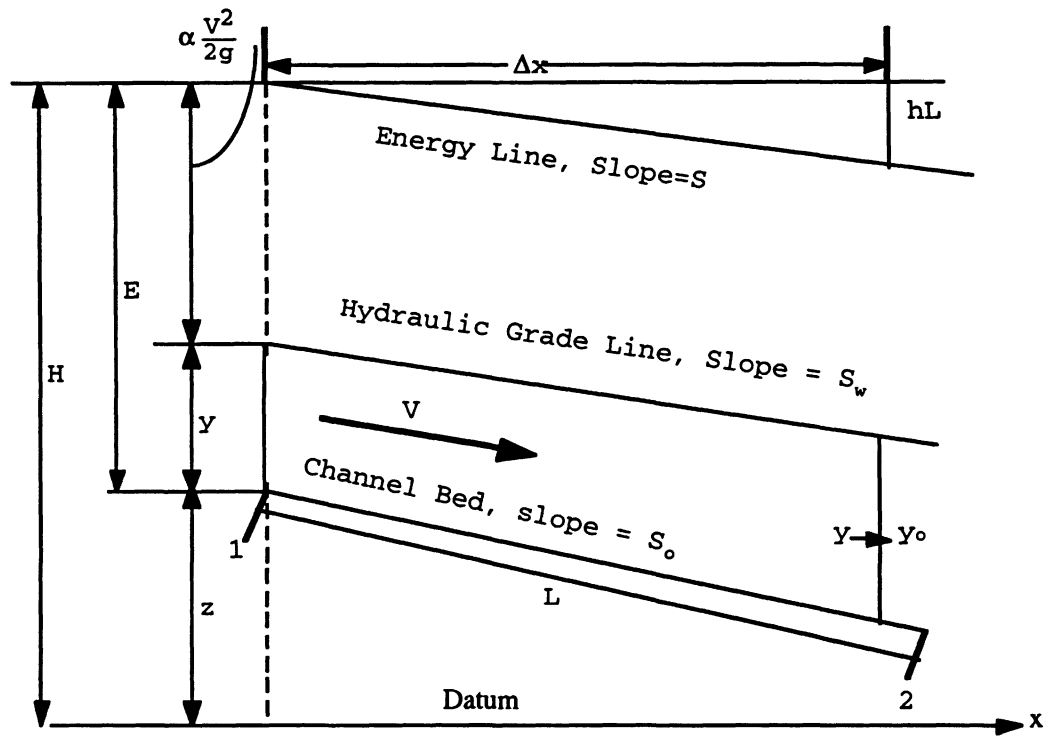
Figure 4.1

Quantities in gradually varied flow
(after Daugherty et al [1985, p. 369]).

where z is the height above an arbitrary datum (metres); y is the height of the hydraulic grade line (i.e. water's surface) above the channel bed (metres); $\propto V^2/2g$ is the kinetic energy head (metres), with V being the average velocity in the cross section (metres per second), and $\propto$ a

factor to account for non-uniform distribution of velocities in the cross section (usually assumed to have a value of one for **low-accuracy** applications), and g the acceleration of gravity (metres per second); E is the specific energy, equal to $y + \propto V^2/2g$ (metres); H is the total energy of an elementary particle of liquid above datum (metres); L is the slope length of the channel subsection in question (metres); S_O is the slope of the channel bed; S_w is the **slope of the water's surface;** S is the slope of the energy line; Δx is the horizontal distance of the channel subsection in question (metres); y_O is the depth for uniform flow (metres); h_L is the head loss due to friction; 1 and 2 indicate channel subsections.

We can obtain the **slope S_w of the water's surface** from:

$$S_w = -\frac{dz}{dx} - \frac{dy}{dx} \tag{4.1}$$

where $S_o = \dfrac{dz}{dx}$ is the rate of change of the datum elevation z with respect to the datum distance x, and $\dfrac{dy}{dx}$ is the rate of change of water depth with respect to datum distance x.

Clearly, the accuracy of the water's surface slope S_w in gradually varied flow is influenced by:

(1)   The validity of assuming that the cross section
        is uniform in the subsection of channel being

54

considered.

(2) Accuracy in knowing the slope S, which in turn depends on the $\propto$ term and the average velocity V in the cross section.

(3) Knowledge of the bottom slope S_O.

(4) Knowledge of the depth y at the beginning of each subsection.

(5) Knowledge of the datum height z along the subsection.

Extensions to uniform channels of non-rectangular cross section can be made. In this situation, the channel is again broken up into sections, but the sections must fit the criteria for the shape of flow being considered.

A further extension can be made to channels with gradually varied or rapidly varied flow. Gradually varied flow means that the channel cross section varies gradually over the channel subsection being considered. Rapidly varied flow means that these changes occur rapidly.

4.2 Models for Representing Water's Surface Elevations in an Estuary

When **unsteady flow** is present, there are fluctuations in velocity and pressure that have large deviations from their mean value, and cover long time periods (for example diurnal and semi-diurnal tidal periods in the estuary, etc.).

The size and shape of the channel cross section must still be considered, as it was for steady flow. However, we should now consider several additional factors -- for example, atmospheric forcing, mean water level, and Coriolis acceleration. Tidal propagation in an estuary is thus governed by a group of differential equations. The number and complexity of these differential equations varies according to the type of hydraulic modeling being implemented. Essentially, the simplest type of model is the one-dimensional model. More accurate results are obtainable in complex tidal systems when the more complex two and three-dimensional models are applied. In sections 4.2.1 and 4.2.2, we use the results of Crean et al [1988] to illustrate the various types of models. Note that Willis [1995] has stated that several advances in hydraulic modeling have occurred since the late 1980's. However, the following descriptions should be sufficient to illustrate the basic model types.

4.2.1 One-Dimensional Model

Crean et al [1988] discuss the results of a 20 year project that looked at the tidal and estuarine characteristics of the waters between Vancouver Island, Canada, and the state of Washington, U.S.A. The survey area is shown in Figure 4.2.

Initially, a one-dimensional model was used to model the entire survey area. The basic differential equations
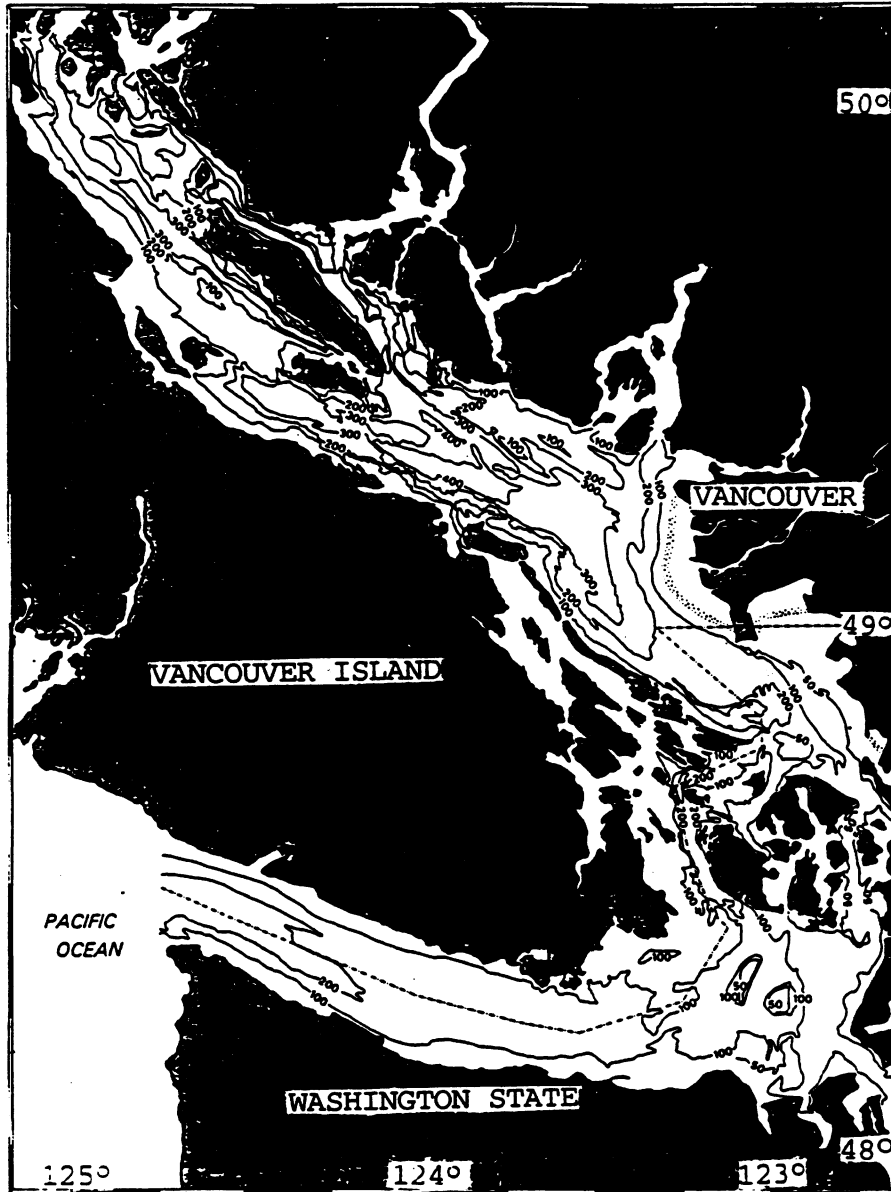
Figure 4.2

Crean et al survey area
(from Crean et al [1988, p. 3]).

for such a model are valid when two assumptions are true: (1) the velocity is essentially in one direction, and (2) the displacements of the water's surface are small with respect to the undisturbed depth. The equations are [Crean et al 1988]:

$$\frac{\partial(AV)}{\partial x} + b\frac{\partial\zeta}{\partial t} = 0,$$

(4.2)

$$\frac{\partial V}{\partial t} + V\frac{\partial V}{\partial x} + \frac{kV|V|}{h} + g\frac{\partial\zeta}{\partial x} = 0,$$

(4.3)

where x is the distance along the medial line of the channel (positive from the mouth); t is time; A(x) is cross-sectional area; V(x,t) is the mean velocity over a cross section; b(x) is the width of the channel; ζ(x, t) is the elevation of the water's surface above the equilibrium depth; g is gravitational acceleration; k is the friction coefficient; h(x) is the mean depth of water below the undisturbed surface.

These equations are solved by breaking the channel up into sections, with the criterion that each section must closely resemble a rectangular channel. The differential equations are then solved using a finite difference scheme.

58

4.2.2 Two-Dimensional Model

Crean et al [1988] state that the fundamental equations of continuity and momentum applicable to tidal motion in a flat rotating sea are:

$$\frac{\partial \zeta}{\partial t} + \frac{\partial U}{\partial x} + \frac{\partial V}{\partial y} = 0 \ , \tag{4.4}$$

$$\frac{\partial U}{\partial t} + \frac{\partial}{\partial x}\left[\frac{U^2}{\zeta + h}\right] + \frac{\partial}{\partial y}\left[\frac{UV}{\zeta + h}\right] - fV +$$
$$+ g(\zeta + h)\frac{\partial}{\partial x}(\zeta - \overline{\zeta}) + \frac{kU\sqrt{U^2 + V^2}}{(\zeta + h)^2} = 0 \tag{4.5}$$

$$\frac{\partial V}{\partial t} + \frac{\partial}{\partial x}\left[\frac{UV}{\zeta + h}\right] + \frac{\partial}{\partial y}\left[\frac{V^2}{\zeta + h}\right] + fU +$$
$$g(\zeta + h)\frac{\partial}{\partial y}(\zeta - \overline{\zeta}) + \frac{kV\sqrt{U^2 + V^2}}{(\zeta + h)^2} = 0 \tag{4.6}$$

where x, y are Cartesian coordinates in the plane of the undisturbed water's surface; t is time; $\zeta(x, y, t)$ is the elevation of the sea surface, about $z=0$; $U(x, y, t), V(x, y, t)$ are components of vertically-integrated velocity in the directions x and y; $h(x, y)$ is the depth of water below the undisturbed surface; f is the Coriolis parameter, assumed uniform over the region; $\overline{\zeta}(t)$ is the equilibrium form of the surface elevation corresponding to the tide - generating

body forces, assumed spatially uniform over the region; $k(x,y)$ is the coefficient of friction; g is the acceleration due to gravity.

4.2.3 Three-Dimensional Model

For an example of one of the fairly recent types of 3-D hydraulic models, we will discuss the results of Leendertse [1988].

The differential equations to be solved are:

$$\frac{\partial u}{\partial t} + u \frac{\partial u}{\partial x} + v \frac{\partial u}{\partial y} + w \frac{\partial u}{\partial z} + v \frac{\partial^2 u}{\partial z^2} + g \frac{\partial \zeta}{\partial x} = 0 \quad , \qquad (4.7)$$

$$\frac{\partial v}{\partial t} + u \frac{\partial v}{\partial x} + v \frac{\partial v}{\partial y} + w \frac{\partial v}{\partial z} + v \frac{\partial^2 v}{\partial z^2} + g \frac{\partial \zeta}{\partial y} = 0 \quad , \qquad (4.8)$$

$$\frac{\partial \zeta}{\partial t} + \frac{\partial (hu)}{\partial x} + \frac{\partial (hv)}{\partial y} = 0 \quad , \qquad (4.9)$$

where u,v,w are the velocities in the x,y, and z directions, respectively; ζ is the distance between the free surface and a reference level; g is the acceleration due to gravity; v is the vertical momentum diffusion coefficient.

Willis [1995] gives an indication of how the latest generation of hydraulic models works. He states that the models used by the National Research Council (NRC) in

Ottawa are of the three-dimensional type, and incorporate time series of wind, salinity, currents, and the water's levels. The model results are compared against two independent data sets before the results are considered fully trustworthy. Willis [1995] states that the prediction accuracy of such models is **0.001 metres.** This accuracy is an estimate of the model fit to observed water level sensor water's surface elevations at **discrete spatial locations.** Model elevation accuracies will still depend on the accuracy of the time series of heights that they are based on. Hydraulic models, therefore, can provide water's surface elevation accuracies that are comparable with water level sensor/OTF DGPS accuracies at these points.

4.2.4 Combining OTF DGPS Water's Surface Elevation Measurements with Hydraulic Models

There are two main applications that could require combining OTF DGPS water's surface elevation measurements with one or more of the hydraulic models mentioned in sections 4.2.1, 4.2.2, and 4.2.3. They are the real time navigation application, and the documentation of flood events on a river.

The real-time navigation application could benefit from a better knowledge of the water's surface elevations along the ship's intended course. There are however two complicating factors to consider: (1) real-time measurements of currents, salinity, wind speed, and water levels may be needed, and (2) the hydraulic models involve

61

an iterative procedure, and must settle (i.e. the iterations must converge) before the results become reliable [Crookshank, 1995].

For documenting flood events on a river, the OTF DGPS water's surface profiles could be used to solve for various parameters in the governing differential equations [Burrells, 1995]. This could be a real-time or post-processing application. The OTF DGPS observations would be used after the flood event to verify some of the assumptions being used in the hydraulic model [Burrells, 1995].

CHAPTER 5

MIRAMICHI RIVER OTF DGPS SURVEY FIELD DATA COLLECTION

In section 5.1 we discuss the field procedures for the various phases of the Miramichi River OTF DGPS surveys. Preliminary reconnaissance took place on May 25-29, 1994. Some static GPS surveys, spirit leveling surveys, water level sensor accuracy assessments, and OTF DGPS river surveys took place from June 7-18, 1994. These surveys were completed during the second week of October, 1994. Section 5.2 provides a physical description of the Miramichi Estuary, including the tidal datum which is in place there. Section 5.3 covers the preliminary reconnaissance. Section 5.4 outlines the survey control establishment. Section 5.5 discusses the Socomar water level sensor data collection. Section 5.6 discusses the current speed data collection. Section 5.7 covers the collection of salinity values. Section 5.8 covers the collection of squat test data. Finally, section 5.9 outlines the OTF DGPS river survey data collection.

5.1 Methodology

The overall goal of this field project was to assess the accuracy and reliability of water's surface elevation

measurements from a typical OTF DGPS package (the Z12/PRISM package) versus a network of digital water level monitoring systems. The water level monitoring systems are an accepted method of water level measurement, and as such served as ground truth for the OTF DGPS water's level measurements.

The Miramichi River field work was composed of four main segments:

(1) Preliminary reconnaissance.

(2) Network control observations.

(3) Vessel squat tests.

(4) Vessel river elevation surveys.

Table 5.1 shows the measurements that were made in each segment of the project, and indicates the purpose behind making the measurements.

5.2 Background Information on the Miramichi Estuary

5.2.1 Physical Structure of the Miramichi Estuary

The information in section 5.2.1 was obtained from Philpott [1978]. The Miramichi Estuary is classified as a bar-built estuary. It is large and shallow, with a width of 22 kilometres at the mouth and a length of 80 kilometres from the barrier islands to the tidal limit.

The physical dynamics of any estuarine system are governed by four boundaries:

64

Table 5.1

Miramichi River field measurements.

Project Segment	Measurement Types	Purpose of Measurements
Preliminary reconnaissance	Initial control point selection Water level sensor calibration vs tide staff	Prepare for network control observations Assess water level sensor accuracy for river elevation survey phase
Network control observations	Static GPS baselines, spirit leveling	Establish 3-D control for the river elevation survey and squat test phases
Squat test	Ellipsoidal water's levels, spirit levels, OTF DGPS antenna elevations, salinity	Calibrate the vessel's antenna height above the water's surface

Table 5.1 Continued

Miramichi River field measurements.

Project Segment	Measurement Types	Purpose of Measurements
River elevation survey	OTF DGPS antenna elevation measurements	Obtain ellipsoidal elevation of antenna phase center
	Salinity measurements	Determine any salinity effects on antenna height
	Current speed measurements	Look for current-related antenna height biases in post-processing
	Water level sensor observations	Water level ground truth for the OTF DGPS water's levels
River elevation survey	Tide staff checks vs water's level sensors	Check accuracy of water level sensors

(1)   The stable bedrock, the less stable sediments above it, and the shorelines which form the bottom and sides of the estuary.

(2)   The upper boundary -- the atmosphere. It acts directly on the surface of the estuary through the action of wind, rain, and heat exchange. This boundary will influence the boundaries in three and four below.

(3)   Upstream of the estuary. This is the river basin which supplies fresh water and fine grained sediment to the estuary.

(4)   The sea. The cycle of the tides causes salt water to ebb and flood, and the tidal currents, along with wind waves, bring sand from the nearby coast.

The Miramichi Estuary can be broken up into five distinct regions (see Figure 5.1), based on differences in the hydrodynamic characteristics (tide action, salinity, wave action, etc.) and on the character of the sedimentary processes. The field work for the assessment of the Z12/PRISM OTF DGPS package took place in Section 1, which is a portion of the **river** section of the estuary.

A shipping channel is present in the Miramichi Estuary. The section used during the OTF DGPS surveys runs from near Newcastle (NEWC) downstream to a point near Gordon Point (FLOY). There are 14 "reaches" or segments in

67

SEDIMENTARY ENVIRONMENTS

1.RIVER
2.RIVER MOUTH
3.INNER BAY
4.TIDAL DELTA&COASTAL BARRIER COMPLEX
5.MIRAMICHI BAY

GORDON POINT

NEWCASTLE

OTF SURVEY

▲ = GPS CONTROL
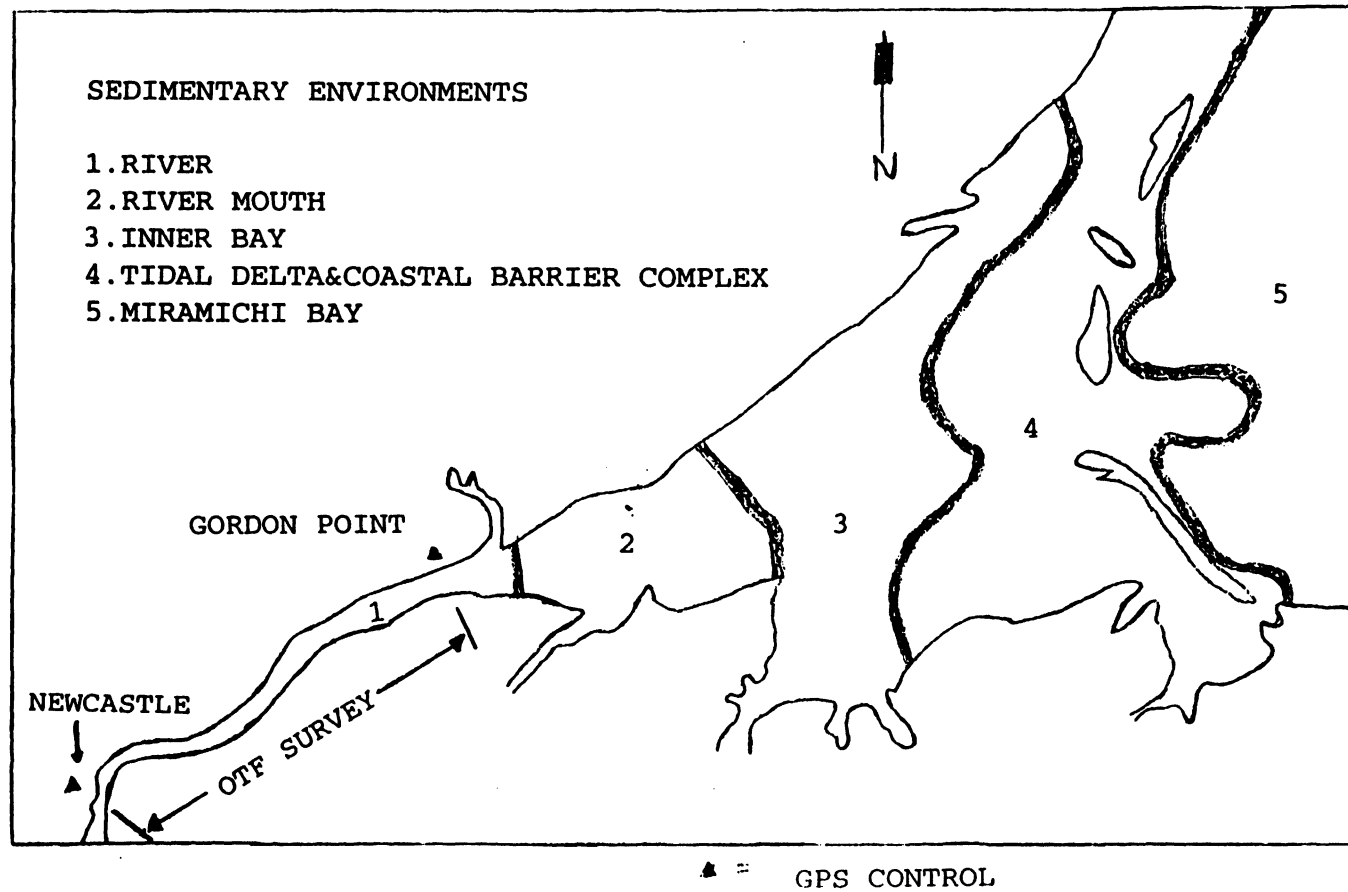
Figure 5.1

Sections of the Miramichi Estuary
(from Philpott [1978, p. 48]).

this section of the channel.

5.2.2 Chart Datum and Hydrographic Surveys on the Miramichi

Within the main channel itself, the Department of Public Works (DPW) performs yearly acoustic sweep surveys. Sweep surveys involve a vessel with two booms suspended outward on each side of the vessel, perpendicular to the vessel heading. Each boom has several single beam, vertical incidence transducers attached to it. The vessel also has two vertical beam echo sounders attached to the hull. These vertical beam transducers determine the depth of the water. It is important to note that the distance from the GPS antenna on the vessel to the transducers on the booms is **not** fixed, due to the flexing of the booms. This could preclude DPW from using a **squat independent** scheme as outlined in section 1.2. Further investigations into the nature of the boom movement are needed, and the possibility of using attitude sensors on the booms needs to be assessed.

The chart datum on the Miramichi Estuary is a "stepped datum" which was established in part by the CHS. Some additional work was carried out by Discovery Consultants Ltd. [no ref.] in 1985. This additional work involved setting intermediate tidal stations between existing CHS tidal stations. The intermediate stations were established during spring tides. The criterion was that the low tide reading at a station between two intermediate primary

stations (with chart datum previously established by the CHS) be zero when the readings at the two primary stations were zero.

The current strategy for sounding reductions on the Miramichi is designed so that the maximum error due to water level measurement/interpolation is **no greater than +/- 0.1 metres.** This by necessity involves some interpolation between tidal stations when the survey vessel is **not immediately adjacent** to a tidal station. The assumption used is that the water's surface is **linear** between the two stations. Hydraulic models exist for the Miramichi, but as stated by Goguen [1995] and Crookshank [1995], the maximum difference between assuming a linear water's surface between water level sensors and the hydraulic model water's surface is about 0.05 metres which is not large enough to justify the effort of having two tide staff readers in place for every survey -- i.e. water level sensors are not present at all tidal stations.

5.3 Preliminary Reconnaissance

In May 1994: (1) several Socomar TMS 1000 digital water level sensors were installed in the estuary (to be used as water level "ground truth" during the OTF DGPS river surveys), (2) horizontal and vertical control was located, and (3) the Chatham water level sensor was calibrated against a tide staff. The FLOY water level

sensor had already been calibrated by DPW. See section 6.2 for the results of this and other water level sensor calibrations. The other water level sensors that would be used in the river water surface elevation surveys (section 6.4) had not yet been installed.

5.4 Survey Control Establishment for the OTF DGPS Surveys

The survey control establishment consisted of static GPS surveys and spirit leveling surveys. The control served two purposes: (1) determining a height for a code differential/OTF DGPS base station, and (2) determining accurate relative ellipsoidal elevations on existing tide staffs, relative to the adopted ellipsoidal height for base station "CHAT". This enabled the use of **ellipsoidal** water's level elevations for the network of digital water level sensors during the OTF DGPS river elevation surveys.

5.4.1 Static GPS Surveys

Static GPS surveys were carried out in June and October, 1994. No baselines were reoccupied, but closed figures involving all control points were produced.

The purpose of the static surveys was to provide an accurate relative 3-D GPS control network throughout the OTF DGPS survey area. The planned OTF DGPS survey lines ran

along the centerline of the Miramichi River shipping channel, from just below NEWC down stream past control stations at Chatham (CHAT), Range Light (RANG), Millbank (MBNK), to FLOY. Triangles indicate GPS control stations only; circled triangles indicate water level sensors and GPS control stations. Figure 5.2 shows the survey control. The GPS control stations were chosen with the following characteristics:

(1) Minimum obstructions to the satellites.

(2) Minimum distance to tide staffs.

(3) Good monument stability.

(4) Easy accessibility.

The stations were nails driven into docks, except for RANG, which was a bolt hole atop a Coast Guard Range tower.

The existing horizontal control consisted of DPW North American Datum '27 (NAD '27) horizontal coordinates for stations CHAT and FLOY. These coordinate values had been derived from an NBGIC (New Brunswick Geographic Information Corporation) control framework in the area.

The existing vertical control on the DPW points consisted of **chart datum** elevations only on all tidal stations except CHAT. These datum elevations were established through water level transfers at some stations and through a time series of tidal observations at others.

The North American Datum '83 (NAD '83) values of CHAT were held fixed in a least-squares network adjustment. Its
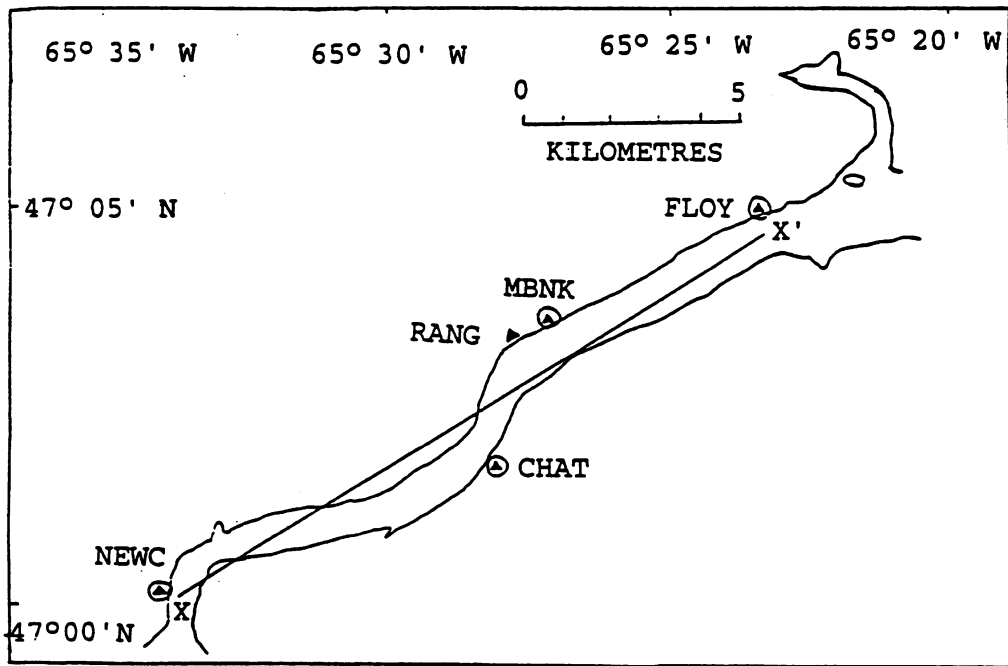
Figure 5.2

Miramichi River control locations
(after Philpott [1978, p.125]).

NAD '83 coordinate values were obtained from NAD '27 using the datum shifts in the National Transformation Software (version 1.1) from the Geodetic Survey of Canada. CHAT was chosen as a base station for two reasons: (1) it was initially intended to be an OTF DGPS base station as well, and (2) it had an orthometric elevation on it. Since it was located near the center of the corridor formed by all the GPS control stations, the baselines from CHAT to each end of the OTF DGPS survey area would have been roughly equal, and less than 10 kilometres in length. Ten kilometres is the maximum length to which the PRISM-PNAV software is claimed to resolve ambiguities with certainty [Ashtech, 1994].

The baselines from NEWC to RANG, NEWC to MBNK, and RANG to FLOY were observed in October, giving a total of seven observed baselines, with geometrical redundancy. One base station and one receiver were used in these observations. No meteorological parameters were measured during any of the static surveys, as it was assumed that the relative positioning technique would remove the tropospheric errors. The best location for the OTF DGPS/differential base station was finally determined to be at station RANG. This was because RANG was a tall coast guard range light tower, with a good line of sight to the survey area, and was still near the midpoint of the OTF DGPS survey area.

5.4.2 Spirit Level Surveys

The second portion of the control surveys involved spirit level surveys at all the Socomar tidal stations. The surveys tied the chart datum elevations from the local CHS benchmarks to the water level sensors. No spirit level surveys were run between tidal stations, due to the large distances involved. Both DPW members and University of New Brunswick (UNB) personnel were involved. At the stations in Figure 5.2 that are also circled, the GPS ellipsoidal elevations of control points were tied to existing tide staffs. This would later allow us to use four existing Socomar water level sensors as **ellipsoidal** water's level references. In addition, the stability of all available tidal benchmarks at each station was assessed, at the request of Parsons [1994]. This was done by comparing spirit levelled elevation differences between benchmarks with published elevation differences. The one exception is the MBNK site, where no tidal benchmarks are in place.

Spirit leveling was also performed on the Newcastle government dock from station NEWC to a second benchmark in preparation for the upcoming squat tests. This benchmark would later be used for measuring ellipsoidal water's level elevations during the squat tests.

5.5 Socomar Water Level Sensor Data Collection

The water level sensor data were collected to provide ground truth for the OTF DGPS water's surface elevations which would be obtained in the river water's surface elevation survey phase. In situ water level sensor calibrations vs tide staffs were also performed.

5.5.1 Water Level Sensor Description

The water level sensors used during the OTF DGPS surveys were Socomar TMS 1000 digital bubbler water level sensors (see Figure 5.3). These water level sensors are temporary water level monitoring systems, designed to be removed/replaced as needed during each survey season.

When installing the Socomar bubbler, the acquisition unit is generally located in a watertight box on the dock. The acquisition unit is basically a small computer, and usually runs on AC power. It is used to modify data collection parameters, collect data, and store data. This data can then be accessed from a laptop computer via modem. The next installation step is to attach the transducer cable tube to the pressure sensor and place them into the water on a rigid support. The tube is then connected to the acquisition unit, which is in turn connected to the modem and power supply.

In terms of physical operation, a gas cylinder inside
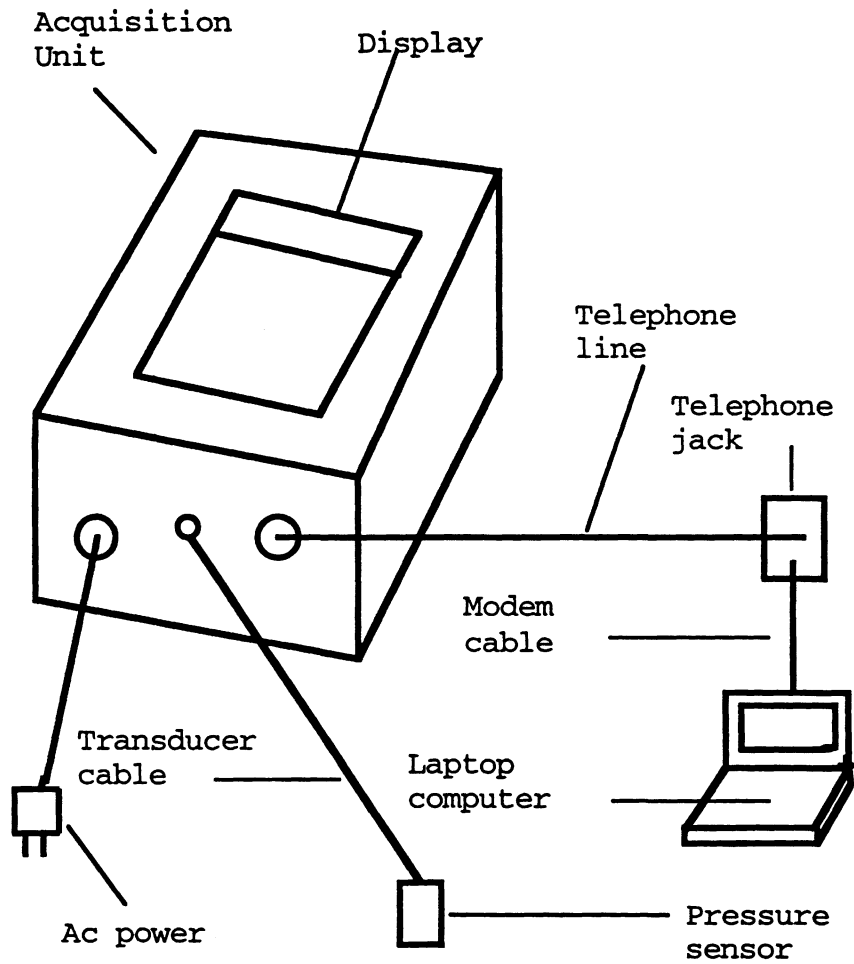
Figure 5.3

Socomar water level sensor setup
(after Phelan [1992, p. 5]).

77

the acquisition unit forces a bubble of gas through the transducer cable and transducer, and into the water. A diaphragm inside the acquisition unit then measures the **difference** between total pressure at the pressure sensor and atmospheric pressure acting on the acquisition unit [Marso, 1995]. Total pressure is the sum of the water column pressure and the atmospheric pressure. Atmospheric pressure changes are automatically compensated for by virtue of the mechanical design of these water level sensors (Parsons [1994]; Marso [1995]; Hare and Tessier [1995]).

As these are temporary water level sensors, some **default** user-estimated salinity and temperature values for the water's column are used. All the water level sensors that were used on this project were set up with the same measurement parameters. Atlantic Daylight Time was used, with a 20 minute recording interval. A 40 second smoothing period was used for filtering out the effect of water's surface waves and swell. During this smoothing period, 40 pressure readings are taken, one every second, and the average obtained.

Knowledge of the water level height measurement accuracy of these water level sensors was critical for the OTF DGPS survey ground truthing. When contacted, the manufacturer's claim was that these water level sensors were accurate to +/- 0.01 metres [Marso, 1995]. **No confidence interval** or **restriction** on **conditions** was stated. Furthermore,

manufacturers claims should always be verified with in-situ accuracy assessments, which better reflect local conditions, and point towards defective equipment. Therefore, in situ accuracy assessments were performed on all water level sensors.

5.5.2 In Situ Water Level Sensor Accuracy Assessments

An in situ accuracy assessment of four water level sensors versus the **tide staffs** was performed before and during the OTF DGPS river surveys. The goal of having height checks throughout the full range of water levels for the FLOY, MBNK, and CHAT water level sensors was met. Note that all the tide staffs used for this purpose were graduated in 0.05 metre increments. It was possible to estimate directly to +/- 0.01 metres on these boards when conditions were calm. During the majority of the accuracy assessments, it is the author's opinion that staff readings were accurate to around +/- 0.01 metres. The NEWC water level sensor was not as well calibrated, because it did not remain running long enough for the author or any DPW employee to get extensive accuracy checks on it. However, enough staff observations were taken on days 166 and 167 to ensure that nothing was grossly wrong with the water level sensor heights.

During the river water surface elevation surveys

themselves, the three water level sensors were compared against the staffs at least once per day. Several systematic height **biases** were found in the water level data collected. These biases were not corrected by resetting the water level sensors in the field, but were recorded for later correction during data processing (section 6.2.1).

5.6 Current Speed Data Collection

Current speed measurements were performed as part of the OTF DGPS river elevation surveys. Measurements were taken at NEWC on Julian Days 166 and 167 only. This was due to: (1) unsuitable measuring conditions at the three other water level sensors, and (2) a lack of current equipment for the October phase of the project. See Table 5.2 for a summary of the results. The current data were needed to attempt to determine any current-related **biases** in OTF DGPS antenna height between upriver and downriver runs.

The current meters were two portable handheld units obtained from Eco Systems Ltd. in Fredericton, New Brunswick. These meters measured the current speed from a sensor lowered into the water on metal poles that were fabricated at a local hardware store in Newcastle. The speed of the current was measured through an electromagnetic technique. The current sensor was placed at depths of 0 to 4.5 metres, in increments of 0.5 metres. At

80

each depth, up to five current readings were taken at a
five second interval. The "noise" (i.e. departure from the
average value) at each depth was +/- 0.03 m/s at most.
Since the draught of the Gulf Surveyor is 0.5 metres, Table
5.2 shows current speeds at a depth of 0.5 metres.

Table 5.2

Current data at Miramichi control stations.

Location	Julian Date	UTC Time	Line Direction	Current Direction	Current speed (m/s)
NEWC	166	15:20	Downriver	Downriver	0.40
		17:40	Upriver	Downriver	0.65
NEWC	166	17:40	Downriver	Downriver	0.65
		19:20	Upriver	Downriver	0.53
NEWC	167	12:20	Downriver	**Upriver**	0.25
		16:00	Upriver	Downriver	0.51

The observations at NEWC were taken from a concrete
structure under the Newcastle Bridge, in the center of the
river. The current flow was unobstructed.

5.7 Salinity Data Collection

Salinity measurements at the water's surface were
needed to establish a theoretical estimate of the change in

81

vessel squat that occurs as a function of salinity change (see section 6.4.3).

The measurements were performed on the following OTF DGPS river survey days: 166, 167, and 293. Samples were taken during the OTF DGPS river elevation survey runs at all control stations -- NEWC, CHAT, MBNK, and FLOY. See Table 5.3 for results.

The samples were taken either directly by dipping a salinity meter into the water, or by collecting water samples for later analysis. The collected samples for days 166 and 167 were measured with a salinity meter. A set of four hygrometers (glass float devices used to measure density) were also calibrated against the salinity meter at this time. The apparent error for both hygrometers was 2 ppt (parts per thousand) versus the salinity meter. These hygrometers were later used to measure the salinity of water samples taken on Julian Day 293. The range of salinity was from 0.5 ppt to 4.9 ppt throughout the entire survey area.

5.8 Vessel Squat Test Data Collection
5.8.1 Squat Test Goals

The goal of the squat tests was to find the **repeatability** of determining **changes** in the GPS **antenna**

82

Table 5.3

Miramichi River salinity measurements.

Location	Day 166	Average Salinity
	Time	
	(GPS)	(ppt)
NEWC	13:04	3.115
CHAT	17:28	0.450
NEWC	22:19	0.670
	DAY 167	
Location	Time	Average Salinity
	(GPS)	(PPT)
NEWC	18:15	1.930
CHAT	15:19	2.530
CHAT	17:00	2.660
FLOY	16:16	4.830
	DAY 293	
NEWC	-----------------	2

height above the water's surface as a function of **vessel Resultant Speed Over Ground (RSOG)**. Resultant Speed Over Ground is given by:

$$RSOG = SQRT(SOGEAST^2 + SOGNORTH^2),$$ (5.1)

where SOGEAST is the Speed Over Ground (SOG) in the geodetic east direction, and SOGNORTH is the SOG in the geodetic north direction. One requirement was for nearly calm conditions during the surveys, because no pitch, roll, and heave sensor was available, and also because a spirit level was being used to observe a level rod on the vessel.

The squat test results would later be used to help derive the ellipsoidal elevation of the water's surface from OTF DGPS ellipsoidal antenna elevation observations taken during the OTF DGPS river survey phase of the project (see section 6.4).

5.8.2 Squat Test Procedure

The squat tests were conducted near the Newcastle government dock (see Figure 5.4). The vessel was run repeatedly toward the spirit level on shore. The squat tests measured the following factors which can affect the squat of the survey vessel:

(1) Changes in vessel RSOG.

(2) Changes in salinity at the water's surface.

84

Vessel
track

Tide
staff

Temporary
Bench
Mark

NEWC

Spirit level

Newcastle government dock

DPW storage shed
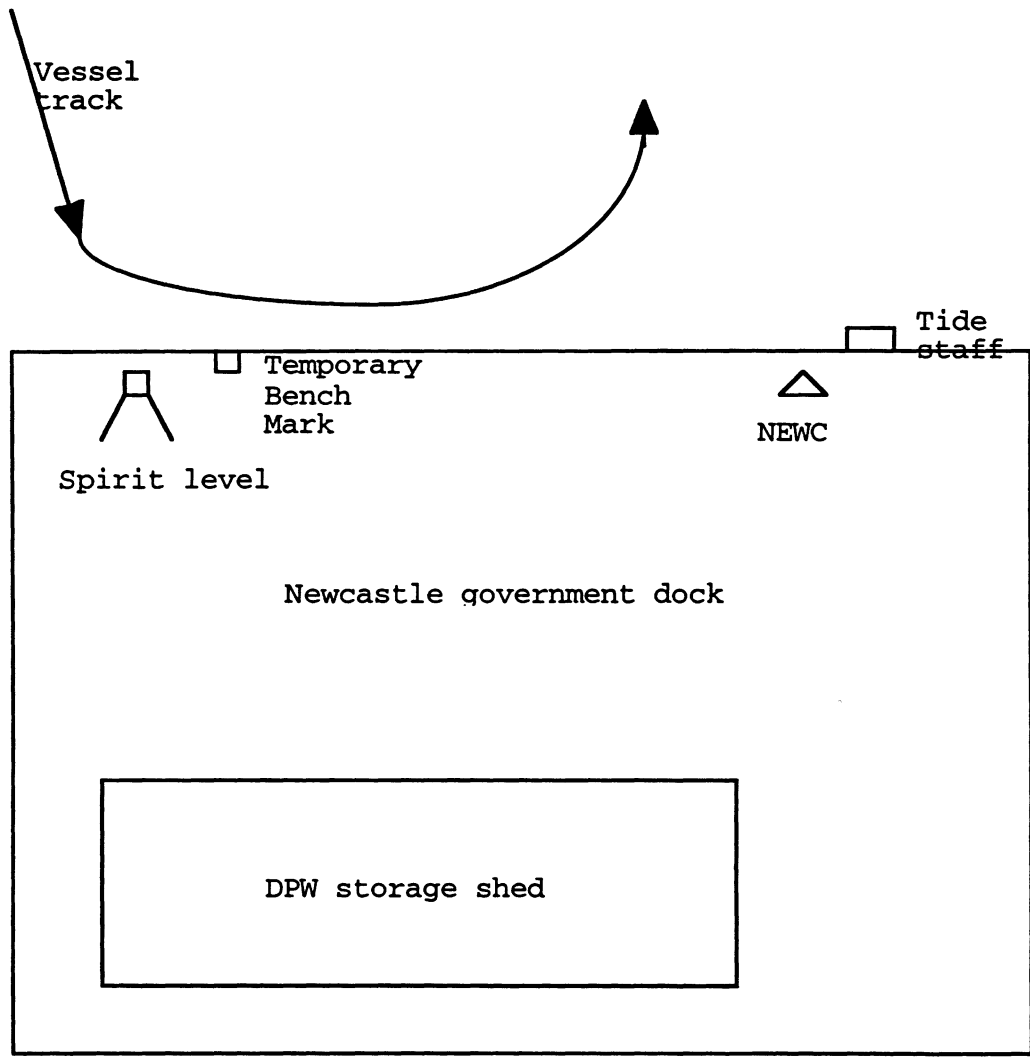
Figure 5.4

Location of vessel squat tests.

(3)   Changes in vessel loading (number of people,

amount of fuel in tank).

Two measurements that should have been made during the
squat tests:

(1)   Changes in current speed and direction.

(2)   Changes in bathymetry.

The main survey equipment for the squat tests (see
Figure 5.5) consisted of one survey vessel, one shore based
spirit level, two laptop computers for logging raw data at
the OTF DGPS base station and the OTF DGPS remote station,
and one tide tape for measuring water levels.

The spirit-leveled ellipsoidal height of the vessel
OTF DGPS antenna above the water's surface was obtained
from the following formula:

$$HANTSP=HI-DH+HTAPE, \hspace{4cm} (5.2)$$

where HTAPE was the tide tape distance from the TBM to the
water's surface; HI was the spirit level backsight reading
taken on the TBM; DH was the height difference between the
rod reading on the vessel and the vessel GPS remote
antenna, corrected for the inclination of the level rod on
the vessel.

The OTF DGPS-derived antenna height was obtained from
the following relationship (valid for the specific

86

situation in Figure 5.5):

$$HANTGPS=ELGPS-(ELTBM-HTAPE),$$ (5.3)

where ELGPS was the height of the OTF DGPS vessel antenna relative to the ellipsoid, and ELTBM was the elevation of the temporary benchmark below the ellipsoid.
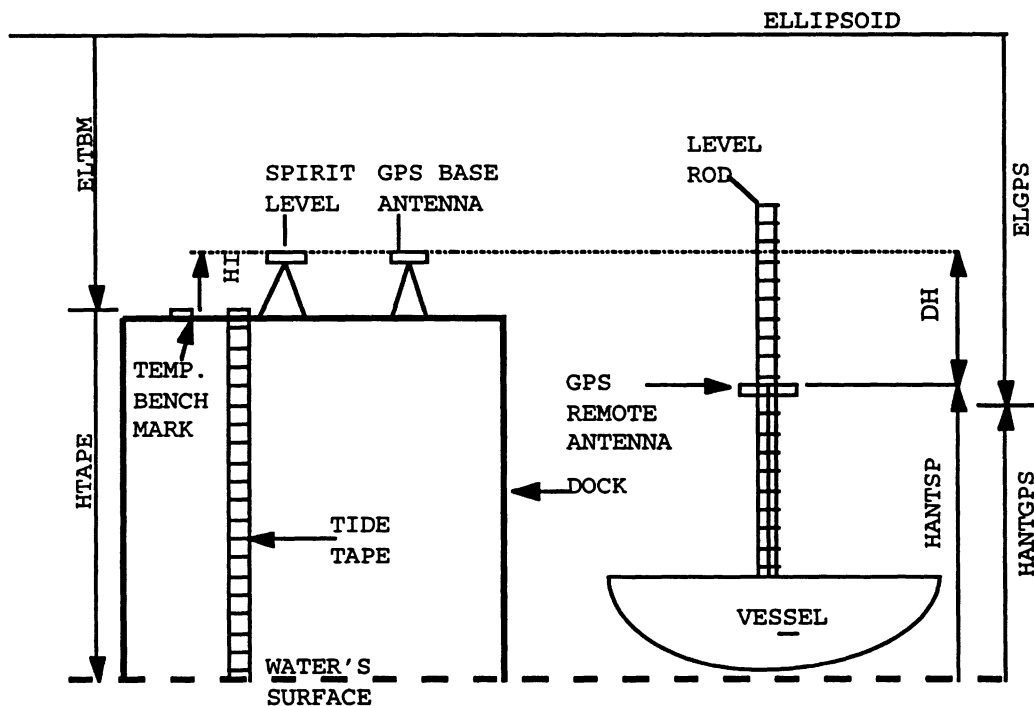
Figure 5.5

Schematic of squat test equipment.

One vessel was used for these squat tests and the OTF DGPS river elevation surveys. This was important, because the antenna height of another vessel would respond differently to changes in vessel speed, making it difficult to interpret the results of the river elevation surveys.

Observations of the water's level below the ellipsoid were taken during the tests, based on a benchmark which was spirit leveled in from station NEWC. The ellipsoidal elevation of the GPS antenna was obtained from OTF DGPS observations and spirit level observations. The vessel antenna height would later be derived separately for both sets of antenna elevation observations by subtracting the observed antenna elevation from the measured water's surface elevations (see section 6.3).

The Gulf Surveyor was driven upriver directly towards a spirit level on shore at RSOG's of 10, 20, 30, and 40 kilometres per hour (kph), which corresponded to the planned RSOG's for the OTF DGPS river surveys. An average of four lines were run at each RSOG.

Raw GPS code and phase data was logged at station RANG directly to a 486 laptop computer at a one second recording interval. The same form of data was logged on the Gulf Surveyor. The spirit level was used to observe a level rod on the ship. The location of the GPS antenna on the level rod was known within +/- 0.01 metres. The ellipsoidal elevation of the water's surface was obtained at approximate 20 minute intervals with a tide tape by measuring downward from the benchmark. Water samples were collected for later salinity measurements.

No sophisticated measurements of motion parameters were performed during these tests. However, it was calm enough to allow an assistant to measure the inclination of

the level rod on the vessel using a carpenter's level. This inclination was measured in an approximate fore-aft direction, relative to the local vertical. A 0° angle would mean the rod was perfectly vertical. This measurement was used to correct the observed level rod readings for inclination in section 6.3.

5.9 OTF DGPS River Survey Data Collection

The purpose of the OTF DGPS river surveys was to assess the accuracy and reliability of using OTF DGPS for the measurement of spatial variations in water's surface elevation throughout the OTF DGPS survey area.

5.9.1 OTF DGPS River Survey Procedure

The OTF DGPS river surveys were carried out on **four** separate days: Julian Days 166, 167, 292, and 293. The OTF DGPS base was always at RANG. The equipment used was the same as the equipment used for the squat tests, except that no spirit level, tide tape, carpenter's level, or level rod was needed. The shore person's duties consisted of taking tide staff readings at the water level sensors, and monitoring the base station at RANG.

The vessel was run upriver and downriver past the water level sensors and staffs at RSOG'S ranging from 10 to

44 kph. No motion sensor measurements were made. Water samples were collected for later salinity measurements, to determine whether changes in vessel squat were correlated with salinity (see section 6.4.3).

The four digital water level sensors were collecting chart datum water's level information at a 20 minute interval, using the parameters defined in section 5.5.1. A tide staff was read at a 20 minute interval whenever a water level sensor went down.

CHAPTER 6
MIRAMICHI RIVER OTF DGPS SURVEY RESULTS

This chapter examines the analysis of the Miramichi River OTF DGPS survey results. In order to assess the accuracy and reliability of the OTF DGPS water's surface elevations, it was necessary to assess the quality of the survey control data, water level sensor data, squat test data, and river elevation survey data. An improved squat test technique is presented in section 6.3.2. An improved OTF DGPS water surface elevation measurement technique for dredging and sounding surveys is presented in section 6.4.8.

Section 6.1 covers the survey control processing results. Section 6.2 discusses the water level sensor processing results. Section 6.3 shows the squat test processing results. Section 6.4 gives the river water's surface elevation survey results.

6.1 Survey Control Processing Results

6.1.1 Choice of Coordinate System

For the horizontal coordinates of the OTF DGPS position fixes, World Geodetic System '84 (WGS '84) ellipsoidal latitude and longitude values were output from

PRISM-PNAV. Ellipsoidal latitude longitude values were output because the PRISM-PNAV software does not allow the user to output mapping plane coordinates. Mapping plane coordinates are two-dimensional (2-D) Cartesian x and y coordinates. For plotting the OTF DGPS water's surface elevations against distance between water level sensors, it was decided that Universal Transverse Mercator (UTM) mapping coordinates would be used to obtain the distances.

It was decided that the heights from OTF DGPS would be expressed as **ellipsoidal heights.** See Wells et al [1996] for up-to-date details on the most appropriate vertical-reference surface for hydrographic data using OTF DGPS measurements.

6.1.2 Network Adjustment Results

The static baseline observations (recall section 5.4.1) were first processed with the software GPPS, which is an Ashtech product that came out before the PRISM software. The resulting baselines were then input along with their estimated accuracies into a software package called GEOLAB [Steeves, 1993], which performed a least-squares network adjustment to determine the adjusted latitude, longitude, and ellipsoidal height of the unknown control points.

A minimally constrained network adjustment was performed with one fixed station -- CHAT, which was

unweighted. Ellipsoidal latitude, longitude, and height coordinates were input for CHAT.

The NAD '83 horizontal coordinates of CHAT were obtained from DPW, and had been derived by transforming from NAD '27 values to NAD '83 values. As long as the radial error in the absolute value of these fixed coordinates is 20 metres or less, a maximum error of about 1 ppm will be present in the GPS baselines [Leick, 1995]. It was assumed that these NAD '83 values for CHAT were the same as WGS '84 values. This is valid, because the two datums now use the same defining parameters for the Geodetic Reference Surface '80 (GRS '80) ellipsoid [Wells, 1996], and have a very small datum shift (on the order of 1 metre). The other contributor to the fixed coordinate error would be the accuracy of the conversion from NAD '27 to NAD '83.

The geodetic height of CHAT was obtained through a spirit level survey using orthometric heights (i.e. heights above the geoid, which is the mean gravitational form of the earth) from nearby CHS tidal benchmarks. The ellipsoidal height of CHAT was then obtained by applying the geoid-ellipsoid separation as determined by the Canadian Geoid Program [Geodetic Research Services, 1989-1992], developed at UNB.

The GPS network adjustment results indicate that in general the seven baseline measurements fit together well. This is evidenced by several factors:

(1) In general, the relative height error between any
     two control stations is on the order of +/- 0.03
     metres at 95% confidence (see Table 6.1). Note
     that the MBNK-RANG baseline was not directly
     observed in the field.

(2) A chi-square goodness of fit test for normality
     on the 21 estimated baseline residuals passes at
     95% confidence (see Table 6.2). This test is
     designed to see if the residuals follow a normal
     distribution. The residuals are in Figure 6.1.

(3) A test for residual outliers using the out-of-
     context Tau test with mean μ = 0 assumed known
     and a-priori variance of unit weight σ_o^2 **unknown**
     detects **no** outliers at 95% confidence. The out-
     of-context Tau test was used, because it is much
     harsher than the in-context Tau test (i.e. it has
     the smallest interval through which observations
     have to pass to be accepted).

One statistical test points to problems, however. The
Chi-Square test on the ratio $\sigma_o^2/\hat{\sigma}_o^2$ between σ_o^2 (assumed to
be one) and the a-posteriori variance factor $\hat{\sigma}_o^2$ (calculated
to be 4.34 in GEOLAB) does **not** pass at 95% confidence (see
Table 6.3). This could be due to several causes, including
[Gagnon and Nassar, 1973]:

94

Table 6.1

95% confidence 1D **relative** confidence region for ellipsoidal height differences.

From	To	Spatial Separation (Metres)	95% Confidence Error Estimate for Height Difference (Metres)
CHAT	FLOY	8141.344	+/- 0.036
CHAT	MBNK	4109.623	+/- 0.024
CHAT	NEWC	7628.988	+/- 0.028
CHAT	RANG	2899.501	+/- 0.030
FLOY	RANG	5977.530	+/- 0.040
MBNK	NEWC	11355.088	+/- 0.030
NEWC	RANG	9751.573	+/- 0.036
MBNK	RANG	1666.358	+/- 0.037
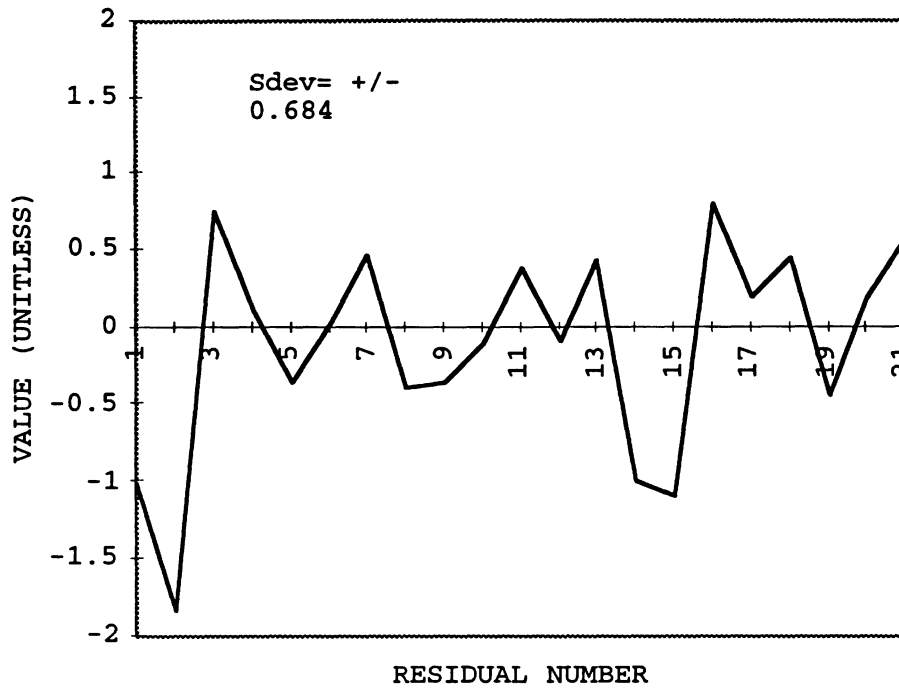
Figure 6.1

Mirimichi network adjustment residuals

Table 6.2

Statistical assessment of network adjustment residuals.

Chi-Square Test Statistic for 2 Degrees of Freedom	Sample Value	Pass at 95% Confidence?
5.99	4.530	**Yes. 4.530<5.99**

(1)   An a-priori weight matrix that was too
      optimistic.

(2)   Presence of systematic errors in the estimated
      single baseline coordinate differences from GPPS.

(3)   Coordinate difference observations did not follow
      a normal distribution.

(4)   An improperly formulated mathematical model.

The cause(s) of the variance factor failure in this
particular dataset were not pinpointed. Instead, to
alleviate the problem, the **covariance matrix** of the
estimated parameters was **scaled** by the estimated variance
factor $\hat{\sigma}_0^2$. This scaling gave more realistic accuracy
estimates for the unknown latitude, longitude, and
ellipsoidal height of the control stations.

Table 6.3

Chi-square test on the estimated variance factor from
Miramichi control network adjustment

Estimated Variance Factor	Equality to be Tested at 95% Confidence	Pass at 95% Confidence ?
4.344	2.055 <1 <14.480	No.

97

6.1.3 Spirit Leveling Results

The spirit leveling loop misclosures were under 0.01 metres. The tidal benchmarks at the FLOY and NEWC tidal sites were stable, because the closed loop height differences agree with the published height differences within +/- 0.01 metres. The tide staffs now agree with the benchmarks within +/-0.01 metres. Note that a 0.08 metre error in the **old** FLOY tide staff due to ice damage was corrected by installing a **new** staff.

Problems were present at the CHAT site, where one benchmark appeared to have moved by 0.03 metres relative to two stable ones. A 0.03 metre misclosure was apparent between this benchmark and the tide staff as well. If the elevation of the unstable benchmark was changed to agree with the leveling results between the two stable ones, the staff would be about 0.015 metres too high. The location of the CHAT tide staff relative to the two stable tidal benchmarks was not corrected. This did **not** affect the accuracy of the CHAT water level sensor as an ellipsoidal water's level reference, since there was an accurate height difference between CHAT and the tide staff. See Table 6.4 for the numerical relationship between tide staff datum and our ellipsoidal datum at the four tidal stations. Figure 6.2 shows the relative ellipsoid-staff datum relationship graphically. The distance "X" is the distance along the

98

Table 6.4

Ellipsoid and staff datum relationships.

Station	Ellipsoidal elevation of **tide staff zero** (metres)
NEWC	-20.509
CHAT	-20.447
MBNK	-20.354
FLOY	-20.318
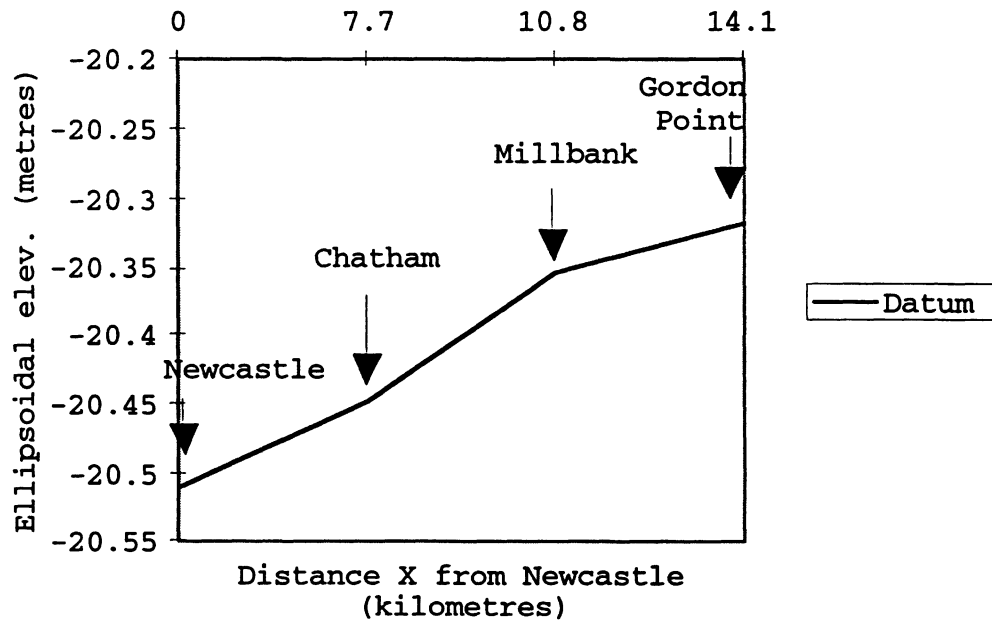
Figure 6.2

Ellipsoidal elevations of tide staff zeroes.

line X-X' which passed through the midpoint of the control stations as shown in Figure 5.2.

6.2 Water Level Sensor Processing Results

Overall, the Socomar water level sensors were sufficiently accurate to ground truth the OTF DGPS water's surface elevation measurements. The in situ accuracy of the water level sensors (see section 6.2.1) turned out to be close to a predicted accuracy value based on:

(1)   The manufacturer's claim for pressure measurement resolution.

(2)   The effects of salinity and temperature error on the calculated changes in water's column height.

(3)   The effects of water level sensor timing error.

By themselves, the Socomar water level sensors were not reliable enough (due to system failures) to completely ground truth all the OTF DGPS water's surface elevations, but a combination of tide staffs and working water level sensors was sufficient for the ground truthing. The CHAT water level sensor stopped recording data on days 166 and 167, with no substitute tide staff readings available. The NEWC water level sensor stopped recording data on Julian dates 291, 292, and 293, with substitute tide staff readings available. The substitute tide staff readings were

100

considered to be as accurate as the NEWC water level sensor, because:

(1) Tide staffs have traditionally been used to calibrate water level sensors.

(2) The waves were generally < 0.10 metres in amplitude.

(3) The staffs were read at a 20 minute interval, which was the same sampling interval as the water level sensors.

6.2.1 In Situ Water Level Sensor Accuracy Assessment Results

For reliable estimates of the in situ water level sensor errors, three conditions were required:

(1) Staff comparisons regularly spaced throughout the full range of water levels for each water level sensor.

(2) A large enough sample of water level sensor - staff comparison errors at each water level sensor to allow a Chi - Square goodness of fit test for normality to be performed on the estimated random water level sensor errors.

(3) Similar conditions during both the staff-water level sensor comparisons and the OTF DGPS river surveys.

6.2.1.1 Bias Removal and Statistical Testing for all Water Level Sensors

The first assessment step involved removing any observed biases in the water level sensor water's surface elevations by subtracting the **average** of the differences between the tide staff and water level sensor from the water level sensor values. These biases were clearly apparent, because the staff-water level sensor comparisons at each water level sensor were always characterized by consistent biases of up to 0.20 metres, with residual noise levels of 0.01 to 0.02 metres. It was very likely that the biases were caused by human reading error on the tide staffs during initial zeroing of the water level sensors against the staff. These biases could have been minimized in the field by re-zeroing the water level sensors in calm or near-calm conditions.

For this project, field correcting the heights would have been unnecessarily tedious; it was much simpler to leave a constant bias in the heights and to subsequently correct the biased heights in post-processing. See Figures 6.3 - 6.6 for graphs of the estimated random errors after bias removal for each individual water level sensor, based on all water level sensor - staff comparisons for that water level sensor.

The second assessment step involved the bias-corrected errors for all of the available water level sensor-staff
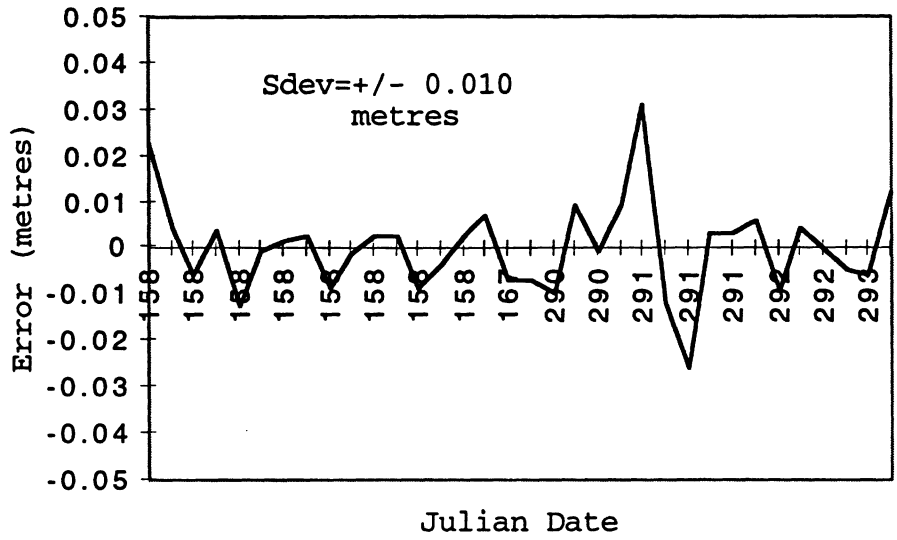
Figure 6.3

Estimated random errors FLOY water level sensor.
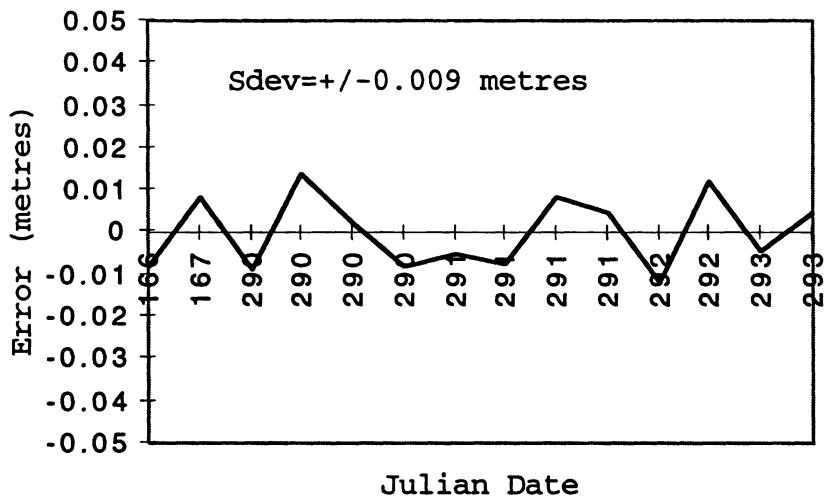
Figure 6.4

Estimated random errors MBNK water level sensor.
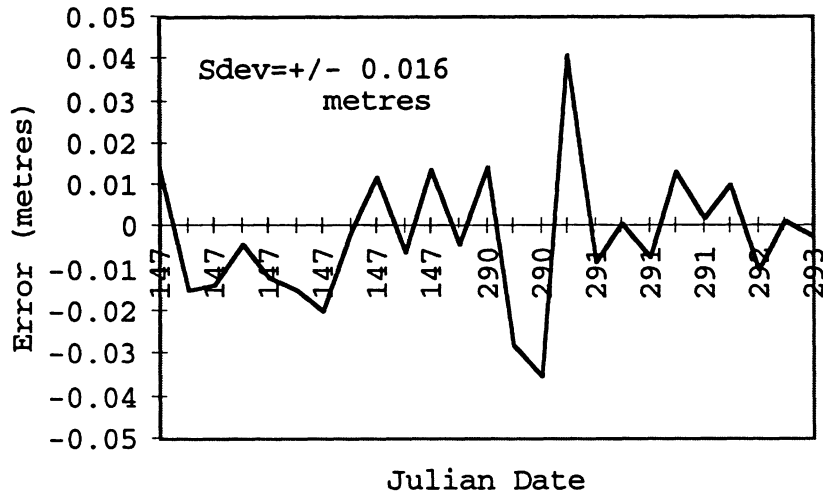
Figure 6.5

Estimated random errors CHAT water level sensor.
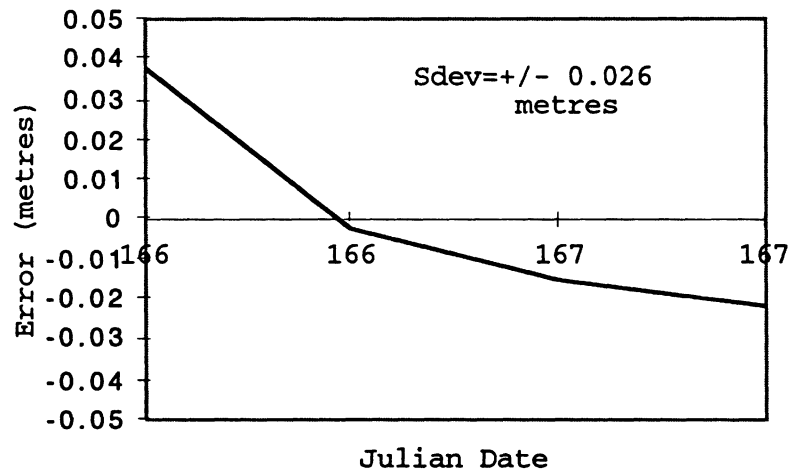
Figure 6.6

Estimated random errors NEWC water level sensor.

comparisons for all four water level sensors. A Chi-Square goodness of fit test for normality was performed on all 77 water level sensor error estimates. The hypothesis that the water level sensor errors were normally distributed with sample **mean -0.0007 metres** and sample **standard deviation +/- 0.013 metres** was **not** rejected at the **5%** significance level. See Table 6.5 for the results of this test and similar tests on the individual water level sensor errors. The corresponding **95% confidence error estimate** for an individual observation at any water level sensor was **+/- 0.025 metres.** The FLOY and CHAT water level sensor errors (Figures 6.3 and 6.5) each have two distinct peaks on Julian Days 290 and 291. These peaks were due to choppy wave conditions, which were **not** the norm during the OTF DGPS river surveys; only day 166 had similar roughness.

6.2.1.2 Accuracy Assessment for Individual Water Level Sensors

The third accuracy assessment on the bias-corrected errors looked at the errors for individual water level sensors. All available water level sensor - staff comparisons at each water level sensor site were used. The most reliable accuracy estimates were obtained for the FLOY, CHAT, and MBNK water level sensors, due to the sizes of the samples involved, and the fact that height checks were obtained throughout most of the available range of water levels.

Table 6.5

Statistical assessment of water level sensor random errors.

Stat-ion	Samp Size	Sample Mean (Metres)	Root Mean Square Error (Met-res)	Sample Sdev (Met-res)	Goodness of Fit Test	95% Conf-dence. Limits (metres)
FLOY MBNK CHAT NEWC	77	-0.0007	0.013	**0.013**	**Pass**	**+/- 0.025**
FLOY	34	$2.94*10^{-5}$	0.009	**0.010**	**Pass**	**+/- 0.020**
MBNK	14	$-7.14*10^{-5}$	0.008	**0.009**	Sample too small to perform test	**+/- 0.018**
CHAT	25	-0.002	0.016	**0.016**	**Pass**	**+/- 0.031**
NEWC	4	0.000	0.023	**0.026**	Sample too small to perform test	**+/- 0.051**

The water level sensor errors were also plotted against tide staff height, in addition to being plotted against Julian Date as in Figures 6.3 to 6.6. No trends were apparent in these plots, indicating that the remaining water level sensor errors appear random. The one exception is the NEWC gauge, where the sample size is too small to determine randomness.

For the FLOY and CHAT stations, a Chi-Square goodness of fit test on the estimated water level sensor random errors, using the sample means and standard deviations, **passed** at 95% confidence. The 95% confidence error estimates for a single water level height measurement with these water level sensors were +/- 0.020 and +/- 0.031 metres, respectively.

The MBNK sample was not quite large enough to perform a Chi-Square test for normality. This was because the water level sensor was not up and running during the preliminary reconnaissance stage (section 5.3). The MBNK errors were assumed to be normally distributed, because:

(1) The entire set of 77 water level sensor errors for all water level sensors was normally distributed.

(2) The MBNK site error estimates were obtained throughout the full range of water levels, in wave conditions that were similar to those at FLOY and CHAT, where the errors were statistically shown to be normally distributed.

Assuming normality in the MBNK water level sensor errors, the 95% confidence error estimate for this water level sensor was +/- 0.018 metres.

The NEWC accuracy estimates are by far the least reliable, as they are from an extremely small sample, and were obtained through a smaller range of water level heights vs the other sensors. This was because the NEWC water level sensor was not up and running during the preliminary reconaissance (section 5.3), or during Julian Days 291, 292, and 293.

Nonetheless, four height checks were obtained at NEWC during Julian Days 166 and 167 (the only days the water level sensor was running), and indicate an approximate 95% confidence error estimate of +/- 0.051 metres for this water level sensor, assuming a normal distribution. The NEWC water level heights were thought to be accurate enough to be used for ground truthing the OTF DGPS water's surface elevations for days 166 and 167, because:

(1)   The staff checks were taken throughout 75% of the full range of observed water levels.

(2)   The staff checks were taken on both day 166 and 167, in wave conditions that were representative of those experienced during the day 166 and 167 river elevation surveys.

6.2.2 In Situ Water Level Sensor Accuracy vs Predicted Accuracy

We will now compare the in-situ accuracy of the Socomar bubbler water level sensors as a whole from section 6.2.1.1 with the predicted accuracy. Following Hare and Tessier [1995], we state that the fundamental equation for the height of the water's column from a differential pressure sensor is given by:

$$h = \frac{dp - \rho_a g \Delta H}{g(\rho_w - \rho_a)} \quad , \qquad (6.1)$$

where h is the water's column height; dp is the measured difference between total pressure and atmospheric pressure; ρ_w is the mean density of the water's column; g is the acceleration of gravity; ΔH is the height difference between the locations of the underwater pressure sensor and the atmospheric pressure sensor; ρ_a is the density of air.

We can then apply the law of propagation of errors to equation (6.1). Since Hare and Tessier [1995] have shown that the effect of errors in ΔH and g can reasonably be neglected, and considering the fact that the atmospheric density error is not applicable due to the mechanical design of these water level sensors, we can obtain the following simplified differential equation for the error in water column height:

$$\sigma_h = \sqrt{\left(\frac{\partial h}{\partial p}\right)^2 \sigma_p^2 + \left(\frac{\partial h}{\partial s}\right)^2 \sigma_s^2 + \left(\frac{\partial h}{\partial t}\right)^2 \sigma_t^2} \quad , \tag{6.2}$$

where σ_h is the 68% confidence error in water's column height; σ_p^2 is the variance of the pressure measurement from the underwater pressure sensor; σ_s^2 is the variance of user-estimated salinity; σ_t^2 is the variance of the user-estimated temperature; ∂h represents the partial derivative with respect to the unknown parameter, h.

We will use approximations for the various partial derivatives in equation (6.2). The partial derivatives in equation 6.2 are very tedious. Evaluating them fully would not improve the accuracy estimates greatly, given the fact that the water level sensors were located in only 3 metres of water at most. Instead, the manufacturer's claim for height error due to pressure measurement error will be used, along with previously derived error estimates for the effects of salinity and temperature measurement errors on water column height. These water column height error estimates were obtained in Phelan [1992] by using an empirical equation of state for sea water to estimate the error in water's column height due to salinity and temperature error.

Marso [1995] claimed a +/- 0.01 metre error for the bubbler water level sensor, independent of water depth (up to a range of 10 metres). It was assumed that: (1) the

110

estimate was a standard deviation, and (2) since this error estimate was **independent** of the water's depth it is logical to assume that the error was a **resolution** on the water's column pressure measurements, independent of the temperature and salinity input by the user. This pressure resolution is similar to the angular resolution on a repeating theodolite -- i.e it is independent of the magnitude of the measurement. These two assumptions were also made by Hare and Tessier [1995]. The corresponding 95% error estimate, assuming a normal distribution for the errors, was +/- **0.020 metres.**

Let us now look at the effect of estimating temperature and salinity values. We will assume that the salinity and temperature errors are uncorrelated. Consider that there is only a 1.5 metre water level range at most in the OTF DGPS survey area (recall Figure 5.1). For a 95% confidence error in the user - estimated salinity of +/- 10 ppt, this would give a 95% confidence error of +/- **0.012 metres** in water column height. A 95% confidence error in user-estimated temperature of +/- 10° C would correspond to a 95% confidence error of +/- **0.002 metres** in water column height [Phelan, 1992].

Timing error in the water level sensors is the final error component. Water level sensor time was compared against a time signal obtained from the Weather Network cable TV broadcast. The time comparison was done by logging into the sensors from a local hotel. The largest

discrepancy between the water level sensors and this time signal was **3** minutes. Let us assume that this is a 95% error estimate. The maximum observed rate of change of water level height is 0.005 metres/minute. This was recorded during the falling tide at CHAT on Julian Day 147 after an onshore gale which diminished at high tide. The corresponding height error was +/- 0.015 metres at the half tide level. This was near the noise level of the water level sensors. Therefore, the timing errors were not corrected in the water level sensor data.

The 95% confidence limits for a single water level sensor height under the worst case conditions mentioned above was obtained by adding the errors quadratically. The result was **+/- 0.028** metres at 95% confidence. This compared favorably with the empirical 95% confidence value of **+/- 0.025** metres obtained for the water level sensors as a whole in section 6.2.1.1.

6.3 Vessel Squat Tests

The squat tests met their goal, which was to obtain the correlation between RSOG changes and changes in the antenna height above the water's surface at RSOG's of 10, 20, 30, and 40 kph. However, several important improvements would be needed for future squat tests. These improvements can be found in section 6.3.2.

6.3.1 Squat Test Results

An average of four lines was run at each RSOG. Restrictions on the amount of available time, however, forced the tests to be much shorter than anticipated. This meant fewer lines at each RSOG, and larger speed increments between lines, than had been planned.

The ellipsoidal elevation HANTSP of the OTF DGPS antenna above the water's surface was obtained using equation 5.2 in section 5.8.2. The ellipsoidal elevation HANTGPS of the OTF DGPS antenna above the water's surface was obtained from equation 5.3 in section 5.8.2.

A problem was present with the reference water levels for the squat tests. A 0.26 metre discontinuity in the Uncorr water level heights was visible at 18:27 GPS time in Figure 6.7. The discontinuity occurred as a switch was made from tide tape readings at the squat test site to readings at the tide staff (200 metres away).

The most likely cause for the discontinuity is a length error in the tide tape that was used to measure the water's surface elevation. The **tide staff** was assumed to be **correct** for two reasons: (1) the leveling between it and point NEWC was in the form of a closed loop, (2) the HANTGPS from this reference matched the HANTGPS from the CHAT, MBNK, and FLOY water level sensor stations within +/- 0.05 metres. The water level discontinuity affected the

absolute value of HANTGPS and HANTSP (recall Figure 5.5) at all RSOG's by about 0.26 metres. This problem was mostly alleviated in the Corr heights by adjusting the earlier tide tape part of the water level curve to fit the later tide staff half.
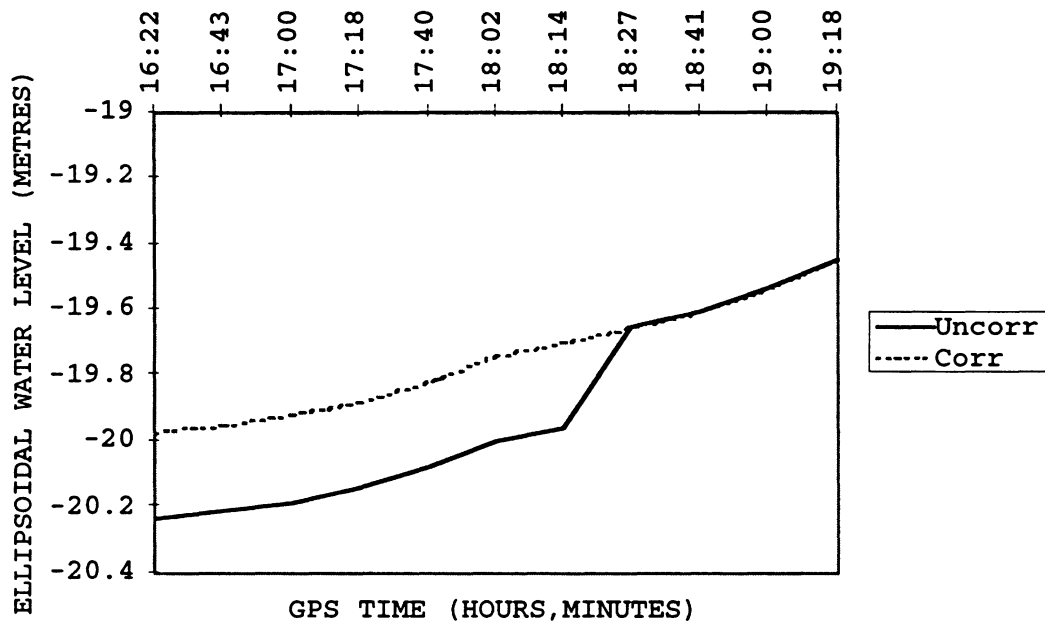
Figure 6.7

Day 293 squat test reference water levels.

It was decided that the squat tests would be used only for the **relative** changes in antenna height, due to: (1) the approximate nature of adjusting the two halves of the water level curve, and (2) an unexplainable bias between the HANTSP and HANTGPS antenna heights. See Table 6.6 for a comparison of the different squat test antenna heights, corrected for the 0.26 metre bias mentioned above. The **best**

114

Table 6.6

Spirit level and OTF DGPS derived antenna heights
from Julian Day 293 squat tests
(corrected for .26 metre bias in reference water level
height).

RSOG (kph)	Level Antenna height (Metres)	GPS Antenna Height (metres)	Difference (Metres)
0	3.277	------------	----------
10.000	3.283	3.165	0.118
10.000	3.281	3.195	0.086
10.000	3.278	3.220	0.058
10.000	3.282	3.218	0.064
Sdev(metres)	**0.002**	**0.026**	
20.000	3.502	3.410	0.092
20.000	3.490	3.408	0.082
20.000	3.487	3.391	0.096
20.000	3.438	3.338	0.100
Sdev(metres)	**0.028**	**0.034**	
30.000	3.576	3.485	0.091
30.000	3.570	3.468	0.102
30.000	3.585	3.496	0.089
Sdev(metres)	**0.008**	**0.014**	
40.000	3.592	3.560	0.032
40.000	3.573	3.528	0.045
40.000	3.602	3.534	0.068
40.000	3.612	3.483	0.129
Sdev(metres)	**0.017**	**0.032**	

115

repeatability (lowest standard deviation (Sdev)) for all runs at all RSOG's was for the HANTSP observations. It was apparent that the rate of change of HANTSP is **greatest** for the range of RSOG's from 10 to 20 kph. See Table 6.7, which shows the **average rate** of HANTSP change versus RSOG.

Table 6.7

Spirit level derived rates of antenna height change versus resultant SOG - Day 293 squat tests

RSOG (kph)	Height Increase (Metres/kph)
0-10	+0.000
11-20	+0.019
21-30	+0.010
31-40	+0.002
41-44	0.002****

****extrapolated from HANTSP height change in 30-40 kph RSOG range

There are two important limitations on the HANTSP and HANTGPS:

(1) **No bathymetry** was measured or used. This is **not acceptable**, because the antenna heights could be different in different water depths.

(2) Correlating antenna height change with RSOG

change will **not** model antenna height changes
due to currents.

Keeping in mind the bathymetry and current limitations
in the previous paragraph, the HANTSP and HANTGPS antenna
heights have good repeatability when RSOG is **mostly**
constant. When the RSOG varies significantly, there is a
clear correlation between changes in HANTSP (due to changes
in ellipsoidal elevation of the remote antenna center) and
changes in RSOG. This correlation is visible in Figure 6.8,
which shows PRISM-PNAV RSOG and ellipsoidal elevation of
the remote antenna center from one of the day 292 river
elevation survey runs between MBNK and FLOY (see section
6.4 for details on the river elevation survey runs). If
uncorrected, this correlation would be significant at the
required 0.10 metre water level measurement/interpolation
accuracy for DPW soundings.

6.3.2 Proposed Squat Test Procedure

The proposed squat tests are very tedious and time
consuming. They must quantify the error in antenna height
above the water's surface, on a **vessel by vessel and**
survey by survey basis, throughout the **full** range of
conditions that would ever be experienced in dredging and
sounding surveys. Therefore, the tests should:

(1)   Be performed in the maximum and minimum salinity

117

values that the vessel would ever undergo, if a-priori calculations such as those performed in section 6.4.3 show squat changes due to salinity effects to be significant.
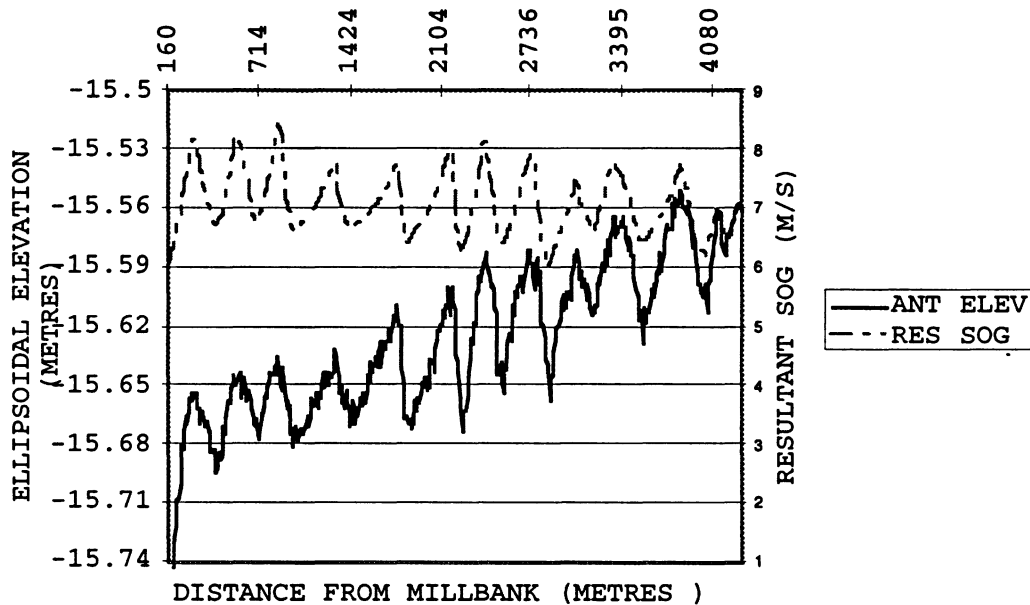
Figure 6.8

Resultant SOG - ellipsoidal antenna elevation correlation MBNK to FLOY day 292.

(2) Assess the effect of all possible variations in vessel loading, especially if the loading is not located symmetrically fore and aft of the center of rotation.

(3) Use **Resultant Speed Through the Water** (RSTW) vs RSOG as the basis for correcting the antenna

118

heights for changes in vessel speed. Two methods
of obtaining RSTW need to be investigated:

(a) The use of engine revolutions per minute
     (RPM) as suggested by Henderson [1995].

(b) The use of current measurements **on the
     vessel.**

(4) Be carried out in the full range of current
     conditions that can ever be expected.

(5) Be run with small increments of speed (say 5 kph
     increments between repeated lines), so that a
     detailed representation of the variation in
     antenna height with respect to vessel RSTW can
     be determined.

(6) Have a high number of repeated lines at each
     RSTW. The number of repeated lines at each
     RSTW should be at least 30 for good
     redundancy, so that a full statistical assessment
     of the errors in antenna height can be made.

(7) Investigate how strongly antenna height
     is affected by squat changes when the vessel
     passes over changing bathymetry -- i.e. narrow
     channels, and areas where the depth to squat
     ratio is less than 2.5 or so [Bowditch, 1984].

(8) Have the OTF DGPS base stations immediately
     adjacent to the squat test area, so that the
     antenna heights determined from OTF DGPS
     observations will be minimally affected by

noise from tropospheric/ionospheric effects.

(9) When wave conditions permit, have a second
     technique besides the OTF DGPS observations
     themselves for determining the antenna heights
     (i.e. spirit level observations).

(10) Use at least three remote stations on the vessel,
     so that:

     (a) The known separations between the
          remotes can be used as quality control
          checks on the OTF DGPS measurements.

     (b) **Investigations** into attitude sensing can
          be performed -- i. e. pitch, roll, and heave
          can be measured, perhaps in combination with
          a pitch/roll/heave sensor. Figure 6.9 shows
          the pitch (θ) and roll (γ) angles. Heave is
          the vertical displacement of the vessel from
          its equilibrium state (i.e. displacement
          from when vessel is completely stationary to
          when vessel is subject to waves and motion
          effects).

(11) Use at least two OTF DGPS base stations on shore
     so that the known baseline length between the
     stations can be used as a quality control check.

(12) Be mostly performed in reasonably calm
     conditions, so that (9) can be used. Some rough
     conditions are needed so that (10b) can be
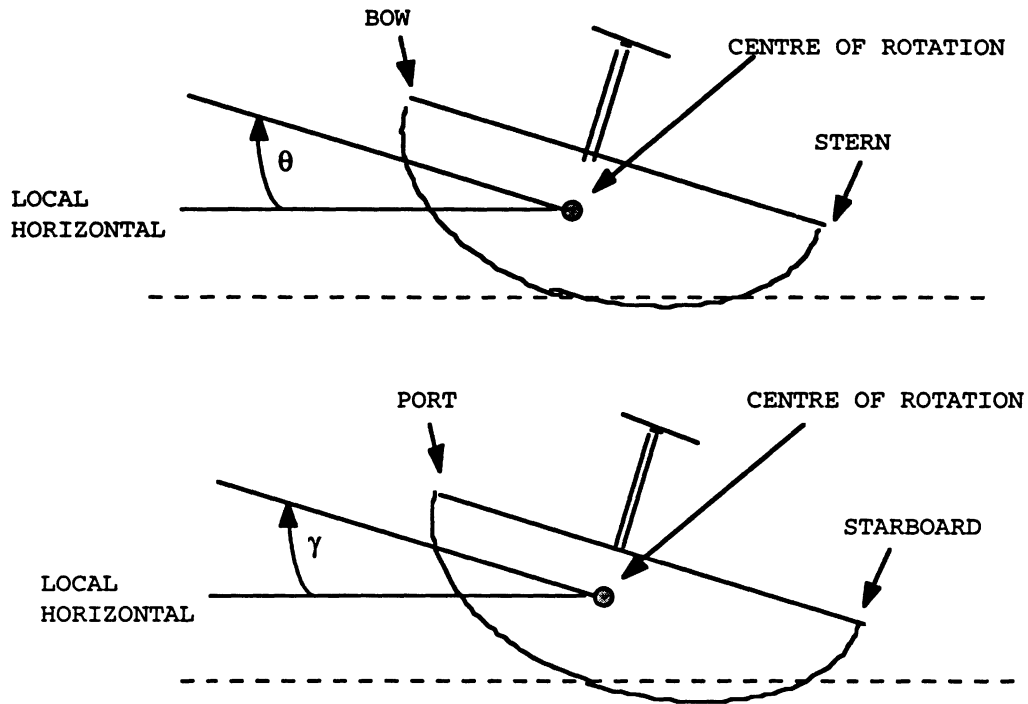
Figure 6.9

Pitch and roll parameters

assessed, however.

(13) Ensure that RSTW magnitudes and RSTW fluctuations
(due to helmsman piloting) are similar to RSTW
magnitudes and fluctuations that would be
experienced during actual dredging and sounding
surveys.

(14) Use a water level sensing technique that filters
out the effects of waves, so that (10b) above can
be used -- i.e. use a digital water level sensor.

6.4 River Water's Surface Elevation Survey Results

The OTF DGPS data was processed with the PRISM-PNAV post-processing OTF DGPS package. Factory default values were used for the various PNAV settings. Note that forward and backward processing was used, with ambiguities fixed. Maximum baseline lengths were less than 10 kilometres. As discussed in section 3.5, this should yield a 1σ RMS accuracy of 0.01 - 0.1 metres after 2-5 minutes of continuous carrier phase data with no cycle slips. The RANG station's 3-D network adjustment coordinates were held fixed for all OTF DGPS processing.

6.4.1 Accuracy of RSOG-Uncorrected OTF DGPS Antenna Heights

The water level sensor ellipsoidal water level ground truth was the most **accurate** when the vessel passed within about 100-200 metres of the water level sensors. In this situation it was unlikely that there was any significant water's surface elevation difference between the vessel location and the water level sensor station.

As a **primary check** on the **vertical accuracy** of the **OTF DGPS** water's surface, the vessel's RSOG-uncorrected antenna height ($Unant_i$) above the water's surface was derived by subtracting the OTF DGPS ellipsoidal antenna elevation from the water level sensor ellipsoidal water's

surface elevation as the vessel passed **near** the water level
stations (within 100-200 metres). The formula was:

$$Unant_i = (Elsm_i - Eltide_i), \qquad (6.3)$$

where $Elsm_i$, i=1,2,...30 was the ith smoothed OTF DGPS
ellipsoidal elevation of the vessel's GPS antenna; $Eltide_i$
was the ellipsoidal elevation of the water's surface from
the water level sensor or tide staff. Figure 6.10
illustrates these terms.
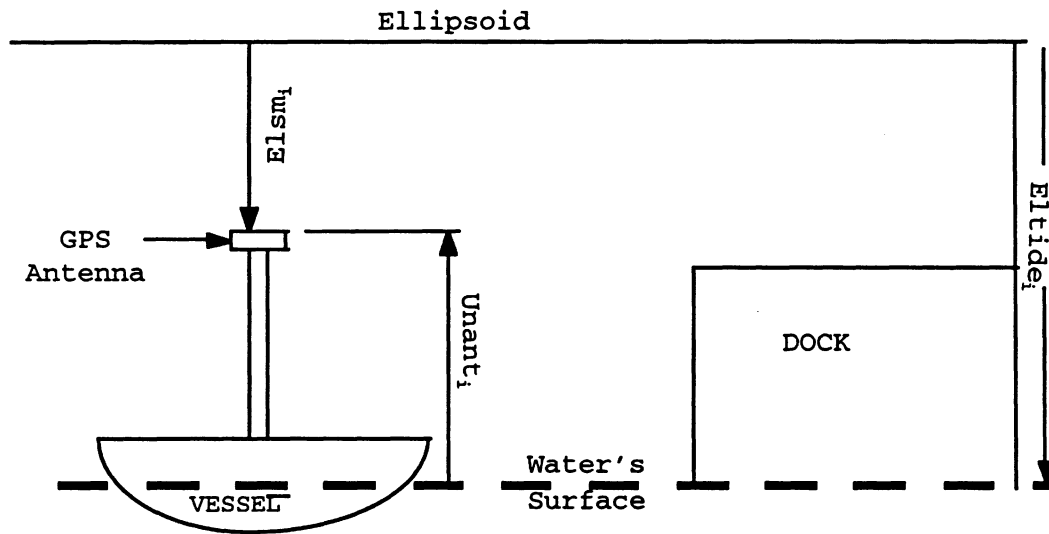
Figure 6.10

Quantities for calculating RSOG-uncorrected antenna heights

Each $Elsm_i$ value was obtained by using a 40 second
numerical average of the observed ellipsoidal antenna
elevations at each water level station. As the OTF DGPS
recording rate was one second, this meant an average of 40

123

numbers. The standard deviation of this estimate was at most +/- 0.015 metres, due to the near-calm water surface conditions. The ellipsoidal water's surface elevation was usually obtained from the Socomar water level sensors, with a linear interpolation between the 20 minute water level heights when needed. The linear interpolation residuals were usually +/- 0.01 metres or less for a series of three 20 minute interval water level heights. Tide staff readings at 20 minute intervals were used when a water level sensor had gone down.

6.4.2 Accuracy of RSOG-Corrected Antenna Heights

Each $Unant_i$ from section 6.4.1 was then corrected back to a **base speed** of **10 kph.** This was done so that all the corrected antenna heights could be statistically tested to see if they belonged to a normal distribution. The equation for correcting to 10 kph was:

$$Corrant_i = Unant_i * Rf_{RSOG},\qquad(6.4)$$

where $Corrant_i$ was the RSOG-corrected antenna height; Rf_{RSOG} was the reduction factor to correct $Unant_i$ back to the 10 kph base speed.

The 10 kph base speed was chosen because the squat tests indicate that between 0 and 10 kph there is no

significant change in $Unant_i$ with increasing vessel speed. The spirit level - derived relative changes in vessel antenna height from the squat tests (recall Table 6.7) were used to derive Rf_{RSOG} for correcting the $Unant_i$ antenna heights back to the 10 kph base speed. The spirit level observations have been used because they show the lowest overall standard deviation for repeated runs at the same speed. Note that the correlation between change in vessel RSOG and change in antenna height **decreases** as we move into the upper speed range between 8 m/s (30 kph) and 11 m/s (40 kph). This has important implications for procedures to be followed in any future squat-dependent OTF DGPS water's surface elevation surveys.

The $Corrant_i$ values will not agree with each other due to the following error sources:

(1) Errors in the water level sensor water's surface elevation $Eltide_i$.

(2) Errors in the ellipsoidal height of the control points.

(3) Errors in the Rf_{RSOG} factor from the squat tests.

(4) Errors in determining the $Elsm_i$ value.

(5) Errors resulting from the fact that RSOG - based antenna height corrections do not account for antenna height changes due to current changes.

The **standard deviation** of the $Corrant_i$ heights is +/- **0.051 metres** for all **30** values derived from Julian

125

Days 167, 292, and 293. Julian Day 166 is **not** included due to problems with loss of lock. A Chi-square test for normality was performed on the $Corrant_i$ heights from Julian Days 167, 292, and 293, with sample mean $Corrant_m$ = **3.231 metres** and sample standard deviation $Corrant_s$ = +/- **0.051 metres**. The hypothesis that the sample was normally distributed with these sample values was **not rejected** at the 95% confidence level. However, a test for outliers using the out-of-context Tau test at the 95% confidence level showed that three $Corrant_i$ heights (3.128 metres, 3.342 metres, and 3.085 metres) had to be removed.

Subsequent to the removal of the three outliers, the Chi-Square test for normality was repeated at the 95% confidence level, with the sample mean $Corrant_m$ = **3.236 metres** and sample standard deviation $Corrant_s$ = +/- **0.035** metres. The normality hypothesis was **not** rejected. The **95% confidence limits** for a single $Corrant_i$ observation were **+/- 0.069 metres.** Note that this accuracy estimate was obtained with surface wave conditions **less than 0.10 metres** in amplitude.

6.4.3 Outlier Investigations on RSOG-corrected Antenna Heights

The first two rejected antenna height observations in section 6.4.2 are at the FLOY water level sensor. The last one is at NEWC. It is of course important to try to determine why these outliers exist. There are six possibilities:

126

(1) Changes in vessel loading affecting vessel squat.

(2) Changes in salinity affecting vessel squat.

(3) Improper squat correction due to rapid changes in vessel RSOG.

(4) Erroneous water level sensor height.

(5) Improper squat correction due to change in current speed.

(6) Unresolved OTF DGPS data improperly flagged as resolved, when in fact it is **not**.

Temperature effects will not be considered because their effect on water density is an order of magnitude less than salinity effects.

Vessel loading changes are not significant. We turn to the Admiralty Manual of Seamanship [1964] for the reasons. The the Tons per Inch Immersion (TPI) is the change in weight necessary to change the mean squat of a ship by 1 inch. It is assumed that the weight change is happening directly above the center of flotation, or is symmetrically disposed fore and aft of it. The TPI is given by:

$$TPI = \frac{A}{420} \text{ Imperial Tons,} \qquad (6.5)$$

where A is the waterplane area of the vessel in feet^2 (i.e. the area of a figure formed by intersecting the plane of the water's surface with the vessel).

For the OTF DGPS surveys, there were always 2 - 3 people on board. The people made a conscious effort to stay **centered** under the OTF DGPS antenna, which would by design be located close to the center of flotation of the vessel if it were at rest. We can now determine if adding and removing people will significantly affect the squat of the vessel. Since for the Gulf Surveyor the waterplane area was about 200 ft^2, the TPI was 0.48 Imperial Tons. The maximum foreseeable change in the weight of people on board was +/- 350 lbs. (difference between having two or three people aboard, and an empty or full gas tank). This corresponded to a +/- **0.009 metre** change in squat, which was **not significant at OTF DGPS accuracies.**

Salinity effects were **not** significant. We again turn to The Admiralty Manual of Seamanship [1964] for the reasons. The formula for determining the change in squat due to a change in salinity was given by:

$$S = \frac{W}{TPIS}\left[\frac{d_s - d_f}{d_f}\right],$$

(6.6)

where S was the sinkage in inches; W ws the displacement in Imperial Tons; TPIS was the Tons Per Inch Immersion in Salt Water; d_s was the density of salt water (64 LB/ft^3); d_f is the density of fresh water (63 LB/ft^3).

For the Gulf Surveyor, we first calculated the displacement. This was suitably done with:

128

$$DISP = (l * w * dr) * d_s ,\qquad\qquad (6.7)$$

where l was the length of the vessel (20 feet); w was the width of the vessel (10 feet); dr was the squat (2 feet); d_s is the density of salt water (64 LB/ft^3).

The displacement was calculated to be 13 Imperial tons, and the sinkage S to be 0.04 feet or **0.011 metres** for a complete change in salinity from salt to fresh water. Since the change of density with salinity is essentially linear, the change in squat per 1 ppt salinity was only 0.0003 metres/ppt. The observed salinity change during the river elevation surveys was only 5 ppt (see Table 5.3); a very pessimistic estimate of +/- 15 ppt change in surface salinity resulted in a **0.005 metre change in squat** which was still **negligible** at OTF DGPS accuracies.

As a check on whether or not the vessel was rapidly accelerating/decelerating, the squat corrections were rechecked. Such rapid acceleration and deceleration was only present at one of the locations with outliers. This may have been the reason that the outlier existed. The other two outliers at FLOY on days 167 and 292 did not occur when there were major changes in acceleration. There was obviously another cause.

In rechecking the water level sensor heights, the FLOY water level sensor data for day 167 does not look suspect,

because:

    (1)   The FLOY water level sensor was accurate, because it had the most extensive in situ calibrations of any of the water level sensors (34 staff checks throughout the full range of water levels).

    (2)   A staff check taken on day 166 matched one taken on day 167 within 0.02 metres.

With regard to the day 292 data, it was even less likely that there was a problem with the FLOY water level sensor heights. This was because four staff height checks were performed on this water level sensor on day 292, in calm conditions, spread throughout the time that the OTF DGPS lines were run to FLOY, with a maximum disagreement of only 0.015 metres between the four staff-water level sensor height biases.

The NEWC water level sensor data was somewhat more suspect. However, height checks were obtained on day 167. The 95% confidence error estimate of +/- 0.050 metres for this water level sensor is not large enough by itself to cause the outlier.

The fifth possibility was that squat changes due to current effects were occurring. Current measurements were unavailable during the day 293 squat tests, and unavailable as well as on day 292. The best that could be done was to look at upriver and down river runs from the day 166 and 167 data to see if Corrant¡ biases existed.

130

The day 166 data at NEWC clearly showed such biases (see Table 6.8). The biases consistently had the same sign. It was certainly possible that current effects caused the day 292 outlier at station FLOY. However, without current measurements for that day, it was impossible to say for certain.

The day 167 current data at NEWC showed somewhat similar current speeds. A clear bias of 0.17 metres was visible when the upriver RSOG - corrected antenna height is subtracted from the down river RSOG - corrected antenna height (see Figure 6.11). The bias had the same sign as the day 166 biases, but was larger, possibly due to the fact that the current was running **upriver**. Tidal plots for this day indicate that the current was probably running upriver due to the fact that the tide was rising at the beginning of this run. Table 6.9 shows the differences between upriver and down river runs for days 167, 292, and 293. For the day 292 and 293 data, only the first run on Julian Day 292 had clear biases with the same sign throughout the OTF DGPS survey area. Current measurements were needed on these days for a proper comparison with the day 166 and 167 data. Further field experiments would be **needed** so that the correlation between RSTW and antenna height bias can be better quantified.

Possibility #6 is that the PRISM software has flagged the OTF DGPS data at FLOY and NEWC as resolved when in fact it is **not**. Without current measurements for Day 292, and a

Table 6.8

Day 166 and 167 derived antenna height biases at NEWC.

Julian Date	Runs Used	Bias (Metres)	Current Direction	Current Speeds (Metres/ Second)
166	Uprun 1- down run1	0.12	Down river	0.65 0.40
166	Uprun 1- downrun 2	0.09	Down river	0.65 0.65
166	Uprun2- downrun1	0.09	Down river	0.53 0.40
166	Uprun 2- downrun 2	0.05	Downriver	0.53 0.65
167	Uprun- downrun	0.17	Downriver **up river**	0.51 0.25
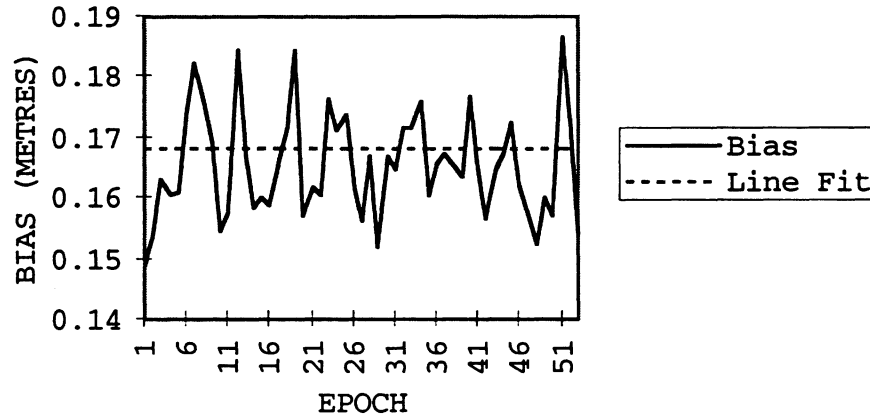
Figure 6.11

Possible current-induced antenna height bias at NEWC day
167.

full understanding of the relationship between current
speed and antenna height bias, we cannot tell if the data
has been improperly flagged as resolved, since the outliers
only failed the out of context Tau test by about 0.03
metres. An obvious loss of lock did not occur on days 167
and 292; day 166 shows water's surface "steps" of 0.3 to 10
metres due to unresolved ambiguities. In summary, then, we
have been able to rule out causes one through four as being
the cause of the day 292 outlier. For the day 167 outliers
only causes one, two, and four were ruled out.

Table 6.9

Comparison of all resultant SOG-corrected antenna heights
from Julian Days 167, 292, and 293.

Station	Julian Date	Down River Antenna Height	Upriver Antenna Height	Upriver Minus Down River
		(metres)	(metres)	(metres)
NEWC	167	3.085	3.250	-0.165
MBNK	167	3.193	3.233	0.040
FLOY	167	3.153	3.128	-0.025
NEWC	292	3.233	3.253	0.020
CHAT	292	3.204	3.236	0.032
MBNK	292	3.209	3.235	0.026
FLOY	292	3.206	3.245	0.039
NEWC	292	3.174	3.262	0.088
CHAT	292	3.311	3.284	-0.027
MBNK	292	3.277	3.214	-0.063
FLOY	292	3.342	3.290	-0.052
NEWC	293	3.243	3.277	0.034
CHAT	293	3.239	3.215	-0.024
MBNK	293	3.231	3.228	-0.003
FLOY	293	3.249	3.221	-0.028

6.4.4 Accuracy of OTF DGPS Water's Surface Elevations

If the $Corrant_m$ and Rf_{RSOG} values were used to obtain water's surface elevations for dredging and sounding surveys, the water's surface elevation would be obtained from:

$$Elwat_i = Elsm_i - Unant_m, \qquad (6.8)$$

where Elwat$_i$ is the OTF DGPS-derived elevation of the water's surface; Elsm$_i$ is the smoothed elevation of the GPS vessel antenna; Unant$_m$ = Corrant$_m$ * $\dfrac{1}{Rf_{SOG}}$ is an average uncorrected antenna height for the given RSOG.

Figure 6.12 shows the OTF DGPS water surface between MBNK and FLOY that was obtained using equation (6.8). Two other surfaces are shown:

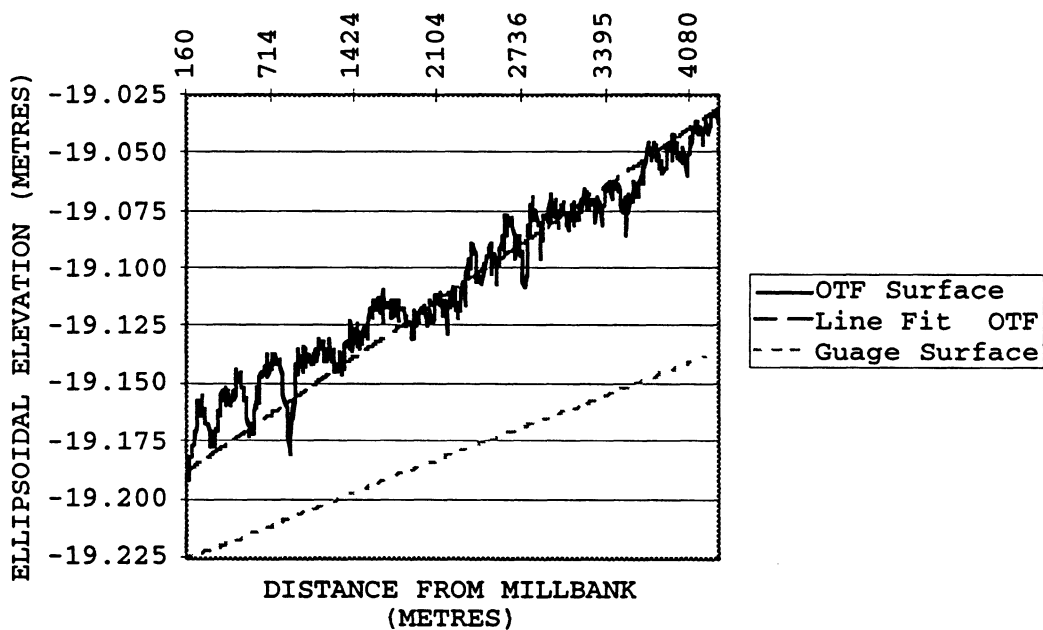   (1)   A line fit to the OTF DGPS water's surface.

Figure 6.12

OTF DGPS-derived ellipsoidal elevation of water's surface
MBNK to FLOY day 292.

    (2)   The linearly interpolated water level sensor
       surface.

135

It is clear in Figure 6.12 that the Rf_{SOG} corrections have been only partially effective in removing the RSOG-induced elevation variation that was visible in Figure 6.8.

The accuracy of Elwat is given by:

$$\sigma^2 Elwat_i = \sigma^2 Elsm_i + \sigma^2 Unant_m,$$ (6.9)

where $\sigma^2 Elwat_i$ is the variance in the OTF DGPS ellipsoidal water's surface elevation; the smoothed ellipsoidal antenna elevation variance $\sigma^2 Elsm_i = \dfrac{\sigma_{ANTEL_i}^2}{n}$, with $\sigma_{ANTEL_i}^2$ being the variance of any one of the n OTF DGPS ellipsoidal antenna elevations used to find the smoothed value $Elsm_i$; the average of a mean RSOG-uncorrected antenna height $\sigma^2 Unant_m = \dfrac{\sigma_{UNANT_i}^2}{n}$, with $\sigma_{UNANT_i}^2$ being the variance of an individual RSOG-uncorrected antenna height for the given RSOG.

For calculating $\sigma Elwat$ for the Miramichi surveys:

(1) $\sigma Elsm = +/-0.016$ metres, obtained using $\sigma_{ANTEL_i} = +/-0.10$ metres (accuracy from Table 3.5), and n =40.

(2) $\sigma Unant_m = +/-0.007$ metres, obtained using σ $Corrant_i = +/-0.035$ metres, and n=27.

Then, **$\sigma Elwat$ = SQRT(0.016^2+0.007^2)*1.96= +/-0.034 metres at 95% confidence.**

It must be made clear that σElwat does **not** include the effects of currents or bathymetry on the antenna heights. Therefore, in section (6.4.8) we present some improved methods for correcting the antenna heights.

6.4.5 OTF DGPS Availability as Indicated by PRISM flag

Previous PRISM OTF DGPS results from other OTF DGPS projects have cast some doubt as to whether the PRISM software is properly flagging unresolved data as being unresolved, especially on baselines over 20 kilometres in length [Wells, 1995b]. As a first approximation, therefore, the number of resolved/unresolved epochs as indicated solely by the PRISM flag value were tabulated (see Table 6.10). The Miramichi surveys, however, have the distinct benefit of having a controlled vertical reference surface -- the ellipsoidal water level sensor water's surface. This surface was later used to determine if unresolved OTF DGPS data was being properly flagged (see section 6.4.6).

6.4.5.1 Flag results on Julian days 167, 292, and 293

The PRISM flag value by itself indicates that on JD's 167, 292, and 293, one could expect around 1% loss of lock, after the effects of the Chatham bridge were manually removed from the total unresolved epoch count. The exception is day 293, where a power failure caused the percent loss of lock without bridge effects to jump to

9.9%. The Chatham bridge effects were easily removable, because they were flagged as unresolved, and in every case as one approached the Chatham Bridge a familiar pattern was

Table 6.10

Resolved and unresolved OTF DGPS epochs as indicated by
PRISM flag value.

Julian Date	Total Epochs at a 1 Second Interval	% Unresolved with Bridge Effects	% Unresolved Without Bridge Effects	Comments
				-----------
166	10,715	75	75**	-----------

167	6971	4.3	1.1	-----------

292	9249	5	1.2	-----------

293	2812	15.2	9.9	Power failure on vessel - - lock regained within 1 minute
293	5899	17.4	N/A	Squat tests at the 10 kilometre baseline limit

** bridge effects could not be removed

observed at essentially the same geographic position: all epochs were resolved (flag = 0), until satellites suddenly began to disappear from the raw data due to blockages. Loss of lock then occurred (flag=1). A sudden discontinuity in the water's surface was observed (up to 0.7 metres in magnitude, usually). Then, on the other side of the bridge,

138

the satellites reappeared, and the flag value returned to zero (lock regained). The water's surface would then be re-acquired within +/- 0.050 metres or so of its previous value before the bridge effects arose.

The water's surface in some of the "lost" lock sections for days 167, 292, and 293 does not show any significant change in water's surface elevation from the "resolved" data immediately before it. This suggests that the PRISM software may actually be flagging resolved data as unresolved in some cases, which is better than the alternative.

6.4.5.2 Day 166 availability results

Day 166 availability proved to be much worse than the other three days, with 75% of the epochs unresolved. It was not possible to separate out the bridge effects, because the OTF DGPS observations were not resolved prior to passing under the bridge. It was however abundantly clear that the bridge exacerbated the existing loss of lock problem, as 0.3 metre to 10 metre vertical steps in the water's surface elevation were observed. One of the possible causes of the Day 166 data being unresolved was ruled out: the Notices to Navstar Users (NANUS) for that time period indicate **no** bad satellites. A graphical analysis of the PDOP and number of satellites for days 166, 167, 292, and 293 was also performed to determine if the

PDOP and number of satellites for day 166 were the cause of the loss of lock. There is no obvious cause for the day 166 problems. A numerical investigation into the PRISM "L" and "J" files should be performed to determine the cause of the day 166 loss of lock problems.

6.4.6 OTF DGPS Reliability Comparisons with Interpolated Water Level Sensor Water Surfaces

A somewhat less accurate check on the accuracy of the OTF DGPS water's surface elevation measurements comes from comparisons with a linear interpolation in time and distance between water level stations. It is less accurate due to the assumption that the water's surface is varying linearly between the water level sensors. The interpolated water surface is, however, a fairly useful method for determining if OTF DGPS data has been flagged as being good when it is not.

The OTF DGPS water surface was obtained by using equation (6.8). The spirit level observations were used because they showed the best repeatability (lowest standard deviation for lines repeated at the same speed). For example, given $Elsm_i$ = -18.000 metres, at an RSOG of 20 kph, the corresponding OTF DGPS water's surface elevation would be -21.426 metres. Since the squat tests were not run at speed increments of 5 kph, it was necessary to **assume** that the antenna height change was **linear** with speed change within each of the four speed ranges. It was

140

apparent that the OTF DGPS water's surface never deviated from the linearly interpolated water level sensor surface by more than **0.20 metres**, and is generally within **+/- 0.05 metres**.

The most important question with respect to OTF DGPS reliability, as stated by Wells [1995b], is whether or not **unresolved data** was properly flagged. The danger was in relying completely on the software to correctly flag unresolved data.

It is crucial to determine how well the linearly interpolated ellipsoidal water's surface can detect loss of lock. Figure 6.13 shows two generic water level stations located 10 kilometres apart. In this figure, we have the following quantities:

(1)   Water level sensor stations A and B.

(2)   Distance DDAB between the two tidal stations.

(3)   Distance DDAX between water level station A and the survey vessel at midpoint X.

(4)   Heights HTA and HTB below the ellipsoid for the survey points at stations A and B.

(5)   Offset GOFFA of water level sensor's water level from survey point at station A.

(6)   Offset GOFFB of water level sensor water level from the survey point at station B.

The linearly interpolated height of the water's surface

Ellipsoid (elevation 0)

HTA

HTB

MIDPOINT

WATER'S
SURFACE
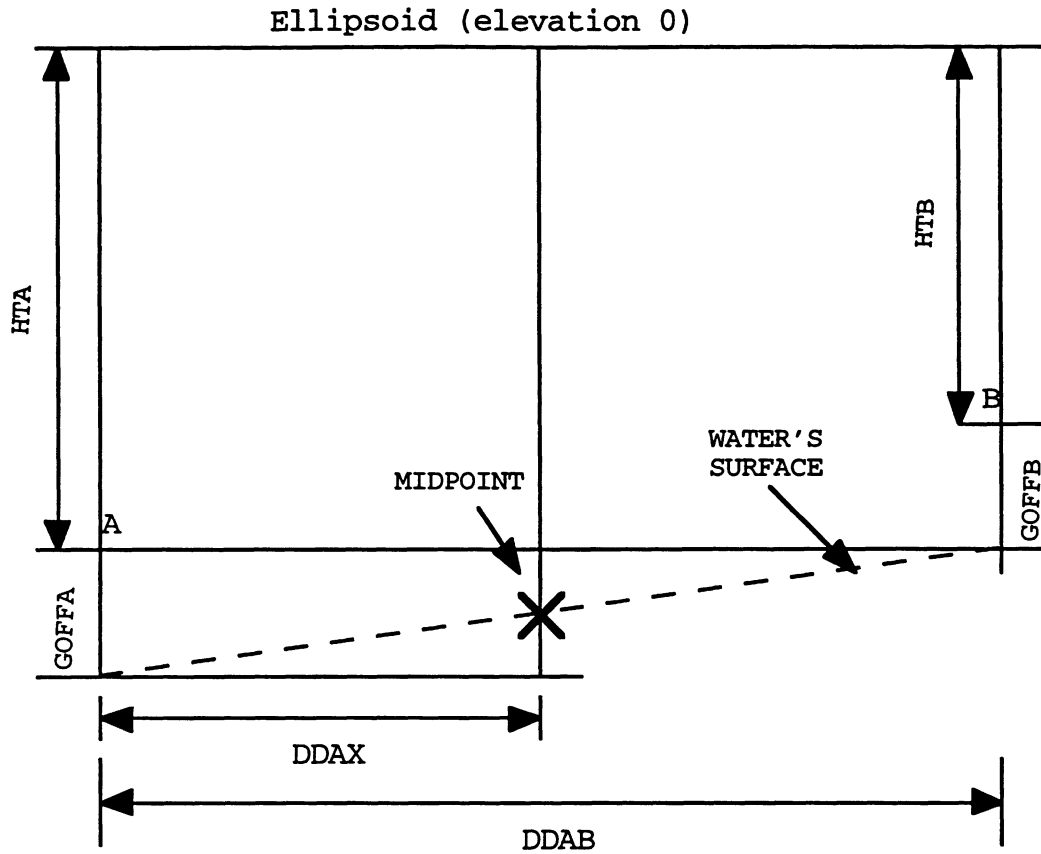
GOFFB

A

GOFFA

B

DDAX

DDAB

Figure 6.13

Generic set of water level sensors.

at point "X" is given by the following relationship:

$$HTX = HTA - GOFFA + \left(\frac{(HTB - GOFFB) - (HTA - GOFFA)}{DDAB} \right) * DDAX,$$

(6.10)

Assuming that all the errors in the above equation are random and uncorrelated, and applying the law of propagation of errors, we obtain the following partial

differential equation for the error in water's surface height at midpoint X:

$$\sigma_{HTX}^2 = \left(1 + \left(\frac{-DDAX}{DDAB}\right)\right)^2 \sigma_{HTA}^2 + \left(-1 + \left(\frac{-DDAX}{DDAB}\right)\right)^2 \sigma_{GOFFA}^2 +$$

$$+ \left(\frac{DDAX}{DDAB}\right)^2 \sigma_{HTB}^2 + \left(\frac{-DDAX}{DDAB}\right)^2 \sigma_{GOFFB}^2 +$$

$$+ \left(DDAX\left((-)\frac{(HTB - GOFFB) - (HTA - GOFFA)}{DDAB^2}\right)\right)^2 \sigma_{DDAB}^2 +$$

$$+ \left(\left(\frac{(HTB - GOFFB) - (HTA - GOFFA)}{DDAB}\right)\right)^2 \sigma_{DDAX}^2 + \sigma_{INTERP}^2,$$

$$(6.11)$$

Let us now discuss the **95% confidence** errors that will be put into equation (6.11). The σ_{HTA} term will be set to zero, since we are dealing with the relative height error between the two stations. The $\sigma_{GOFFA} = \sigma_{GOFFB}$ term will be set to +/-0.030 metres, based on the worst case water level sensor error of +/- 0.028 metres and on a very pessimistic spirit leveling error of +/- 0.01 metres between the OTF DGPS survey point and the tide staff. The σ_{HTB} term is set to +/- 0.04 metres (based on the worst case relative height error from the control network adjustment). For $\sigma_{DDAB} = \sigma_{DDAX}$ the accuracy is +/- 0.03 metres, again based on the control network adjustment results. Finally, for the σ_{INTERP} term, we will assume

143

that the error in the linear interpolation is random, with magnitude +/- 0.098 metres. This error comes from statements made by Crookshank [1994], and Goguen [1994], that assuming a straight line water's surface between water level sensors in the OTF DGPS survey area will cause a difference of about 0.050 metres (we will assume it is a standard deviation) versus the water's surface obtained from a one-dimensional hydraulic model for this section of river.

Table 6.11 shows the estimated error in the linearly interpolated water's surface for a worst case scenario where the vessel is located exactly in the **middle** of a section between two water level sensors. Thus the linearly interpolated ellipsoidal water's surface reference has the ability to detect OTF DGPS water's surface elevation errors **greater than +/- 0.110 metres 95% of the time** at the midpoint X. At the water level sensor location itself, we are essentially able to detect any OTF DGPS water's surface elevation errors greater than the 95% error estimate for the water level sensor heights.

The important point to note is that since we do not have current observations for the majority of the OTF DGPS river survey data (days 292 and 293 to be specific), or for the day 293 squat tests, we are only able to see **combined** effects of current biases and loss of lock biases (if they exist). Without actual current observations for these days, we cannot say for sure that the ambiguities are unresolved,

144

Table 6.11

95% confidence error estimate for interpolated water level sensor surface at the midpoint.

Description	Numerical Value (Metres)	95% Confidence Error Estimate (Metres)
HTA	-19	$\sigma_{HTA} = +/-\ 0.00$
GOFFA	1.2	$\sigma_{GOFFA} = \ +/-\ 0.03$
HTB	-18	$\sigma_{HTB} = +/-\ 0.04$
GOFFB	2	$\sigma_{GOFFB} = \ +/-\ 0.03$
DDAB	10,000	$\sigma_{DDAB} = \ +/-\ 0.04$
DDAX	5,000	$\sigma_{DDAX} = \ +/-\ 0.04$
INTERP	N.A.	$\sigma_{INTERP} = \ +/-\ 0.\ 098$
σ_{HTX}	N.A.	**$+/-\ \ 0.11$**

145

unless there are obvious step functions in the water's surface.

6.4.7 A Search for Spatial Variations

Since the goal of this field project was to see if OTF DGPS is capable of measuring spatial variations in water's surface elevation, two day 293 OTF DGPS runs between MBNK and FLOY were analyzed. A spatial variation should be visible in the **line fit residuals** for **both** an upriver and downriver run, if: (1) both runs pass over the **same** physical locations, and (2) the time interval between passing over the same locations is **short**. The day 293 runs met these criteria, with a difference of only 2 minutes between the end of the downriver run and the beginning of the upriver run.

Figure 6.14 shows the residuals from a line fit to the OTF DGPS water's surface from the MBNK-FLOY run. This water's surface was obtained by using the equation (6.8) from section 6.4.4. An attempt was made to use a simple fixed antenna height correction, but RSOG variations were too large.

The only spatial variations that can be detected are ones that are larger than the noise level of OTF DGPS. This noise level will be at least as high as the estimated network adjustment height difference accuracy -- around +/- 0.03 metres at 95% confidence. The magnitude of the line

fit residuals in Figure 6.14 is at or below the noise level
of the OTF DGPS measurements. Thus we **cannot** say that any
spatial variations have been detected.

Figure 6.15 shows the residuals from a line fit to the
OTF DGPS water's surface for the FLOY-MBNK run. Again, all
structure is at or below the noise level of the OTF DGPS
network adjustment ellipsoidal height differences.

6.4.8 Proposed OTF DGPS River Elevation Survey Procedure

Future real-time or post-processing squat-dependent
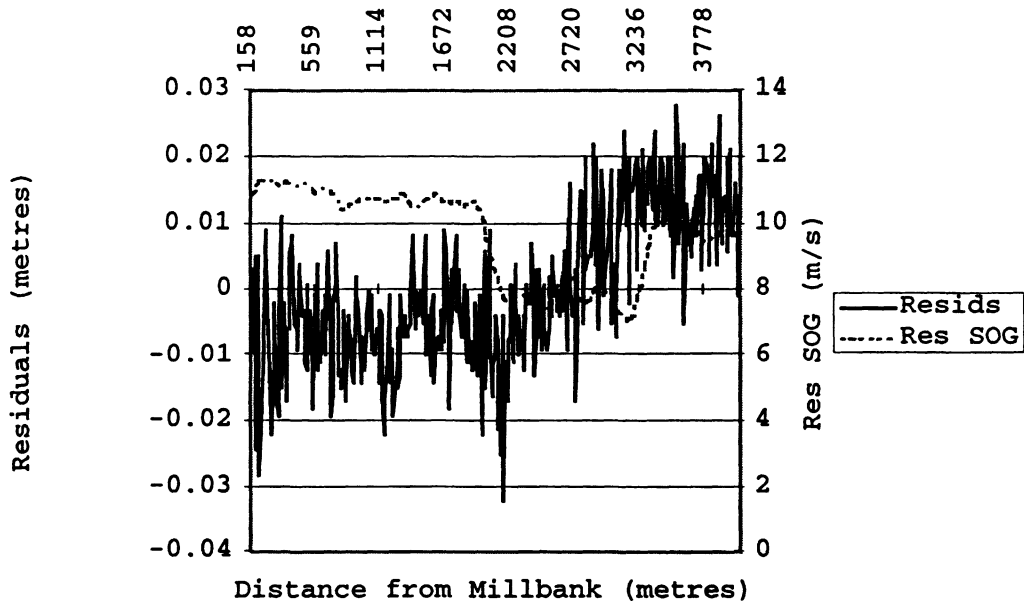OTF DGPS water surface elevation surveys would have to

Figure 6.14

Residuals from line fit to OTF DGPS water's surface
MBNK to FLOY day 293.
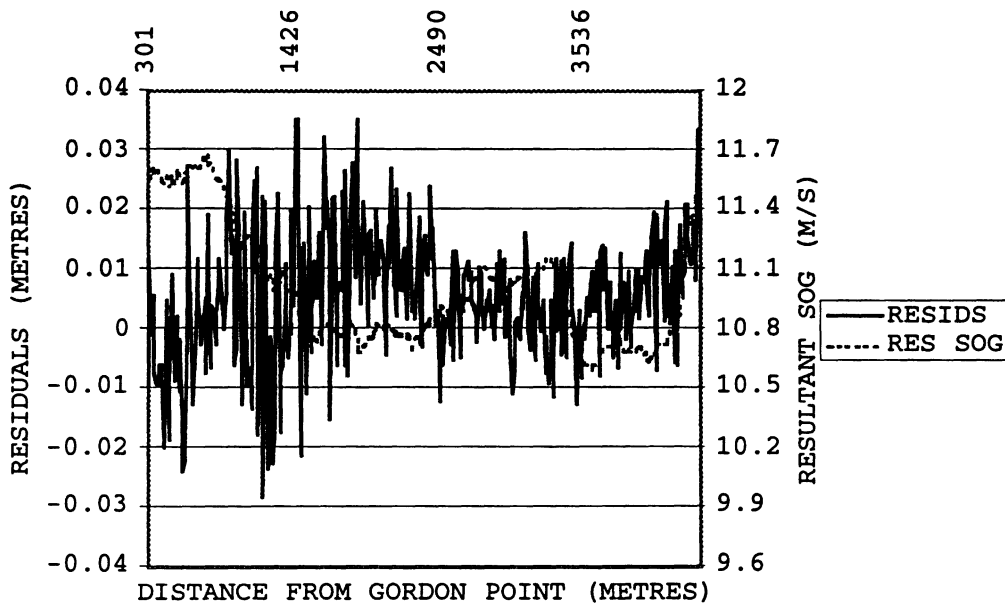
Figure 6.15

Residuals from line fit to OTF DGPS water's surface
FLOY to MBNK day 293.

follow guidelines (3), (10) and (11) that were established
for the squat tests in section 6.3.2. Even more guidelines
would need to be followed as well. In particular:

(1)   The RSTW should be controlled -- i.e. the surveys
      should:

      (a)   Be run at an RSTW that minimizes the
            correlation between RSTW changes and changes
            in the vessel's antenna height above the
            water's surface.

      (b)   Be run with RSTW as constant as possible, so

148

that antenna height fluctuations are
minimized.

(2)   Changes in salinity, bathymetry, and vessel
loading must be monitored, if the results of the
squat tests deem it to be necessary.

CHAPTER 7

CONCLUSIONS AND RECOMMENDATIONS

Under limited conditions, PRISM/Z12 post-processing OTF DGPS accuracy is acceptable for squat-dependent dredging and sounding surveys in an estuarine region. These conditions are:

(1) Baselines less than **10** kilometres in length.

(2) Water waves less than **0.10** metres in amplitude.

(3) No large changes in vessel **Resultant Speed Over Ground.**

For the work described here, the PRISM/Z12 post-processed OTF DGPS water's surface elevation accuracy was **+/-0.034 metres at 95% confidence.** This accuracy is generally in agreement with literature on current OTF DGPS performance.

PRISM/Z12 post-processing reliability was acceptable under the limited conditions stated above. The PRISM/Z12 software **does not** incorrectly flag unresolved data as being resolved, when obvious step functions of +/- 0.20 metres or more were present in the water's surface elevation.

Availability (i.e. the percent resolved epochs as indicated by the post-processing PRISM/Z12 software flag) was:

(1) Acceptable for three out of four survey days, ranging from 90-99%. This generally agrees with

the 99% value stated by Frodge et al. [1994].

(2)   Unacceptable for day 166, at 25%.

Three recommendations are pertinent:

(1)   Since squat is unique to every **vessel** and every
      survey area, future OTF DGPS dredging and
      sounding surveys should investigate **squat-
      independent** methods of obtaining accurate and
      reliable bathymetry. The water's surface
      elevation from conventional water level sensors
      might only be used as:

      (a)   A **quality control check** to ensure OTF
            DGPS ambiguities are resolved, and/or

      (b)   A solution to the problem of availability.

(2)   The use of multiple base and remote OTF
      DGPS stations should be investigated for:

      (a)   Measuring attitude parameters, perhaps in
            combination with a conventional attitude
            sensor.

      (b)   Using known baseline components on shore and
            known baseline lengths on the vessel as
            quality control checks.

(3)   OTF DGPS accuracy and reliability need to be
      investigated further, especially during the
      upcoming sunspot maximum in the year 2001, to

determine:

(a) Maximum baseline length for reliable ambiguity resolution.

(b) Percent ambiguity resolution at that maximum length.

(c) Accuracy (at 95% confidence) of the OTF DGPS bathymetry at that maximum length.

Due to the complexity of the squat parameter, the OTF DGPS technique for dredging and sounding surveys will reach its full potential with a rigorous investigation into the accuracy and reliability of **squat-independent** methods of obtaining accurate and reliable bathymetry.

REFERENCES

Abidin, H. (1994). "On - the - Fly Ambiguity Resolution."
GPS World, Vol. 5, No. 4, pp. 40 - 50.

Abidin, H., Wells D. E. , and Kleusberg A. (1992). "Some
Aspects of 'On-the-Fly' Ambiguity Resolution"
*Proceedings of the Sixth International Geodetic
Symposium on Satellite Positioning.* Vol II., pp. 660-
669.

Ashtech, Inc. (1994). "Precise GPS Navigation and Surveying
(PNAV-PRISM) Software User's Guide". Document No.
600248, Revision A, U.S.A.

Ashtech, Inc. (1995). "Supplement to Z-12 Receiver
Operating Manual Covering RTZ Functions". Document No.
600292, Revision A, USA.

Bowditch, N. (1984). *American Practical Navigator   An
Epitome of Navigation.* Vol I. 2nd Ed. Defense Mapping
Agency Hydrographic / Topographic Center.

Burrells, B. (1995). Personal Communication. Engineer,   New
Brunswick Provincial Environment Department, New
Brunswick, Canada, August.

Crean et al. (1988). *Mathematical Modeling of Tides and Estuarine Circulation*. Managing Eds. Malcolm J, Bowman, Richard T. Barber, Christopher N. K. Mooers, and John A. Raven. In Lecture Notes on Coastal and Estuarine Studies.

Crookshank, N. (1995). Personal Communication. Hydraulic Engineer, National Research Council of Canada, Ottawa, Canada.

Daugherty, R. L., Franzini, J. B., and Finnemore, J. E. (1985). *Fluid Mechanics with Engineering Applications*. 8th ed., McGraw-Hill, Inc.

Deloach , S. (1994). Personal Communication. Presentation made at the Bedford Institute of Oceanography, Bedford, Nova Scotia, Canada, June, 1994. Engineer, Logan Technologies Ltd., Stafford, VA, U.S.A.

Euler, Hein, G. and Landau (1992). "Investigation of Global Positioning System (GPS) Carrier Phase Ambiguity Resolution On-The-Fly." Contract Report prepared by TerraSat, Ottobrunn, Germany, for the U.S. Army Topographic Engineering Center, Fort Belvoir, VA, U.S.A., March.

Frodge, S.L., Shannon, B., Remondi, B.W., Lapucha ,D.,   and
    Barker, R.A.(1993). "Results of Real-Time Testing of GPS
    Carrier Phase Ambiguity Resolution On-The-Fly".
    Proceedings of the Sixth International Technical Meeting
    of the Satellite Division of the Institute of
    Navigation, Salt Lake City , UTAH, September.

Frodge , S.L. , Remondi, B., Lapucha, D. and   Barker, R.
    A.(1994). "Real-Time on-the-Fly Kinematic GPS System
    Results." *Navigation : Journal of the Institute of*
    Navigation, Vol. 41, No. 2, Summer 1994, pp. 175-185.

Gagnon, P. and Nassar, M. (1973). "External Appendix to the
    Lecture Notes No. 18 - The Method of Least-Squares".
    Department of Surveying Engineering Lecture Notes No.
    18, University of New Brunswick, Fredericton, N.B.,
    Canada.

Geodetic Research Services Lt.(1989-1992). CndGeoid:
    Canadian Geoid Ver 2.0(a). University of New Brunswick,
    Fredericton, New Brunswick, Canada.

Goguen , M. (1995). Personal Communication. Engineer,
    Department of Public Works, Moncton, New Brunswick,
    Canada, May.

Hare, R. and Tessier, B. (1995). "Water level accuracy

estimation for real-time navigation in the St. Lawrence
River". Internal Report for the Canadian Hydrographic
Service.

Hatch, R. (1989). "Ambiguity Resolution in the Fast
Lane". *Proceedings of the Second International Technical
Meeting of the Satellite Division of the Institute of
Navigation*, Colorado Springs, Colorado, pp. 45-50.

Henderson, G. (1995) Personal Communication. Hydrographer,
Canadian Hydrographic Service, Bedford, Nova Scotia,
Canada.

Lachapelle, G., Liu, C., Liu, G., Weigen, Q., and Hare,
R. (1993). "Water Level Profiling with GPS" *ION GPS 93,
Proceedings of the Sixth International Technical
Meeting of the Satellite Division of the Institute of
Navigation*. The Institute of Navigation, Salt Lake City,
UTAH, 22-24 September, pp. 1-7.

Lacroix, P, and Kightley, J. (1996). "An Under Keel
Clearance Guidance System for Ports and Waterways."
Proceedings of the Canadian Hydrographic Conference.
Bedford Institute of Oceanography, Bedford, Nova Scotia,
May 1996.

Langley, R. (1997). "The GPS Error Budget". *GPS World*, Vol.

3, No. 8, pp. 51-56.

Langley, R, and Komjathy, A. (1994). "Report on Accuracy
Assessment of Ashtech Ground Truth System" Contract
Report Prepared by the Department of Geodesy and
Geomatics Engineering, University of New Brunswick,
Fredericton, N.B., Canada for Transport Canada Aviation
and Cougar Helicopters, August.

Leendertse, J. (1988). "A New approach to Three-Dimensional
Free-Surface Flow Modeling". Contract Report No. DIV-78
for the Netherlands Rijkswaterstaat and the Rand Report.
Santa Monica, California : The Rand Report.

Leick, A. (1995). *GPS Satellite Surveying.* 2nd ed., John
Wiley and Sons, New York.

London, Her Majesty's Stationary Office (1964). "Admiralty
Manual of Seamanship".Vol II. Edinburgh, Scotland.

Marso, D. (1995). Personal Communication. Engineer,
Socomar Incorporated, Quebec City, Quebec, May.

Parsons, S. (1994). Personal Communication. Hydrographer,
Canadian Hydrographic Service, Bedford, Nova Scotia,
Canada.

Phelan, R. (1992). "Suitability and Technical Aspects of
the Socomar TMS 1000 Digital Tide Monitoring System".
Undergraduate Report, Department of Surveying
Engineering, University of New Brunswick, Fredericton,
Canada.

Philpott, K.L. (1978). "Miramichi Channel Study". Contract
Report Prepared for the Department of Public Works
Canada Design and Construction Marine Directorate.

Remondi, B. W. (1991). Kinematic GPS Results Without Static
Initialization. NOAA Technical Memorandum NOS NGS-55,
National Geodetic Information Center, Silver Spring,
Maryland, May.

Steeves, R. [1993]. GEOLAB Ver 2.6 a. Bitwise Ideas Ltd.

Wells, D. E. (1995a). "Vertical Positioning, Requirements
and Methods" . Presented at the 1995 Multibeam Training
Course in Saint Andrews, New Brunswick, Canada. pp. 28 -
29. Section V-3 of Multibeam Course Class Notes.

Wells, D. E. (1995b) Personal Communication. Professor,
Department of Geodesy and Geomatics Engineering,
University of New Brunswick, Canada, July.

Wells, D. E. (1996) Personal Communication. Professor,

Department of Geodesy and Geomatics Engineering, University of New Brunswick, Canada, June.

Wells, D.E., A. Kleusberg , and P. Vanicek (1996). "A Seamless Vertical-Reference Surface for Acquisition, Management, and Display of ECDIS Hydrographic Data". Final Contract Report prepared by the Department of Geodesy and Geomatics Engineering, University of New Brunswick, Fredericton, New Brunswick, Canada, for the Canadian Hydrographic Service, Department of Geodesy and Geomatics Engineering Technical Report No. 179, University of New Brunswick, Fredericton, New Brunswick, Canada, 64 pp.

Willis, D.H. (1995). Personal Communication. Hydraulic Engineer, National Research Council of Canada, Ottawa, Canada, October.

VITA

Candidate's full name: Richard Bradford Phelan

Place and date of birth: Halifax, Nova Scotia July 16,1966

Permanent Address: 59 Queen Street, Bridgetown, Nova
Scotia, Canada.

Schools attended: Nova Scotia Land Survey Institute
Sept. 1985-May 1987

Universities Attended   University of New Brunswick
Sept. 1987-May 1993

University of New Brunswick
Sept. 1993-May 1997